

UNCLASSIFIED

AD 258 979

*Reproduced
by the*

**ARMED SERVICES TECHNICAL INFORMATION AGENCY
ARLINGTON HALL STATION
ARLINGTON 12, VIRGINIA**



UNCLASSIFIED

NOTICE: When government or other drawings, specifications or other data are used for any purpose other than in connection with a definitely related government procurement operation, the U. S. Government thereby incurs no responsibility, nor any obligation whatsoever; and the fact that the Government may have formulated, furnished, or in any way supplied the said drawings, specifications, or other data is not to be regarded by implication or otherwise as in any manner licensing the holder or any other person or corporation, or conveying any rights or permission to manufacture, use or sell any patented invention that may in any way be related thereto.

CATALOGED BY ASTIA

AS AD No. _____

258 979

The Plasma Core Reactor

10 MAY 1961

Prepared by SEYMOUR T. NELSON

For AIR FORCE BALLISTIC MISSILE DIVISION
AIR RESEARCH AND DEVELOPMENT COMMAND
UNITED STATES AIR FORCE, *Inglewood, California*



AEROSPACE CORPORATION

CONTRACT NO. AF 04 647-594

ASTIA
RECEIVED
JUL 5 1961
RECEIVED
TIPDR

4/10/61
XEROX

THE PLASMA CORE REACTOR

by
Seymour T. Nelson

AEROSPACE CORPORATION
El Segundo, California

Contract No. AF 04(647)-594

10 May 1961

Prepared for
AIR FORCE BALLISTIC MISSILE DIVISION
AIR RESEARCH AND DEVELOPMENT COMMAND
UNITED STATES AIR FORCE
Inglewood, California

ACKNOWLEDGMENT

The author wishes to acknowledge the stimulation about this subject that resulted from discussions with G.W. Elverum, Jr., of Space Technology Laboratories, Inc., and R.W. Bussard of Los Alamos Scientific Laboratory.

Also gratefully acknowledged is the indispensable assistance given by Shirley Nelson, of the Technical Publications Section of Aerospace, in preparing this manuscript for publication.

ABSTRACT

Two types of plasma core reactor, considered as a space propulsion system of thrust-to-weight ratio exceeding unity, are investigated; viz, the simple magnetic bottle and the homopolar configurations. The principal system variables are indicated, and some upper- and lower-bounds for these are derived. The major problem areas and difficulties affecting feasibility are discussed.

CONTENTS

<u>Section</u>		<u>Page</u>
I.	INTRODUCTION	1
II.	NUCLEONICS	5
III.	PLASMA PHYSICS.	12
	A. Magnetic Bottle Confinement of a Plasma Core	12
	B. Radial Diffusion	13
	C. Radial Diffusion: Alternative Treatment	38
	D. Axial Diffusion: Magnetic Mirror Losses	43
IV.	GENERAL DISCUSSION	67
V.	CONCLUSIONS.	76
	SYMBOLS	105
	REFERENCES	111

LIST OF ILLUSTRATIONS

FIGURES

<u>Number</u>		<u>Page</u>
1	$\langle \sigma_a \rangle$ vs Neutron Energy	77
2	$\eta \langle \sigma_a \rangle$ vs Neutron Energy	78
3	Critical Mass and Particle Density vs Radius for U-233/D ₂ O	79
4	Critical Mass and Particle Density vs Radius for U-235/D ₂ O	80
5	Critical Mass and Particle Density vs Radius for Pu-239/D ₂ O	81
6	Critical Mass and Particle Density vs Radius for U-233/C	82
7	Critical Mass and Particle Density vs Radius for U-235/C	83
8	Critical Mass and Particle Density vs Radius for Pu-239/C	84
9	Critical Mass and Particle Density vs Radius for U-233/Be.	85
10	Critical Mass and Particle Density vs Radius for U-235/Be.	86
11	Critical Mass and Particle Density vs Radius for Pu-239/Be.	87
12	Fraction of Singly Ionized Uranium Atoms vs Temperature for Various Pressures	88
13	B vs n_e and T	89
14	Moderator-Reflector Mass vs Radius of Spherical Critical Cavity	90
15	Fraction of Singly Ionized Hydrogen Atoms vs Temperature for Various Pressures	91
16	Maxwell-Boltzmann Energy Distribution.	92
17	Schematic Diagram of Magnetic-Bottle Type of Plasma Core Reactor	93

LIST OF ILLUSTRATIONS (Continued)

<u>Number</u>		<u>Page</u>
18	Particle Density Decay Due to Plasma Loss Through a Magnetic Mirror	94
19	Magnetic-Bottle Type of Plasma Core Reactor with Divertor.	95
20	Plasma Core Reactor with Homopolar Geometry	96
21	Q vs a for different values of b	97
22	Homopolar Confinement.	98
23	Homopolar Confinement (Detail)	99

TABLES

<u>Number</u>		<u>Page</u>
I	Nucleonic Temperature Data	100
II	$\ln \Lambda$	103
III	Limitations Upon Principal System Variables	104

SECTION I

INTRODUCTION

By way of definition, let us call a propulsion system "low acceleration" if the ratio of its thrust to the initial vehicle gross weight is less than 1, and "high acceleration" if this ratio exceeds 1. If we confine our attention to the so-called advanced systems, it is immediately evident that there exists a bewildering variety of concepts for low-acceleration systems, such as the different types of electrical devices, but rather few ideas in the booster or high-acceleration category. In particular, if we arbitrarily consider a high-acceleration propulsion system to be "advanced" only if its I_{sp} exceeds the 800 to about 1000 seconds promised by solid-core nuclear reactors (like those under development in the Rover program), then, only two such systems have been proposed. One of these employs a series of nuclear explosions and is currently under investigation in Project Orion. The other is the plasma-core fission reactor.

This paucity of advanced concepts becomes understandable when we realize that, for all high-acceleration systems, the I_{sp} is proportional to $\sqrt{T/M}$, where T is the engine operating temperature and M is the molecular mass of the exhaust gas. If the exhaust material were dissociated hydrogen, M would equal 1 and be essentially minimized. The only way engine performance could then be further improved would be by raising the temperature. However, the maximum steady-state temperatures which even the most refractory structural materials can withstand correspond to I_{sp} values in the neighborhood of 1000 seconds.

The two ideas which have been proposed to overcome this formidable limitation both involve restricting the interaction between extremely high temperature gases and the adjacent solid materials. The first, the Orion approach, limits the interaction in time¹ by operating in pulses of short duration. The other limits the interaction in space by simply eliminating all solid structure from the immediate vicinity of the hot gas, and replacing

¹An oversimplification, to be sure, but nevertheless useful for purposes of categorization.

the confining walls by electromagnetic fields. This approach is represented by the plasma core reactor.

The object of this paper is to examine the latter concept. It should be remembered, however, that all analysis will be subject to the constraint that the propulsion system must be capable of imparting a vehicle acceleration greater than 1 g. Removal of this constraint vastly simplifies the problem, but results in a device which does not appear to compete favorably with alternative low-acceleration schemes, such as the hydrodynamically-driven gas-phase vortex reactor proposed by Kerrebrock and Meghreblian (Ref. 1). Conversely, a free-vortex gaseous-core reactor does not appear attractive for application to high acceleration systems due to propellant flow rate limitations imposed by hydrodynamic instabilities. If, however, one ionizes the fissionable material, one may (in principle at least) stabilize or "straightjacket" the core by means of electromagnetic fields. One hopes, therefore, that use of external fields to stabilize the plasma against boundary layer turbulence and Helmholtz instabilities will permit flow rates of hydrogen propellant through the core which are consonant with high acceleration propulsion.

In its simplest form, such as proposed by Taylor (Ref. 2), the plasma core reactor consists of a plasma of fissionable material which is confined within a roughly cylindrical or ellipsoidal zone about the axis of a cylindrical chamber by means of a longitudinal magnetic field. The latter is generated by electrically conducting coils bearing strong currents, which surround the chamber. The field is uniform except for the ends of the cylinder, where it is more intense due to a higher concentration of coils. The resultant arrangement of parallel lines of force bunched in at the ends is frequently referred to as a "magnetic bottle", and each end is called a "magnetic mirror". Charged particles gyrate in helical paths about the magnetic lines of force. When the magnetic moment is an adiabatic invariant of the motion, as is here assumed; i. e., when $\mu = W_{\perp} / B$ is constant for slow changes in the magnetic field strength, B , during a single gyration, it follows that the component of kinetic energy of a particle in the plane orthogonal to B , W_{\perp} , must adjust itself to compensate for an increase in B (at the magnetic mirrors). Since the total kinetic energy, $W = W_{\parallel} + W_{\perp}$,

is conserved, any increase in W_{\perp} must be offset by a decrease of equal magnitude in the parallel component, W_{\parallel} . If the mirror field is sufficiently strong, W_{\parallel} diminishes to zero at some point in the axial direction, and the sense of the particle's helical trajectory is reversed. This is the physical explanation for the "reflection" of an ion or electron by a magnetic mirror. It is thus possible in principle to confine a plasma indefinitely within a magnetic bottle. Unfortunately, diffusion phenomena alter this situation. As will be shown in Section III, it is theoretically feasible to optimize (i. e., sufficiently minimize) the plasma diffusion rate, but the price comes high.

Surrounding the glob of fissioning plasma, in the simplest device, is a layer of hydrogen propellant which forms an annulus coaxial with the plasma but nevertheless inside the solid (but porous) chamber wall, through which it is radially injected. The hydrogen flows axially down the chamber, absorbing enthalpy from the plasma core. It is finally exhausted through a suitable nozzle, after being heated to dissociation but not ionization.

The reason why hydrogen is not ionized in this case is basic to all nuclear rocket-propulsion systems, regardless of type. Fissionable material is much too expensive to waste, and must therefore be largely retained, while the hydrogen is of course expelled. Fox (Ref. 3) has demonstrated the impracticality of a system wherein the reactor core contains hydrogen mixed with a critical mass of fissionable material at all times, and the mixture is exhausted with no attempt at separation. Furthermore, Bussard and DeLauer (Ref. 4) have shown that rather large separation ratios must be achieved in order to attain economic feasibility. The hydrodynamic vortex system seeks to realize adequate separation by means of a mechanically-generated centrifugal field. The plasma core reactor, on the other hand, relies upon magnetic confinement of an ionized fissionable gas which "sees" the confining field barrier, and upon the escape of non-ionized flowing hydrogen which does not.

Nucleonically, the system resembles an externally moderated "cavity" reactor, since the particle density of the fissionable material, as will be shown in Section II, need be only about 1 percent of that of a gas at standard temperature and pressure. External moderation is achieved by a layer of

suitable solid material surrounding the core (and actually comprising the wall itself). This cladding performs the dual function of moderation and reflection, in that fission neutrons born in the core are thermalized in this external layer, and eventually reflected back into the core.

SECTION II

NUCLEONICS

In order to fix the range of values of the important variables and parameters corresponding to a working plasma core reactor, it is necessary to first consider the nucleonic aspects. In particular, we wish to know the minimum critical size and mass, as well as the corresponding particle density. In order to perform even a crude systems analysis, it is also necessary to know the way in which the critical mass and critical particle density vary with core size. The nucleonic calculations made here follow the method of Safonov (Ref. 5 and 6), whose results agree with those of the different approach used by Bell (Ref. 7). Elaborate machine computations are avoided with the help of the following simplifying assumptions:

1. The cylindrical geometry of the core, which is the most natural for propulsion applications, is approximated by a sphere. The simplification thus introduced is great, while the final results should not be much in error (because the obvious requirement that the critical mass and particle density be minimized will keep the L/D ratio within reasonable bounds). In other words, the "pancake" and "salami" extremes of cylindrical geometry are definitely precluded.
2. The thickness of the layer of moderator-reflector surrounding the core is taken to be essentially infinite. This means that the layer is at least a few thermal-diffusion-lengths thick. Since the critical mass and density are relatively insensitive functions of the moderator-reflector thickness (provided the latter exceeds about half a thermal diffusion length), it follows that this assumption need not introduce any serious errors.
3. The moderating and neutron-absorbing effects of the hydrogen propellant flowing in the vicinity of the core are completely ignored. The justification for this assumption is that, while proper accounting for the nucleonic effects of the hydrogen would not affect criticality calculations by more than about a factor of 2 at reasonable densities, it would increase the complexity of calculation enormously.

The only modification of Safonov's treatment has been to eliminate his assumption that the reactor is at room temperature. Thus, instead of the

absorption cross section corresponding to a kinetic temperature of .0253 ev, we have employed the mean absorption cross section averaged over a Maxwell-Boltzmann distribution about each of several distinct moderator temperatures of interest. These are the lowest temperatures to which neutrons may, on the average, be "thermalized". Figure 1 shows how the Maxwellianized cross section varies with kinetic temperature. The quantity η ; which is the number of neutrons released per thermal neutron capture in the core; also varies significantly with temperature, and this variation has also been taken into account. The much smaller temperature dependences of the Fermi age, thermal diffusion length, and transport mean free path for thermal neutrons in the moderator, have all been neglected. The first-order temperature effect is illustrated in Figure 2, which plots the product of η and the mean absorption cross section against kinetic temperature. This product turns out to be inversely proportional to the critical mass and particle density.

Most of the neutrons are moderated to the ambient temperature of the moderator-reflector and return to the core to cause fissions. Although this temperature may be as high as several thousands of degrees Kelvin instead of room temperature, it is nevertheless about an order-of-magnitude lower than the temperature of the plasma core itself. This raises the question of warmed-over neutrons. If a neutron undergoes a scattering event inside the plasma core before being absorbed, it will, on the average, gain energy in the process from the hotter nucleus of fissionable material. This will cause a decrease in effective fission cross section. Thus, one would expect a leakage of slow neutrons in velocity space radially outward from the origin, the magnitude of which would depend upon the ratio of the probability that a neutron will be scattered to the probability that it will be absorbed in fission or capture. The maximum value of this ratio for any fissionable material occurs for a head-on collision between a U-233 nucleus and a neutron, in which case it is still less than 4 percent. This means that, even under such extreme circumstances, an average of more than 25 neutron absorptions will occur for each scattering event. Thus we see that this effect may be neglected in the first approximation.

We can now proceed with the criticality calculations as follows:
The thermal diffusion kernel is

$$\phi(r, \rho) = \frac{3Le^{-\frac{\rho}{L}}}{8\pi\ell\rho r} \left[e^{\frac{r}{L}} - \left(\frac{1 + \frac{3a\gamma}{\ell} - \frac{a}{L}}{1 + \frac{3a\gamma}{\ell} + \frac{a}{L}} \right) e^{\frac{2a}{L}} e^{-\frac{r}{L}} \right] \quad (1)$$

for $a \leq r < \rho$, and

$$\phi(r, \rho) = \frac{3Le^{-\frac{\rho}{L}}}{8\pi\ell\rho r} \left[e^{\frac{2\rho}{L}} - \left(\frac{1 + \frac{3a\gamma}{\ell} - \frac{a}{L}}{1 + \frac{3a\gamma}{\ell} + \frac{a}{L}} \right) e^{\frac{2a}{L}} \right] e^{-\frac{r}{L}} \quad (2)$$

for $r \geq \rho$. This kernel gives the thermal-neutron flux at a point r due to a unit shell source of thermal neutrons at ρ , where both r and ρ are within the moderator. L is the thermal diffusion length, a is the core radius, and ℓ is the transport mean free path for thermal neutrons in the moderator. γ is a dimensionless constant, defined as the ratio of thermal current into the interior to the thermal flux at the interior boundary, which is a measure of the thermal-neutron sink strength of the core, i. e., the "interior greyness".

The diffusion kernel must satisfy the boundary condition

$$\frac{1}{3} \left[\frac{d\phi(r, \rho)}{dr} \right]_{r=a} = \gamma \phi(a, \rho), \quad (3)$$

which essentially says that the core acts as a sink for thermal neutrons. From Eq. (3), the directional flux at the interior boundary ($r = a$) can be written as

$$Nv = \frac{\phi(a, \rho)}{4\pi} (1 - 3\gamma \cos \theta), \quad (4)$$

Where θ is the angle between the directional flux and the radial vector from the center of the system.

From the assorted boundary conditions available, one obtains, to first-order approximation, the relation

$$3\gamma \approx \frac{a}{\Lambda} \quad (5)$$

where Λ is the absorption mean free path of thermal neutrons in the core. This approximation is valid for $\gamma < 1$, which is the only range of practical interest.

The distributed source of thermal neutrons applicable to the present case was first given by Wallace and Le Caine (Ref. 8) as

$$q(r) = \frac{S e^{-\frac{(r-a)^2}{4\tau}}}{4ar \sqrt{\pi^3 \tau}} \left\{ 1 - \frac{\sqrt{\pi \tau}}{a} e^{\left(\frac{r-a}{2\sqrt{\tau}} + \frac{\sqrt{\tau}}{a}\right)^2} \left[1 - \operatorname{erf}\left(\frac{r-a}{2\sqrt{\tau}} + \frac{\sqrt{\tau}}{a}\right) \right] \right\} \quad (6)$$

for $r > a$, and

$$q(r) = 0 \quad (7)$$

for $0 \leq r < a$. $q(r)$ is the thermal source strength per unit volume at a distance r from the center of the system, S is the total fast-neutron source strength which is symmetrically distributed in the core of radius a , τ is the Fermi age of thermal neutrons in the moderator, and $\operatorname{erf}(x)$ is the error function:

$$\operatorname{erf}(x) = \frac{2}{\sqrt{\pi}} \int_0^x e^{-t^2} dt. \quad (8)$$

The thermal flux in the moderator due to the source $q(r)$ is

$$\Phi(r) = \int_a^\infty 4\pi \rho^2 q(\rho) \phi(r, \rho) d\rho, \quad a < r, \quad (9)$$

which integrates to

$$\Phi(a) = \frac{3S}{4\pi a \ell \left(1 - \frac{a}{L}\right) \left(1 + \frac{a}{L} + \frac{3\gamma a}{L}\right)} \left\{ e^{\frac{\tau}{a^2}} \left[1 - \operatorname{erf} \left(\frac{\sqrt{\tau}}{a} \right) \right] - \frac{a}{L} e^{\frac{\tau}{L^2}} \left[1 - \operatorname{erf} \left(\frac{\sqrt{\tau}}{L} \right) \right] \right\}. \quad (10)$$

The net current at the boundary is therefore

$$J(a) = -\gamma \Phi(a). \quad (11)$$

The multiplication constant of the system may now be written as

$$k = \frac{4\pi a^2 \gamma \eta \Phi(a)}{S}, \quad (12)$$

since S is the number of fission neutrons released in a given generation, $-4\pi a^2 J(a) = 4\pi a^2 \gamma \Phi(a)$ is the number absorbed in the core, and η is the number born per thermal neutron captured in the core. Substituting Eq. (10) into Eq. (12), and setting $k = 1$ for criticality, and rearranging, yields the following expression for 3γ :

$$3\gamma = \frac{\frac{\ell}{a} \left[1 - \left(\frac{a}{L}\right)^2 \right]}{\eta \left\{ e^{\frac{\tau}{a^2}} \left[1 - \operatorname{erf} \left(\frac{\sqrt{\tau}}{a} \right) \right] - \frac{a}{L} e^{\frac{\tau}{L^2}} \left[1 - \operatorname{erf} \left(\frac{\sqrt{\tau}}{L} \right) \right] \right\} - 1 + \frac{a}{L}} \quad (13)$$

Near $a = L$, which is a singularity of Eq. (13), 3γ may be approximated by the relation

$$3\gamma = \frac{2 \frac{a}{L}}{\eta \left\{ \left(1 + \frac{2\tau}{L^2}\right) e^{\frac{\tau}{L^2}} \left[1 - \operatorname{erf} \left(\frac{\sqrt{\tau}}{L} \right) \right] - \frac{2}{L} \sqrt{\frac{\tau}{\pi}} \right\} - 1} ; a \rightarrow L. \quad (14)$$

Since $1/\Lambda$ is proportional to the core density, the critical mass is given by

$$M_c = \frac{4 \pi a^2 A}{3N \langle \sigma_a \rangle} \left(\frac{a}{\Lambda} \right), \quad (15)$$

so that the critical particle density is just

$$n_c = \frac{1}{a \langle \sigma_a \rangle} \left(\frac{a}{\Lambda} \right). \quad (16)$$

By virtue of Eq. (5), Eqs. (13) or (14) may be substituted for a/Λ in Eqs. (15) and (16). A is the atomic mass, N is Avogadro's number, and $\langle \sigma_a \rangle$ is the mean absorption cross section for a Maxwell-Boltzmann distribution about the moderator temperature of interest ("thermal"). $\langle \sigma_a \rangle$ is given (Ref. 9 and 10) by

$$\langle \sigma_a \rangle = \langle \sigma_a(T) \rangle = g_a(T) \sigma_{oa} \sqrt{\frac{\pi T_o}{4T}} \quad (17)$$

$$= \begin{cases} 10535 & g_a(T) T^{-1/2} & \text{for U-235} \\ 8831.4 & g_a(T) T^{-1/2} & \text{for U-233} \\ 15663 & g_a(T) T^{-1/2} & \text{for Pu-239} \end{cases}$$

Making use of the numerical values for the temperature-dependent variables presented in Table I, one can plot the critical mass and particle density vs core radius. This has been done for all combinations of the fuels U-233, U-235 and Pu-239 with the moderators Be, C (graphite) and D₂O. Four different representative values of the moderator kinetic temperature have been used, and the resultant curves plotted in Figures 3-11.

We are now in a position to calculate, from magnetohydrodynamic considerations, sets of values of system parameters which are consistent with the nucleonic constraints represented by these curves.

SECTION III
PLASMA PHYSICS

A. Magnetic Bottle Confinement of a Plasma Core

The Sherwood program is directed toward heating a plasma to thermonuclear temperatures ($\approx 10^8$ -deg K) and confining it within a physical chamber for seconds, or for at least significant fractions of a second. The heating problem is much more acute than that of confinement. In the plasma core reactor, however, the situation is reversed. We are dealing with a plasma which is some 10,000 times colder, and 1000 times denser, than that in a thermonuclear reactor, and this plasma must be confined for several minutes (corresponding to rocket burnout) rather than for seconds. One of the principal reasons why it is harder to confine a cool dense plasma than a hot rarified one is the Coulomb collisions between the constituent charged particles which result in diffusion of the plasma across the confining magnetic field. That is, the "guiding centers" of the Larmor (or cyclotron) orbits shift from one magnetic line of force to another as a result of collisions between the particles. It is clear that the denser the plasma, the greater the frequency of such collisions. Furthermore, the collision frequency increases with decreasing temperature. This is because the Coulomb scattering cross section varies inversely as the square of the kinetic temperature, as may be seen immediately by replacing $2mv^2$, which is four times the particle kinetic energy, by the equivalent expression, $6kT$, in the Rutherford formula for the differential Coulomb scattering cross section:

$$\begin{aligned} \frac{d\sigma}{d\Omega} &= \left(\frac{e_1 e_2}{2mv} \right)^2 \csc^4 \left(\frac{\theta}{2} \right) \\ &= \left[\frac{e_1^2 e_2^2}{\sin^4 \left(\frac{\theta}{2} \right)} \right] \left(\frac{1}{6kT} \right)^2 \end{aligned} \tag{18}$$

Effective confinement within a magnetic bottle entails both radial confinement by means of an axial field and longitudinal confinement by means of magnetic mirrors at the ends. Let us consider each of these modes in turn.

B. Radial Diffusion

It is well known (Ref. 11 and 12) that, to first-order in the density gradient (where the divergence of the stress tensor is replaced by the gradient of an isotropic pressure), like-particle collisions produce no net diffusion. In this approximation, therefore, the ion-electron collisions are solely responsible for the diffusion of plasma across magnetic lines of force.

In order to study plasma diffusion as a function of reactor-operating parameters such as temperature, magnetic-field strength and radial dimension, it is necessary to calculate the flux across the confinement zone due to ion-electron collisions. For every ion diffusing across the magnetic field there will be $\langle \mathcal{D} \rangle$ electrons, where $\langle \mathcal{D} \rangle \equiv$ the mean degree of ionization of the plasma atoms. Figure 12 plots the Saha equation (Ref. 13 and 14)

$$x = \left[\frac{3.16 \times 10^{-7} T^{2.5} e^{-E_v/kT}}{p + 3.16 \times 10^{-7} T^{2.5} e^{-E_v/kT}} \right]^{1/2} \quad (19)$$

for gaseous uranium. The curves give the fractional ionization, x , as a function of temperature and pressure, under the assumption that

$$\mathcal{D}_{\max} = 1 ; \quad (20)$$

i. e., that no atom is more than singly ionized. For optimum confinement with this restriction, let us also assume that no atom is un-ionized; i. e.,

$$\langle \mathcal{D} \rangle = \mathcal{D}_{\max} = \mathcal{D} = 1 . \quad (21)$$

At a pressure of 1 atm., for example, this implies a temperature upwards of 15,000-deg K. Unless otherwise noted, it will be assumed throughout this paper that Eq. (21) holds for the fissionable material, while for the hydrogen propellant,

$$\langle \mathcal{D}_H \rangle = \mathcal{D}_H \approx 0, \quad (22)$$

so that the electrically neutral hydrogen will be unaffected by the presence of the magnetic field confining the fissionable material.

Since electrons and ions occur in equal numbers in the plasma, they must diffuse at the same rate. The justification for this assertion is based upon the fact that, for temperatures and particle densities of interest, the Debye length or "shielding distance",

$$h = \left(\frac{kT}{4\pi n_e e^2} \right)^{1/2} \quad (23)$$

is very small compared with a characteristic plasma dimension. The Debye length is a measure of the distance over which n_e can deviate appreciably from $\mathcal{D}n_i$. (In general, $1 \leq \mathcal{D} \leq Z$, Z being the atomic number.) n_e and n_i are, of course, the electron and ion particle densities; respectively. Thus, for $T = 10^5$ -deg K and $n_e = 10^{16} \text{ cm}^{-3}$, we have, for the maximum value of h which might ever be realistically contemplated,

$$h_{\text{max}} \approx 2.7 \times 10^{-5} \text{ cm} .^1 \quad (24)$$

This implies, for example, that over a region whose thickness is 27 microns, n_e must equal $\mathcal{D}n_i$ to within one-hundredth of 1 percent. The existence of charge neutrality in the macroscopic domain greatly simplifies many calculations, and will be implicitly used throughout the subsequent analysis.

The particle flux due to plasma diffusion has been calculated by Simon², Longmire and Rosenbluth³, and others. In a previous, more detailed, paper (Ref. 15), Longmire derives an expression for the flux of particles of Type 1 due to collisions with particles of Type 2, viz.:

$$F(1, 2) = F_1 + F_2, \quad (25)$$

¹ Actually, a more typical value for h would be some two orders of magnitude smaller than h_{max} .

² Op. cit.

³ Op. cit.

where

$$\begin{aligned}
 F_1 = & - \frac{8\pi}{3} \frac{c^2 e^2}{B^2} \ln \left(\frac{2}{\theta_{\min}} \right) \sqrt{\frac{m}{2\pi kT}} n_1(x_1) n_2(x_1) \\
 & \times \left\{ \frac{e_1 B}{kT} \frac{V_D}{c} + \frac{e_1}{e_2} \frac{1}{B} \frac{\partial B}{\partial x_1} - \left(\frac{e_1}{e_2} + 1 \right) \frac{1}{n_2(x_1)} \frac{\partial n_2(x_1)}{\partial x_1} \right. \\
 & \left. + \frac{e_1}{M} \left[\left(\frac{m_1}{e_1} - \frac{m_2}{e_2} \right) + \left(\frac{1}{e_1} + \frac{1}{e_2} \right) \frac{m_1}{2} \right] \frac{1}{kT} \frac{\partial kT}{\partial x_1} \right\} \quad (26)
 \end{aligned}$$

and

$$F_2 = \frac{\partial}{\partial x_1} \left[\frac{8\pi}{3} \frac{c^2 e^2}{B^2} \ln \left(\frac{2}{\theta_{\min}} \right) \sqrt{\frac{m}{2\pi kT}} n_1(x_1) n_2(x_1) \right] \quad (27)$$

In Eqs. (26) and (27) the following definitions were assumed:

m_j, e_j, n_j \equiv mass, charge and particle density, respectively, of particles of type j ($j = 1, 2$);

x_1 \equiv $x + (v_y/\omega)$ = x -coordinate of the guiding center of a particle whose coordinates in phase space are x, v ;

V_D \equiv relative drift velocity of unlike particles;

M \equiv $m_1 + m_2$;

m \equiv $m_1 m_2 / M$;

and

$$\frac{2}{\theta_{\min}} \equiv \frac{mv^2}{e_1 e_2} \left(\frac{kT}{4\pi n_2 e_2^2} \right)^{1/2} \quad (28)$$

If we associate particles of Type 1 with ions and particles of Type 2 with electrons, and substitute $3kT$ for mv^2 , Eq. (28) can be written

$$\begin{aligned}
 \frac{2}{\theta_{\min}} &= \frac{3}{2e^3} \left(\frac{k^3 T^3}{\pi n_e} \right)^{1/2} \\
 &= \langle h/p_o \rangle \quad (29)
 \end{aligned}$$

This is the mean value of the ratio of the Debye length to the value of the classical impact parameter corresponding to $\pi/2$ deflection,

$$p_0 = e^2 / m_e v_e^2. \quad (30)$$

(p_0 is that value of the classical impact parameter, p , for which the potential energy is just twice the original kinetic energy of the scattered electron). For convenience, we will employ the notation of Spitzer (Ref. 16) and put

$$\Lambda = \frac{2}{\theta_{\min}} \quad (31)$$

We now list some of the changes of notation, assumptions and other simplifications introduced:

1. Put 1 \equiv ion and 2 \equiv electron, so that (32)

$$n_1 \equiv n_i = n_e / \mathcal{D} = n_e \quad (33)$$

$$n_2 \equiv n_e \quad (= \mathcal{D} n_i = n_i) \quad (34)$$

$$e_1 \equiv -e_i = -\mathcal{D} e_e \equiv -\mathcal{D} e = -e \quad (35)$$

$$e_2 \equiv e_e \equiv e = 4.8 \times 10^{-10} \text{ esu.} \quad (36)$$

2. Assume cylindrical geometry, in which the plasma is confined radially by means of a magnetic field $B = B_z$ in the z -direction, and diffusion occurs in the radial direction only. In particular, we calculate the outward flux (or current, which is the same thing in the one-dimensional case) of particles originating within an infinitesimal volume about the axis. The system is axi-symmetric; i. e., independent of azimuthal coordinate. Eqs. (26) and (27) are evidently invariant under a coordinate transformation from x_1 to r , so that r may be substituted everywhere for x_1 without modifying the final results in any way.
3. The magnetic field is homogeneous in the annular region between the coils and the plasma boundary. The plasma is sufficiently dense, however, for diamagnetic effects to be significant. The magnetic field vanishes inside the plasma, so that in the region $0 \leq r \leq R$, the con-

tribution to the diffusion flux of the field intensity gradient terms must not be neglected.

4. The plasma temperature is constant throughout the core volume.
5. Charge neutrality considerations discussed earlier require that the ion-electron relative drift velocity be negligible, i. e., that V_D effectively vanish. Consequently, no ambipolar diffusion takes place.
6. Assume that $n_e(r)$ falls off linearly from the value n_e at the axis to zero at $r = R$. Thus we may write

$$n_e(r) = n_e - \frac{n_e r}{R}, \quad (37)$$

whence

$$\frac{\partial n_e(r)}{\partial r} = \frac{dn_e(r)}{dr} = -\frac{n_e}{R} = \text{const.} \quad (38)$$

7. The electron rest mass, m_e , will be used in place of the reduced mass, m , throughout. (Actually, $m/m_e = 0.999 +$).

Since the plasma is taken to be spatially isothermal (4 above), the last term in the braces of Eq. (26) vanishes. From 5, the first term in the braces also vanishes. The third term drops out because $e_1 = -e_2$, by Eqs. (35) and (36). The remaining (second) term may be evaluated as follows:

The linearized equation of motion for a steady-state plasma with no electric or external field is simply

$$\nabla P = \bar{j} \times \bar{B}, \quad (39)$$

where ∇P is the magnetic pressure gradient which, by means of Maxwell's curl \bar{B} equation can be written

$$\left. \begin{aligned} \nabla P &= \frac{1}{4\pi} \nabla \times \bar{B} \times \bar{B} \\ &= \frac{1}{4\pi} \left(\bar{B} \cdot \nabla \bar{B} - \frac{\nabla^2 \bar{B}}{2} \right) \end{aligned} \right\} \quad (40)$$

The last expression results from expansion of the triple vector product. For an uncurved field, i. e., where the magnetic mirrors at the ends are

neglected (as indicated in 2 above), the first term on the right-hand side of Eq. (40) vanishes, so that we have

$$\nabla P = -\frac{1}{4\pi} \frac{B^2}{2} = -\nabla \left(\frac{B^2}{8\pi} \right). \quad (41)$$

Integrating both sides yields

$$P + \frac{B^2}{8\pi} = \text{constant}. \quad (42)$$

This can be written

$$P_o = \frac{B_R^2 - B_o^2}{8\pi}, \quad (43)$$

where the subscript o refers to the axis and the subscript R to the outer boundary of the plasma. P_o is maximum when B_o vanishes. Taking this to be the case, the (maximum) magnetic pressure is

$$P_o = B_R^2 / 8\pi. \quad (44)$$

(Eq. (44), incidentally, is numerically equal to the magnetic energy density.)

For equilibrium confinement, the magnetic pressure must exactly balance the hydrostatic pressure of the plasma at the outer boundary, so that we have

$$n_o kT = \beta \frac{B_R^2}{8\pi}, \quad (45)$$

where n_o is the total number of free particles per cubic centimeter of plasma at the axis; it is, by virtue of the present assumptions, numerically the same as n_c in Section II. Making use of Eqs. (33) and (34),

$$n = (\mathcal{L} n_e + n_i) = 2n_e. \quad (46)$$

By definition, β is the ratio of the hydrostatic pressure at the axis to the magnetic pressure at the boundary:

$$\beta = \frac{n k T}{\frac{B^2}{8\pi}} = \frac{16 \pi n_e k T}{B^2}, \quad (47)$$

where the subscripts have been dropped for simplicity. Henceforth all hydrostatic pressures and particle densities will refer to the axis and all magnetic-field intensities will refer to the outer boundary of the plasma unless otherwise noted, as in the functions $n_e(r)$ and $B^2(r)$ appearing below, which depend upon the radial coordinate.

Obviously

$$0 < \beta \leq 1. \quad (48)$$

Eq. (47) can also be written as

$$B^2 = 16 \pi n_e k T / \beta \quad (49)$$

The square root of the right-hand side of Eq. (49) is numerically the same as the magnetic field intensity which serves to confine the plasma. It is minimum when $\beta = 1$ and becomes infinite as $\beta \rightarrow 0$. In Figure 13, B is plotted vs. T and n_e for $\beta = 10^{-2}$, 10^{-1} and 1. The smaller values of β are of interest chiefly because magnetically confined plasmas of high β tend to be unstable.

We have assumed (4 above) that

$$\frac{\partial T}{\partial r} = 0, \quad (50)$$

so that Eq. (49) implies that

$$B^2(r) = B^2 - \frac{16 \pi n_e(r) k T}{\beta}. \quad (51)$$

This means that since, by Eq. (37), $n_e(r)$ varies inversely as r , it follows that the magnetic pressure inside the plasma must vary directly as r , and the magnetic-field intensity inside the plasma is consequently proportional to $r^{1/2}$. Thus we are assuming that as a result of plasma diamagnetism, $B^2(r)$ falls off linearly from the value B^2 at $r = R$ to the value zero at the axis, while the hydrostatic pressure increases linearly from the value zero at the boundary to its maximum at the axis, since the density gradient is

$$\beta = \frac{n k T}{\frac{B^2}{8\pi}} = \frac{16 \pi n_e k T}{B^2}, \quad (47)$$

where the subscripts have been dropped for simplicity. Henceforth all hydrostatic pressures and particle densities will refer to the axis and all magnetic-field intensities will refer to the outer boundary of the plasma unless otherwise noted, as in the functions $n_e(r)$ and $B^2(r)$ appearing below, which depend upon the radial coordinate.

Obviously

$$0 < \beta \leq 1. \quad (48)$$

Eq. (47) can also be written as

$$B^2 = 16 \pi n_e k T / \beta \quad (49)$$

The square root of the right-hand side of Eq. (49) is numerically the same as the magnetic field intensity which serves to confine the plasma. It is minimum when $\beta = 1$ and becomes infinite as $\beta \rightarrow 0$. In Figure 13, B is plotted vs. T and n_e for $\beta = 10^{-2}$, 10^{-1} and 1. The smaller values of β are of interest chiefly because magnetically confined plasmas of high β tend to be unstable.

We have assumed (4 above) that

$$\frac{\partial T}{\partial r} = 0, \quad (50)$$

so that Eq. (49) implies that

$$B^2(r) = B^2 - \frac{16 \pi n_e(r) k T}{\beta}. \quad (51)$$

This means that since, by Eq. (37), $n_e(r)$ varies inversely as r , it follows that the magnetic pressure inside the plasma must vary directly as r , and the magnetic-field intensity inside the plasma is consequently proportional to $r^{1/2}$. Thus we are assuming that as a result of plasma diamagnetism, $B^2(r)$ falls off linearly from the value B^2 at $r = R$ to the value zero at the axis, while the hydrostatic pressure increases linearly from the value zero at the boundary to its maximum at the axis, since the density gradient is

constant and the temperature gradient vanishes.

Differentiating Eq. (51) thus yields

$$2B(r) \frac{\partial B(r)}{\partial r} = - \frac{16\pi kT}{\beta} \frac{\partial n_e(r)}{\partial r} \quad (52)$$

Substituting for the density gradient from Eq. (38) and dividing both sides of Eq. (52) by $B^2(r)$ and substituting Eq. (51), we obtain

$$\frac{1}{B(r)} \frac{\partial B(r)}{\partial r} = \frac{8\pi n_e kT}{\beta R \left[B^2 - \frac{16\pi n_e(r)kT}{\beta} \right]} \quad (53)$$

If this expression is evaluated at the axis (from which region it is desired to calculate the diffusion flux), B^2 vanishes and $n_e(r) = n_e$, so that we have

$$\left. \begin{aligned} \left[\frac{1}{B(r)} \frac{\partial B(r)}{\partial r} \right]_{r=0} &= - \frac{8\pi n_e kT}{R (16\pi n_e kT)} \\ &= - \frac{1}{2R} \end{aligned} \right\} \quad (54)$$

Hence, using Eqs. (35) and (36), the second term in the braces of Eq. (26) finally reduces to

$$\left. \begin{aligned} \frac{e_1}{e_2} \frac{1}{B} \frac{\partial B}{\partial x_1} &= - \frac{1}{B(r)} \frac{\partial B(r)}{\partial r} \\ &= \frac{1}{2R} \end{aligned} \right\} \quad (55)$$

With all the previous simplifications, Eq. (26) now reduces to

$$F_1 = - \frac{8\pi}{3} \frac{c^2 e^2}{B^2} \ln \Lambda \sqrt{\frac{m_e}{2\pi kT}} \frac{n_e^2}{2R} \quad (56)$$

Writing Eq. (27) as

$$F_2 = - \frac{\partial}{\partial r} \left(\frac{8\pi}{3} c^2 e^2 \ln \Lambda \sqrt{\frac{m_e}{2\pi kT}} \right) \frac{n_e^2(r)}{B^2(r)} \quad (57)$$

and performing the indicated differentiation, we have

$$\begin{aligned}
 F_2 = & -\frac{8\pi}{3} c^2 e^2 \ln \Lambda \sqrt{\frac{m_e}{2\pi kT}} \left[\frac{2n_e(r)}{B^2(r)} \frac{\partial n_e(r)}{\partial r} \right. \\
 & \left. - \frac{2n_e^2(r)}{B^3(r)} \frac{\partial B(r)}{\partial r} \right] \\
 = & -\frac{8\pi}{3} \frac{c^2 e^2}{B^2} \ln \Lambda \sqrt{\frac{m_e}{2\pi kT}} \left[2n_e(r) \frac{\partial n_e(r)}{\partial r} \right. \\
 & \left. - \frac{2n_e^2(r)}{B(r)} \frac{\partial B(r)}{\partial r} \right].
 \end{aligned} \tag{58}$$

Substituting, as before Eqs. (37), (38) and (54), and evaluating the resultant expression at $r = 0$, we obtain

$$\begin{aligned}
 F_2 = & -\frac{8\pi}{3} \frac{c^2 e^2}{B^2} \ln \Lambda \sqrt{\frac{m_e}{2\pi kT}} \left[\left(-\frac{2n_e^2}{R} \right) - \left(-\frac{2n_e^2}{2R} \right) \right] \\
 = & \frac{8\pi}{3} \frac{c^2 e^2}{B^2} \ln \Lambda \sqrt{\frac{m_e}{2\pi kT}} \frac{n_e^2}{R}.
 \end{aligned} \tag{59}$$

From Eq. (25), we can at last write the radial diffusion flux as the sum of Eqs. (56) and (59):

$$\begin{aligned}
 F(1, 2) & \equiv F(i, e) \equiv F \\
 & = \frac{4\pi}{3} \frac{c^2 e^2}{B^2} \ln \Lambda \sqrt{\frac{m_e}{2\pi kT}} \frac{n_e^2}{R}.
 \end{aligned} \tag{60}$$

Eq. (60) may be simplified still further, but perhaps it would be more illuminating to evaluate it first for a numerical example of possible interest.

Table II gives values of $\ln \Lambda$ for some representative temperatures and particle densities. It should be noted, however, that for low temperatures and high densities (corresponding to the upper right-hand portion of the table), the theory tends to break down.¹ This is precisely the regime

¹Spitzer, Op. cit. p. 73.

which is of practical concern. However, since in the present approximation we are interested only in gross order-of-magnitude effects, this complication will be ignored.

Since the plasma core reactor is to ultimately constitute the heart of the propulsion system of a space vehicle, it is natural to require that its size and critical mass be minimal, in order to minimize the launching weight and overall cost per mission. A significant fraction of the latter will undoubtedly be the cost of the fissionable material alone. Figures 3-11 indicate that a plutonium core moderated by means of a heavy water reflector should satisfy this requirement for a plasma radius of 30-40 cm. This in turn would imply a critical mass of less than 600 grams and a corresponding critical particle density of about $5 \times 10^{18} \text{ cm}^{-3}$. It is clear, however, that most of the weight of the entire vehicle aft of the tankage is likely to be concentrated in the moderator-reflector. Figure 14 shows, as might be anticipated, that when overall system weights are taken into account, D_2O loses its great attractiveness, even neglecting the intrinsic engineering disadvantages of a liquid relative to a solid. In fact, if two thermal diffusion lengths are deemed necessary for effective moderation, a 40-cm radius core surrounded by a layer of D_2O will weigh some 14 times that of a Be-reflected core of the same size, or about 63 metric tons. It is clear that a weight penalty of 58.5 metric tons is unacceptable, so we turn to a beryllium-clad core (see Figures 9-11).

The choice of fissionable material will, in the final analysis, depend upon such factors as economics, relative safety, and the temperature to which the moderator-reflector can be cooled. For concreteness, however, let us assume that the fuel is U-233 and that the moderator-reflector is maintained at 293-deg K (0.0253 ev). In this case, Figure 9 implies a minimum radius of about 45 cm and a corresponding critical mass of 5 kg and critical particle density, n_c , of $3.3 \times 10^{19} \text{ cm}^{-3}$.

Anticipating a later result, viz., that diffusion considerations require that R be maximized, and for purposes of simplifying calculations, let us compromise by taking $R = 220 \text{ cm}$, which is quite large, but certainly not impossible. A glance at Figure 14, incidentally, shows that enlarging the dimension in this manner will bring the weight of the Be layer up to the same

value the D_2O layer had for a 40-cm radius core. Although it appears we are back where we started weight-wise, we have nevertheless (by enlarging the core) vastly improved the diffusion properties of the plasma and consequently ameliorated the confinement problem. Moreover, it is possible that a thickness of only one-half diffusion length (about 12 cm for Be) might prove worthwhile in spite of somewhat increased fuel inventories, particularly for the larger cores.

A U-233 core 220-cm in radius, surrounded by "thermal" Be, corresponds to a critical mass of 34-kg (6.8 times the minimum value possible, which occurs at $R = 45$ cm), and, even more significantly, reduces the critical particle density to $2 \times 10^{18} \text{ cm}^{-3}$ (which represents a 16.5-fold decrease from the 45-cm value). Thus, identifying $n = n_c$, Eq. (46) implies that

$$n_e = n_c / 2 = 10^{18} \text{ cm}^{-3} . \quad (61)$$

At a temperature of 2.5×10^4 -deg K, this corresponds to a hydrostatic pressure

$$\begin{aligned} P = nkT &= 2 \times 10^{18} \times 1.38 \times 10^{-16} \times 2.5 \times 10^4 \\ &= 6.9 \times 10^6 \text{ dyne cm}^{-2} \end{aligned} \quad (62)$$

or about 6.8 atmospheres. If $\beta = 0.1$, this corresponds to a magnetic energy density of $6.9 \text{ joule cm}^{-3}$. Figure 12 shows that at this pressure and temperature effectively all of the uranium is at least singly ionized. Figure 15, which plots the Saha equation for hydrogen ($E_v = 13.6 \text{ ev}$) in the same way that Figure 12 does for uranium, shows that if the hydrogen temperature is not permitted to exceed about 40 percent of the plasma temperature, or about 10,000-deg K, at a pressure of the order of 10 atm., then its fractional ionization should be less than one-half of 1 percent.

Figure 13 shows that these values of n_e and T imply that a minimum ($\beta = 1$) magnetic-field strength of 13.17 kilogauss is necessary for plasma confinement. Therefore, if we assume, as before, that plasma stabilization will require a value of $\beta = 0.01$, we are faced with the task of generating the enormous field strength of 131.7 kilogauss. Although this is smaller than fields which have already been produced in the laboratory

(albeit, for short periods of time), it still represents a formidable engineering difficulty, principally because of the requirement that the coils and associated field-generating apparatus be lightweight; i. e., flyable. It is possible, however, that by resorting to a pulsed B-field instead of a steady-state one¹ and to "force-free" coils, such as described by Furth, Levine and Waniek (Ref. 17), such strong fields may be rendered flyable.

Let us summarize the values of the system variables thus far selected as representative:

$$\left. \begin{aligned} R &= 220 \text{ cm,} \\ n_e &= 10^{18} \text{ cm}^{-3}, \\ T &= 2.5 \times 10^4 \text{ deg K,} \\ \beta &= 0.01 \\ B &= 1.317 \times 10^5 \text{ gauss.} \end{aligned} \right\} (63)$$

Substituting these values into Eq. (60), along with the value

$$\ln \Lambda = 3.89 \quad (64)$$

from Table II, we have

$$\left. \begin{aligned} F &= \frac{4\pi \times 8.99 \times 10^{20} \times 23.07 \times 10^{-20} \times 3.89}{3 \times 1.73 \times 10^{10}} \\ &= \sqrt{\frac{9.11 \times 10^{-28}}{2\pi \times 1.38 \times 10^{-16} \times 2.5 \times 10^4} \frac{10^{36}}{220}} \\ &= 5.74 \times 10^{18} \text{ cm}^{-2} \text{ sec}^{-1}. \end{aligned} \right\} (65)$$

This implies a radial diffusion velocity

$$v_r = \frac{F}{n_e} = 5.74 \text{ cm sec}^{-1}, \quad (66)$$

¹Indeed, it appears that pulsing B may prove to be the only practical method of stabilizing the plasma-hydrogen interface against Helmholtz waves.

which compares with the thermal electron velocity

$$v_e^{(th)} = \sqrt{\frac{3kT}{m_e}} = \sqrt{\frac{3 \times 1.38 \times 10^{-16} \times 2.5 \times 10^4}{9.11 \times 10^{-28}}} \quad \left. \vphantom{\frac{3kT}{m_e}} \right\} (67)$$

$$= 1.07 \times 10^8 \text{ cm sec}^{-1}$$

in the ratio

$$v_r/v_e^{(th)} = 5.36 \times 10^{-8} . \quad (68)$$

Of course the ions move, on the average, $\sqrt{233} = 15.26$ times slower than the electrons, i. e.,

$$v_i^{(th)} = 6.99 \times 10^6 \text{ cm sec}^{-1} , \quad (69)$$

but enormous space charge effects would quickly develop unless the macroscopic diffusion rates were equal.

The diffusion time across the core, from the axis to the plasma-hydrogen interface at $r = R$, is simply

$$t_d = R/v_r = 220/5.74 = 38.33 \text{ sec} . \quad (70)$$

There are several alternative methods for achieving at least a theoretical degree of feasibility for the system (insofar as radial diffusion alone is concerned). Since the propulsion-system burning time, t_b , is not likely to be less than, say, 230 sec (which is just $6t_d$) for typical astronautic missions, we can either accept the loss of about seven critical masses per mission by this particular diffusion mechanism¹, or we can choose to increase the diffusion time, t_d . For the numerical case under consideration, the critical mass is 34 kg, so that radial diffusion alone would account for the dissipation of some 238 kg of fissionable material.

Although, for a sufficiently large vehicle, this situation need not be regarded as intolerable, a plasma-core propulsion system nevertheless

¹In order to maintain criticality during the last "throughput" (i. e., from $t_b - t_d$ sec to t_b sec after launch), we take the total number of throughputs, n , to be

$$n \approx \frac{t_b}{t_d} + 1 \quad (71)$$

loses much of its appeal when the fuel cost per mission is comparable with the research and development cost of the entire vehicle program. Moreover, other loss mechanisms are also present, such as end losses out of the magnetic mirrors and surface erosion of the plasma due to the frictional effect of axially-flowing hydrogen. This erosion will be enhanced by Helmholtz waves at the plasma boundary and other instabilities which might exist inside the plasma.

It is not unreasonable, therefore, to establish as a prerequisite for the demonstration of system feasibility that (insofar as radial diffusion processes alone are concerned) the reactor must not lose all of its initial charge of fissionable material before the first 230 seconds of flight have elapsed. Perhaps this requirement is too stringent. Indeed, it may be removed if there is a decrease in the unit cost of fuel, an increase in budget, or if some way can be found to retain within the vehicle most of the plasma which is lost to the magnetic bottle proper, and to continuously re-inject this plasma back into the magnetic bottle. A possible method of accomplishing this for losses in the axial direction will be discussed later.

Let us see where both directions lead. First we will retain the limitation

$$t_d \geq 230 \text{ sec}, \quad (72)$$

and subsequently we will weaken it.

Accepting Ineq. (72) for the moment, it remains to manipulate the values selected for the system parameters in the numerical example above in such a way as to multiply t_d by the required factor of 6. It would appear from Eq. (60) that there are four different ways of doing this, viz., to increase B or T , decrease n_e , or increase R . The interdependence of these variables, however, should be immediately evident. There are, in fact, only two independent ways of increasing t_d . Combining Eqs. (49), (60), (66) and (70), we get

$$\begin{aligned}
t_d &= \frac{R}{v_r} = \frac{Rn_e}{F} \\
&= \frac{3B^2R^2}{4\pi n_e c^2 e^2 \ln \Lambda} \sqrt{\frac{2\pi kT}{m_e}} \\
&= AR^2 T^{3/2}
\end{aligned}
\tag{73}$$

where

$$A = \frac{12k}{\beta c^2 e^2 \ln \Lambda} \sqrt{\frac{2\pi k}{m_e}}
\tag{74}$$

A is approximately constant, since the $\ln \Lambda$ does not vary much over the range of temperatures to which we are limited by ionization and heat transfer phenomena, and over the range of particle densities to which we are limited by nucleonic considerations and fabrication problems. (See Table II).

Instead of eliminating B in Eq. (73), we could have eliminated one of the remaining variables. The present form, however, appears to suggest the available avenues of manipulation in a physically more realistic way.

Thus, Eq. (73) tells us that, in order to multiply the left-hand side by 6, we can either increase R by a factor of $6^{1/2} = 2.45$, or T by a factor of $6^{2/3} = 3.30$, or else increase both by smaller factors.

Considerations of pressure vessel weight and plasma stability set an upper limit on the axial flow rate of propellant. It therefore appears that the hydrogen flowing past the plasma core will be heated to a final (exhaust) temperature somewhat lower than, but nevertheless of the same order as, that of the core. If one denies the inevitability of this, several shortcuts to feasibility present themselves. These will be mentioned in the General Discussion. For the meanwhile, let us assume that the possibility of more than tripling the plasma temperature does not hold much promise. Figure 15 shows that if the hydrogen is permitted to exceed about 12,000-deg K at the pressures of interest, the fractional ionization becomes quite significant; the newly created hydrogen ions, being electrically charged, then respond to the externally imposed magnetic field, thereby tending to nullify

the preferential confinement of the fissionable material within the magnetic bottle, which is the crux of the entire propulsion system.

This temperature limitation is unfortunate for several reasons, even though the "electric bill" for energy supplied to the magnetic coils, (which, of course, we wish to minimize) is directly proportional to T (see Eq. (45)). First, it sets an upper limit to the exhaust velocity and specific impulse ultimately attainable by any magnetically confined plasma core reactor system which expels hydrogen, although this limit is indeed substantially higher than that corresponding to a solid core (i. e., fixed-bed) nuclear rocket. Secondly, there is a very definite reason, independent of rocket performance as such, for desiring to raise the plasma temperature to about 40,000-deg K. Since the ionization potential of hydrogen is 13.6 volts, the $n = 2$ level (where $n \equiv$ principle quantum number) corresponds to an energy of $13.6/2^2 = 3.4$ electron volts. This is equivalent to a temperature of very nearly 4×10^4 -deg K. Strictly speaking, it would be most desirable for the kinetic temperature, kT , to be 6.8 ev, in which case the mean energy of the plasma particles would be 10.2 ev, but the most probable energy, $1/2 (kT)$, would be just 3.4 ev. This is depicted in Figure 16, where the peak (most probable value) of the Maxwell-Boltzmann energy distribution precisely corresponds to the second hydrogen quantum level at 3.4 volts. Since the slope of Figure 16 is not too steep between the abscissas $E = 1/2 (kT)$ and $E = kT$, an operating temperature of 4×10^4 -deg K instead of 8×10^4 -deg K ($kT = 6.8$ ev) would not represent an extremely large sacrifice in energy transfer efficiency.

Thus, if we were able to "tune" the maximum of the Maxwell-Boltzmann temperature distribution of the fissioning plasma to this resonance for hydrogen, we should expect that the hot plasma would "talk" better to the hydrogen, i. e., the rate of absorption by the hydrogen propellant of radiant energy emitted by the plasma would be at a relative maximum.

Actually, the absorptivity of hydrogen is seriously small only for very low pressures at temperatures in the 10-20,000-deg K range. In fact, for pressures ≥ 50 atm, the absorptivity approaches unity (Ref. 18). Thus the real problem in the annular flow device is getting the hydrogen heated up to,

say, 8000-deg K, rather than from 8000 to the final exhaust temperature of 10-12,000-deg K since radiation is the primary energy transfer mechanism. However, some preliminary radiative transfer calculations indicate that wall-cooling considerations will prohibit any further increase of T, even in devices with significant rates of radial hydrogen diffusion through the plasma.

In passing, it is interesting to note that Eq. (73) predicts a sort of Maxwell demon effect in the plasma, which preferentially retains the more energetic particles and allows the less energetic ones to escape. In other words, the colder the plasma, the faster the diffusion rate. The explanation of this intuitively anomalous circumstance lies in the fact that the Coulomb scattering cross section for ion-electron collisions (the dominant diffusion mechanism) decreases with increasing temperature.

We now turn to the remaining method for increasing t_d : by virtue of Eq. (73), the only recourse available is to enlarge the radius of the core to

$$R = 2.45 \times 220 = 539 \text{ cm} . \quad (75)$$

This alternative looks as unattractive as the former one. A chamber almost 11 meters in diameter (even excluding the space occupied by the concentric layer of propellant!) would present formidable fabrication problems. Also, the volume which the confining magnetic field must occupy would be so large that the total amount of energy supplied by the coils to maintain this field would be excessive. Furthermore, according to Figure 9, the critical mass for a core of this size would be about 180 kg, substantially defeating the purpose of the core enlargement.

It would appear, then, that the simple magnetic bottle mode of confining a plasma core reactor is rather unpromising, on the basis of radial diffusion alone, unless methods can be found to remove or weaken at least one of the above restrictions. Thus, it might become possible, either by means of a reduction in the cost of fuel or by some scheme whereby a fraction of the critical mass, perhaps up to 50 percent, is embedded within the moderator-reflector cladding, or by a combination of such factors, to weaken Ineq. (72) by as much as a factor of 4. If such were the case, Ineq. (72) would be replaced by

$$t_d \geq 57.5 \text{ sec} , \quad (76)$$

and the still-needed factor of 1.5 further increase in t_d might easily be achieved by increasing R by a factor of $1.5^{1/2} = 1.22$, from 220 to 269 cm. An enlargement of this small order would, almost certainly, not introduce any serious complications. Note that the remaining restriction, viz., the temperature limitation, has not been modified. This is because it is felt to be the most recalcitrant of all.

Accepting the above optimistic concessions for the sake of illustration, let us calculate some of the principle characteristics of the resultant system. Since we now have

$$R = 269 \text{ cm} , \quad (77)$$

and since we assume, as before, that we are dealing with a U-233 core moderated by an external layer of beryllium one thermal-diffusion length (23.6-cm) thick, it follows that the diameter of the entire system (excluding the coils, which would undoubtedly be embedded within the Be) is

$$D = 2 (R + L_{\text{Be}} + Y) , \quad (78)$$

where L_{Be} is the cladding thickness and Y is the thickness of the hydrogen layer surrounding the plasma. For simplicity, let us circumvent the elaborate heat-transfer analysis necessary to evaluate Y, and assume that

$$Y \approx R . \quad (79)$$

Preliminary calculations indicate that, in the core size range of interest, this approximation should hold fairly well.

Eq. (78) then becomes

$$\left. \begin{aligned} D &= 2 (2R + L_{\text{Be}}) \\ &= 2 (2 \times 269 + 23.6) \\ &= 11.23 \text{ meters} , \end{aligned} \right\} (80)$$

or slightly less than 37 feet, of which over 17 feet is actual plasma.

According to Figure 14, the beryllium layer has a mass

$$M_r = 160 \text{ metric tons} . \quad (81)$$

From this value alone it may be deduced that, in order for the vehicle acceleration to exceed 1 g, the thrust developed by the plasma-core propulsion system must be rated in the millions of pounds at the least.

Figure 9 tells us that the critical mass is

$$M_c = 49 \text{ kg} \quad (82)$$

and

$$n_c = 1.6 \times 10^{18} \text{ cm}^{-3} \quad (83)$$

so that

$$n_e = 8 \times 10^{17} \text{ cm}^{-3} \quad (84)$$

As before,

$$T = 2.5 \times 10^4 \text{ -deg K} \quad (85)$$

and

$$\beta = 10^{-2} \quad (86)$$

Thus, from Figure 13 we see that

$$B = 117.8 \text{ kilogauss.} \quad (87)$$

This corresponds to a magnetic energy density

$$\left. \begin{aligned} \frac{E}{V} &= \frac{B^2}{8\pi} = \frac{2n_e kT}{\beta} = 1.6 \times 10^{18} \times 1.38 \times 10^{-16} \times 2.5 \times 10^4 \times 10^2 \\ &= 5.52 \times 10^8 \text{ erg cm}^{-3} \end{aligned} \right\} (88)$$

and therefore a magnetic pressure

$$\left. \begin{aligned} P_M &= 5.52 \times 10^8 \text{ dyne cm}^{-2} \\ &= 545 \text{ atm} \\ &= 8012 \text{ psi.} \end{aligned} \right\} (89)$$

Of course, the hydrostatic pressure of the plasma is only

$$\left. \begin{aligned} P_H &= 5.45 \text{ atm} \\ &= 80.12 \text{ psi.} \end{aligned} \right\} (90)$$

Neglecting ohmic losses, we can calculate from Eq. (88) the electrical energy which must be supplied to the magnetic coils:

$$\begin{aligned}
 E &= 5.52 \times 10^8 \times \frac{4}{3} \pi \times 269^3 \\
 &= 4.50 \times 10^{16} \text{ erg} \\
 &= 4500 \text{ megajoules ,}
 \end{aligned}
 \quad \left. \vphantom{\begin{aligned} E &= 5.52 \times 10^8 \times \frac{4}{3} \pi \times 269^3 \\ &= 4.50 \times 10^{16} \text{ erg} \\ &= 4500 \text{ megajoules ,} \end{aligned}} \right\} (91)$$

where the chamber has been assumed spherical for simplicity, as in the nucleonic calculations of Section II.

There are two reasons why it might be of interest to consider time-varying B-fields. First, there is the possibility of recovering a significant fraction of the externally-supplied ohmic power losses by means of periodically varying the multiplication constant in a manner appropriately related to the variation in B and in plasma volume.

If B were pulsed so as to compress the plasma during part of each cycle, after which the plasma were allowed to expand nonadiabatically after having generated nuclear energy at an increased rate, it would do work against the confining field which could be tapped from external windings as electrical energy. Thus there would exist a process of direct conversion of nuclear-generated thermal energy into electrical energy whose efficiency would depend, of course, upon the ratio of maximum-to-minimum plasma volume, and therefore upon B'/B , where B' is the field intensity peak and B is the minimum value of the field intensity in each cycle. For a sinusoidally-varying magnetic field, it is clear that the root-mean-square field intensity must at least equal the steady-state value which would ordinarily be required for plasma confinement, and the field intensity minimum, B , should be greater than zero.

Secondly, Helmholtz waves and other plasma oscillations might be smoothed out by superimposing, upon the confining field, a time-varying component whose frequency is comparable with the wave frequency, or is related to the rate of growth in amplitude of the disturbance. Although the magnitude of such a component could, in principle, equal the magnitude of the entire confining field, in practice there is no reason why it could not be much smaller.

In view of the above considerations, it is of interest to calculate the magnitude of the ohmic losses in the plasma for the case where B varies, but where there is no time-varying electric field. In particular, let us

investigate how long it takes for the ohmic losses in the plasma to dissipate an energy comparable with the magnetic energy density, $B^2/8\pi$. We assume that

$$\frac{\partial \bar{j}}{\partial t} \approx 0, \quad (92)$$

$$\frac{\partial \bar{v}}{\partial t} \approx 0, \quad (93)$$

$$\nabla p/2 \approx \nabla p_i \approx \nabla p_e \approx 0, \quad (94)$$

and

$$\nabla \phi \approx 0, \quad (95)$$

where $\nabla \phi$ is an external force, such as gravity. Then the linearized equation of motion,

$$\rho \frac{\partial \bar{v}}{\partial t} = \bar{j} \times \bar{B} - \nabla p - \rho \nabla \phi \quad (96)$$

reduces to

$$\bar{j} \times \bar{B} = 0. \quad (97)$$

Making use of Eqs. (92), (94) and (97), we can simplify the generalized Ohm's law,

$$\frac{m_e c^2}{n_e e^2} \frac{\partial \bar{j}}{\partial t} = \bar{E} + \bar{v} \times \bar{B} + \frac{c}{en_e} \nabla p_e - \frac{c}{en_e} \bar{j} \times \bar{B} - \eta \bar{j}, \quad (98)$$

to

$$\bar{E} + \bar{v} \times \bar{B} = \bar{j}. \quad (99)$$

Now since we assume that

$$\frac{\partial \bar{E}}{\partial t} = 0, \quad (\text{steady state}) \quad (100)$$

Maxwell's equation,

$$\nabla \times \bar{B} = \frac{1}{c^2} \frac{\partial \bar{E}}{\partial t} + 4\pi \bar{j} \quad (101)$$

reduces to

$$\nabla \times \bar{B} = 4\pi \bar{j} \quad (102)$$

or

$$\bar{j} = \nabla \times \bar{B} / 4\pi. \quad (103)$$

Substituting Eq. (103) into Eq. (99) yields

$$\bar{E} + \bar{v} \times \bar{B} = \frac{\eta}{4\pi} \nabla \times \bar{B}. \quad (104)$$

Taking the curl of both sides of Eq. (104) and assuming the resistivity, η , to be constant, we have

$$\left. \begin{aligned} \nabla \times (\bar{E} + \bar{v} \times \bar{B}) &= \frac{\eta}{4\pi} \nabla \times \nabla \times \bar{B} \\ &= \frac{\eta}{4\pi} \left[\nabla \left(\nabla \cdot \bar{B} \right) - \nabla^2 \bar{B} \right], \end{aligned} \right\} (105)$$

after resolution of the triple vector product. The first term on the right-hand side of Eq. (105) vanishes because of Maxwell's equation,

$$\nabla \cdot \bar{B} = 0, \quad (106)$$

so that

$$\nabla \times (\bar{E} + \bar{v} \times \bar{B}) = -\frac{\eta}{4\pi} \nabla^2 \bar{B}. \quad (107)$$

Let us approximate $\nabla^2 \bar{B}$ by \bar{B}/R^2 . Making this substitution in Eq. (107) yields

$$-\nabla \times (\bar{E} + \bar{v} \times \bar{B}) \approx -\frac{\eta}{4\pi} \frac{\bar{B}}{R^2}. \quad (108)$$

The change of magnetic flux through a moving surface whose element of area is $d\bar{S}$, may be easily shown to be¹

$$\frac{d\Phi}{dt} = -\iint \nabla \times (\bar{E} + \bar{v} \times \bar{B}) \cdot d\bar{S}. \quad (109)$$

Substituting for the integrand from Eq. (108) yields

$$\begin{aligned} \frac{d\Phi}{dt} &= \frac{\eta}{4\pi R^2} \iint \bar{B} \cdot d\bar{S} \\ &= \frac{\eta}{4\pi R^2} \Phi. \end{aligned} \quad (110)$$

¹See, e. g., Spitzer, Op. cit., p. 37.

Therefore

$$t = \int dt = \frac{4 \pi R^2}{\eta} \int \frac{d\Phi}{\Phi} = \frac{4 \pi R^2}{\eta} \ln \Phi, \quad (111)$$

so that

$$\Phi = e^{-\frac{\eta}{4 \pi R^2} t} \quad (112)$$

Hence the time constant (e-folding time), τ , is just

$$\tau = \frac{4 \pi R^2}{\eta}. \quad (113)$$

It is interesting to note that, for the same resistivity, Eq. (113) tells us that our 269-cm radius core will dissipate only two-thirds the power of the previously considered 220-cm core.

Let us approximate our plasma (for which, it will be recalled, $\mathcal{D} = 1$) by a Lorentz gas; i. e., a hypothetical fully-ionized ($z = \mathcal{D} = 1$) gas in which the electrons do not interact with each other and all the positive ions are at rest. Since the ions are actually moving with about one-fifteenth the thermal velocity of the electrons, the latter approximation is not excessively erroneous. We can then use the well-known expression for the electrical resistivity of a Lorentz gas,

$$\eta_L = \frac{\pi^{3/2} m_e^{1/2} Z e^2 c^2 \ln \Lambda}{2(2kT)^{3/2}}. \quad (114)$$

In order to arrive at a more accurate expression for the resistivity, the electron-electron collisions must be taken into account.¹ In the present case ($z = \mathcal{D} = 1$), this may be done by dividing η_L by the correction factor 0.582. Eq. (114) then becomes, after collecting constants,

$$\eta = \frac{\eta_L}{0.582} = 6.53 \times 10^{12} \frac{\ln \Lambda}{T^{3/2}}. \quad (115)$$

¹ Although negligible for calculating diffusion effects, collisions of this type are significant in determining η .

Substituting Eq. (115) in Eq. (113) yields

$$\tau = \frac{4 \pi R^2 T^{3/2}}{6.53 \times 10^{12} \ln \Lambda} \quad (116)$$

With $T = 2.5 \times 10^4$ deg K, $R = 269$ cm, and (from Eqs. (28) and (31), with $n_e = 8 \times 10^{17} \text{ cm}^{-3}$) $\ln \Lambda = 4.00$, Eq. (116) becomes

$$\begin{aligned} \tau &= \frac{4 \pi \times 269^2 \times 2.5^{3/2} \times 10^6}{6.53 \times 10^{12} \times 4} \\ &= 0.138 \text{ sec} \end{aligned} \quad (117)$$

Since the time during which the ohmic dissipation occurs is taken to be 230 sec (even though we have assumed the original charge of plasma to be confined only 57.5 sec), it follows that the number of times, N' , which the magnetic energy, E , must be supplied to compensate for the losses in the pulsating plasma is

$$\begin{aligned} N' &= 230/\tau = 230/0.138 \\ &= 1667 \end{aligned} \quad (118)$$

But τ is only the e-folding time and perhaps it would be slightly more accurate (as well as simpler) to take

$$N' \approx 1000 \quad (119)$$

Using Eqs. (91) and (119), and neglecting losses in the coils themselves,¹ we find that the total electrical energy which must be expended in the course of one mission in order to maintain the confining magnetic field against dissipation in the plasma is

¹ These may actually be quite significant, since the heat energy density stored in the solid coil material generally exceeds the energy density stored in the field itself. However, since we are interested here only in order-of-magnitude effects, let us ignore this complication.

$$\begin{aligned}
 E_{\text{tot}} &\approx N'E \approx 10^3 \times 4.50 \times 10^{16} \\
 &= 4.50 \times 10^{19} \text{ erg} \\
 &= 4.50 \times 10^6 \text{ megajoules.}
 \end{aligned}
 \quad \left. \vphantom{\begin{aligned} E_{\text{tot}} &\approx N'E \approx 10^3 \times 4.50 \times 10^{16} \\ &= 4.50 \times 10^{19} \text{ erg} \\ &= 4.50 \times 10^6 \text{ megajoules.} \end{aligned}} \right\} (120)$$

The rate at which this energy must be supplied; i. e., the ohmic-power dissipation of the plasma, is, of course, simply

$$\begin{aligned}
 \frac{dE}{dt} &= \frac{E}{\tau} = \frac{4.50 \times 10^6}{0.138} \\
 &= 3.26 \times 10^{17} \text{ erg sec}^{-1} \\
 &= 32,600 \text{ MW} ,
 \end{aligned}
 \quad \left. \vphantom{\begin{aligned} \frac{dE}{dt} &= \frac{E}{\tau} = \frac{4.50 \times 10^6}{0.138} \\ &= 3.26 \times 10^{17} \text{ erg sec}^{-1} \\ &= 32,600 \text{ MW} , \end{aligned}} \right\} (121)$$

or, in the approximation of Eq. (119)

$$\begin{aligned}
 \frac{dE}{dt} &= \frac{E_{\text{tot}}}{t_b} = \frac{4.50 \times 10^{19}}{230} \\
 &= 1.96 \times 10^{17} \text{ erg sec}^{-1} \\
 &= 19,600 \text{ MW.}
 \end{aligned}
 \quad \left. \vphantom{\begin{aligned} \frac{dE}{dt} &= \frac{E_{\text{tot}}}{t_b} = \frac{4.50 \times 10^{19}}{230} \\ &= 1.96 \times 10^{17} \text{ erg sec}^{-1} \\ &= 19,600 \text{ MW.} \end{aligned}} \right\} (122)$$

We neglect the correction factor ($V_{\text{skin}}/V_{\text{plasma}}$), which is introduced in Eqs. (120) - (122) by the use of a time-varying magnetic field instead of a steady-state field, since the skin thickness becomes appreciably smaller than R only for very high plasma frequencies. Detailed discussion of this point would be premature, because engineering considerations involving inductance problems will undoubtedly set an upper limit on the frequency, while the growth rate of Helmholtz waves at the plasma-propellant interface will set a lower limit.

If it is to propel a spaceship with a thrust of, say, 10^7 -lb at an I_{sp} in the neighborhood of 2000 sec, the plasma-core reactor system must pump hydrogen at a rate of some 2 tons/sec, continuously raising its enthalpy by about 10^5 -cal gm^{-1} . These figures imply a total reactor-power level of the order of 10^6 MW! For a system of such magnitude, the fraction of

reactor-power output which must be employed merely to confine the plasma is of the order of 5 percent, if coil losses are added to the plasma losses given by Eq. (122).

The volume of the core (assumed spherical) is

$$\begin{aligned} V &= 4\pi (269)^3 / 3 = 8.154 \times 10^7 \text{ cm}^3 \\ &= 81.54 \text{ m}^3 \end{aligned} \quad \left. \vphantom{\begin{aligned} V &= 4\pi (269)^3 / 3 = 8.154 \times 10^7 \text{ cm}^3 \\ &= 81.54 \text{ m}^3 \end{aligned}} \right\} (123)$$

Thus we are dealing with a core-power density of about 12.27-KW cm^{-3} , which is rather high by the standards of nuclear reactors currently in operation, but certainly comparable with the power densities contemplated in some of the more advanced fixed-bed reactors proposed for rocket propulsion.

C. Radial Diffusion: Alternative Treatment

As a check on the foregoing calculations, it is worthwhile to derive the diffusion velocity, v_r , by a different (although somewhat cruder) method than that employed in the previous subsection. It will also be intuitively enlightening, in that typical numerical values for several physically significant quantities hitherto not discussed will be presented, as they are needed for calculating v_r .

Simon (Ref. 19) derives the following expression for the diffusion flux or current¹ of plasma particles across the magnetic lines of force:

$$F = n_e v_r = - \frac{D_o}{1+(\omega\tau)^2} \frac{dn_e}{dr} \quad (124)$$

This is nothing but the one-dimensional statement of Fick's law, which governs the diffusion of neutrons in a reactor core, the diffusion of foreign matter in a crystal, and other mathematically analogous phenomena. The coefficient of the negative density gradient is usually referred to simply as the "diffusion coefficient". In Eq. (124), this coefficient is a combination of

¹Since we always restrict plasma diffusion to one dimension, it will be noted that flux and current are synonymous throughout this study.

several factors. τ is defined as the mean time between ion-electron collisions, ω is the electron cyclotron frequency given by

$$\omega = \frac{eB}{m_e c} \quad , \quad (125)$$

and D_0 is the hypothetical diffusion coefficient in the absence of a magnetic field, given by

$$D_0 = \frac{\lambda v_e}{3} \quad , \quad (126)$$

where v_e is the same as $v_e^{(th)}$ in Eq. (67), viz.,

$$v_e = (3kT/m_e)^{1/2} = 1.07 \times 10^8 \text{ cm sec}^{-1} \quad , \quad (127)$$

and λ is the ion-electron collision mean free path, given by

$$\lambda = \frac{1}{n_e \sigma} \quad . \quad (128)$$

Here σ is the usual Coulomb scattering cross section for ion-electron collisions, but multiplied by the correction factor $8 \ln \Lambda$ to account for the multiplicity of long-range collisions relative to the number of close encounters. The predominance of long-range effects, wherein the typical scattering involves the vector sum of numerous minute deflections of a particle as a result of its simultaneous interaction with thousands of other particles, is a peculiar characteristic of all relatively dense plasmas. Thus

$$\sigma = 8 \pi \ln \Lambda \left(\frac{e^2}{3kT} \right)^2 \quad . \quad (129)$$

In the presence of a magnetic field the diffusion coefficient, which is then defined as one-third the mean-square displacement of electron guiding centers divided by the mean time between ion-electron collisions, is

$$D' = \frac{\langle r^2 \rangle}{\tau} = \frac{D_0}{1 + (\omega \tau)^2} \quad , \quad (130)$$

which is just the coefficient of the negative density gradient appearing in Eq. (124).

First, let us evaluate Eq. (129), which is physically just the integrated (omnidirectional) cross section for ion-electron collisions which result in 90-degree deflection of the electron:

$$\begin{aligned} \sigma &= \frac{8\pi \times 4.00 \times 4.8^4 \times 10^{-40}}{9 \times 1.38^2 \times 6.26 \times 10^8} \\ &= 4.99 \times 10^{-14} \text{ cm}^2 \end{aligned} \quad \left. \vphantom{\begin{aligned} \sigma &= \frac{8\pi \times 4.00 \times 4.8^4 \times 10^{-40}}{9 \times 1.38^2 \times 6.26 \times 10^8} \\ &= 4.99 \times 10^{-14} \text{ cm}^2 \end{aligned}} \right\} (131)$$

Considered as a geometric cross section, this value corresponds to an "effective diameter" of 2.52×10^{-7} cm, which is about 10 times the actual diameter of a uranium atom.

The collision mean free path is, from Eq. (128), then

$$\begin{aligned} \lambda &= \frac{1}{8 \times 10^{17} \times 4.99 \times 10^{-14}} \\ &= 2.50 \times 10^{-5} \text{ cm} \end{aligned} \quad \left. \vphantom{\begin{aligned} \lambda &= \frac{1}{8 \times 10^{17} \times 4.99 \times 10^{-14}} \\ &= 2.50 \times 10^{-5} \text{ cm} \end{aligned}} \right\} (132)$$

This implies that, on the average, an ion travels approximately 100 times its effective diameter and 1000 times its physical diameter before colliding with an electron.

The mean time between ion-electron collisions is

$$\begin{aligned} \tau &= \frac{\lambda}{v_e} = \frac{2.50 \times 10^{-5}}{1.07 \times 10^8} \\ &= 2.34 \times 10^{-13} \text{ sec} \end{aligned} \quad \left. \vphantom{\begin{aligned} \tau &= \frac{\lambda}{v_e} = \frac{2.50 \times 10^{-5}}{1.07 \times 10^8} \\ &= 2.34 \times 10^{-13} \text{ sec} \end{aligned}} \right\} (133)$$

This corresponds to a collision frequency

$$\nu_c = 1/\tau = 4.27 \times 10^{12} \text{ sec}^{-1} \quad (134)$$

Substituting the field strength given by Eq. (87) into Eq. (125), we find that the electron cyclotron frequency is

$$\omega = \frac{4.80 \times 10^{-10} \times 1.18 \times 10^5}{9.11 \times 10^{-28} \times 3.00 \times 10^{10}} \quad \left. \vphantom{\omega} \right\} (135)$$

$$= 2.07 \times 10^{12} \text{ sec}^{-1}$$

This implies that the magnetic field corresponding to the particular plasma density in question is not strong in the usual magnetohydrodynamic sense. A strong field is one for which the radius of gyration (Larmor radius), a_L , is less than the collision mean free path, λ . The following equivalent criterion is often used:

$$\frac{\omega}{\nu_c} > 1, \quad (\text{strong field}) \quad , \quad (136)$$

$$\frac{\omega}{\nu_c} < 1, \quad (\text{weak field}) \quad . \quad (137)$$

In the present case

$$\frac{\omega}{\nu_c} = \frac{2.07 \times 10^{12}}{4.27 \times 10^{12}} \quad \left. \vphantom{\frac{\omega}{\nu_c}} \right\} (138)$$

$$= 0.48 \quad ,$$

so that our 118-kilogauss field is indeed a weak one. This may appear rather strange, until it is realized that the plasma with which we are dealing is perhaps 1000 times denser than the most dense plasmas ordinarily treated in astrophysical or thermonuclear work.

Another way of seeing that the field is weak is to compare the magnetic diffusion coefficient, D' , with the nonmagnetic diffusion coefficient, D_0 . According to Eq. (130), this is equivalent to comparing $(\omega\tau)^2$ with unity. But $(\omega\tau)$ is, by Eq. (134), the same as ω/ν_c , so that

$$(\omega\tau)^2 = 0.23 \quad \left. \vphantom{(\omega\tau)^2} \right\} (139)$$

$$< 1 \quad .$$

Hence

$$D' \approx D_o \quad (140)$$

In particular,

$$\begin{aligned} D_o &= \frac{\lambda v_e}{3} = \frac{2.50 \times 10^{-5} \times 1.07 \times 10^8}{3} \\ &= 891.67 \text{ cm}^2 \text{ sec}^{-1} \end{aligned} \quad (141)$$

and

$$D' = 891.67/1.23 = 724.93 \text{ cm}^2 \text{ sec}^{-1} \quad (142)$$

Thus D' is about 19-percent smaller than D_o . Substituting Eq. (38) into Eq. (124) and using Eqs. (130) and (142) yields

$$\begin{aligned} F &= D' n_e / R = 724.93 \times 8 \times 10^{17} / 269 \\ &= 2.16 \times 10^{18} \text{ cm}^{-2} \text{ sec}^{-1} \end{aligned} \quad (143)$$

This corresponds to a radial diffusion velocity

$$v_r = F/n_e = 2.70 \text{ cm sec}^{-1} \quad (144)$$

and a diffusion time

$$\begin{aligned} t_d &= R/v_r = 269/2.70 \\ &= 99.74 \text{ sec} \end{aligned} \quad (145)$$

These compare with the following values obtained by the methods discussed in subsection B:

$$F = 3.74 \times 10^{18} \text{ cm}^{-2} \text{ sec}^{-1} \quad (146)$$

$$v_r = 4.68 \text{ cm sec}^{-1} \quad (147)$$

$$t_d = 57.5 \text{ sec} \quad (148)$$

Thus it is seen that the method of the previous subsection leads to results which, although perhaps more precise, differ from the results obtained by the simpler treatment of the present section by only 42 percent.

In conclusion, it is of interest to evaluate the Debye length, h , in the plasma. According to Eq. (23),

$$\begin{aligned}
 h &= \sqrt{\frac{kT}{4\pi n_e e^2}} \\
 &= \sqrt{\frac{1.38 \times 10^{-16} \times 2.5 \times 10^4}{4\pi \times 8 \times 10^{17} \times 23.07 \times 10^{-20}}} \\
 &= 1.22 \times 10^{-6} \text{ cm} .
 \end{aligned}
 \tag{149}$$

Using Eq. (132), we find that

$$\begin{aligned}
 \frac{\lambda}{h} &= \frac{2.50 \times 10^{-5}}{1.22 \times 10^{-6}} \\
 &= 20.5 .
 \end{aligned}
 \tag{150}$$

This means that, on the average, an electron traverses a distance of some 20 Debye lengths, i. e., 20 times its own "neighborhood", between successive scattering events.

D. Axial Diffusion: Magnetic Mirror Losses

The particle loss rate due to leakage through a magnetic mirror has been calculated by Judd, MacDonald and Rosenbluth (Ref. 20) and others (Ref. 21), starting from the spatially-independent Fokker-Planck equation or from the Boltzmann equation:

$$\frac{\partial f_1}{\partial t} = \int \left(f'_0 f'_1 - f_0 f_1 \right) v \frac{d\sigma}{d\Omega} d\bar{c}_0 , \tag{151}$$

where f is the velocity space-distribution function, $d\sigma/d\Omega$ is the Rutherford differential-scattering cross section, \bar{c}_0 is the velocity vector, and v is the relative velocity of collision. Since the Coulomb

collisions result mainly in small-angle deflections, the integrand, in Eq. (151) may be expanded in terms of vector velocity increments $\delta \bar{c}_0 = \bar{c}'_0 - \bar{c}_0$ and $\delta \bar{c}'_1 = \bar{c}'_1 - \bar{c}_1$. It is then assumed that all particles whose velocity vectors lie within the "cone of escape" in velocity space, which is the coaxial cone defined by

$$\theta < \theta_c \quad , \quad (152)$$

where

$$\theta_c = \arcsin \sqrt{R} \quad , \quad (153)$$

and

$$R \equiv \text{mirror ratio} \equiv B_{\text{max}}/B_0 \quad , \quad (154)$$

are immediately lost from the system.

The criterion for reflection implied by Eqs. (152) - (154); viz., that the angle between the axis and the velocity vector exceed a critical value, θ_c (which depends on the mirror ratio) is an immediate consequence of the adiabatic approximation, in which the magnetic moment is an integral of the motion,¹ and of the conservation of total particle kinetic energy.

The assumption that particles which are scattered into the escape cone disappear from the system is approximately valid only when the collision mean free path is much larger than the linear dimension, L , of the system. In the present case, however, the latter is likely to be of the order of 10^3 cm, while λ , from Eq. (132), is only 2.50×10^{-5} cm. Thus, for the actual system under consideration, back-scattering is all-important; i. e., the average particle which is deflected into the escape cone will be scattered out of it, and perhaps back into it, many times before arriving at the physical boundary of the system where the magnetic mirror is located. In other words, that region of the plasma which is much more than a single mean free path from the end will not "know" what is going on at the end. (See Figure 17).

¹The justification for this approximation will be examined at the end of Subsection E.

We will nevertheless assume immediate loss of all particles which are deflected into the escape cone, as above, but all results obtained from the subsequent analysis must be modified by the factor

$$N_\lambda = \frac{2L}{\lambda} , \quad (155)$$

which is twice the number of mean free paths contained in the system length, as though there were N_λ magnetic bottles laid end to end. The reason for the factor of 2 in Eq. (155) may be seen as follows: Let the initial rate of particle-density decrease be $dn_e/dt = \dot{n}_e$. Now, \dot{n}_e will itself decrease with time, so that in the limit as $t \rightarrow \infty$, i. e., when $n_e = 0$, \dot{n}_e will also vanish. Since the process is linear, it follows that the mean value of \dot{n}_e , during the time when the entire chamber of length L is being emptied, is just

$$\langle \dot{n}_e \rangle = \frac{\dot{n}_e}{2} . \quad (156)$$

Thus the relaxation time is twice what it would be if \dot{n}_e remained at its initial value instead of decreasing.

Returning, then, to the simplified model in which all particles inside the escape cone are considered to have vanished from the system, we see that this assumption is equivalent to the boundary condition

$$f(c^2, \theta) = 0 \quad \text{for } \theta \leq \theta_c . \quad (157)$$

If it is further assumed that f is factorable as follows:

$$f(c^2, \theta, t) = h(c^2, t) g(\cos \theta) \quad (158)$$

and that $g(\cos \theta)$ is nearly isotropic outside the escape cone, one is led to the following expression for the density loss rate:

$$\dot{n}_i = \dot{n}_e = \frac{dn_e}{dt} = -n_e^2 \left[\frac{4\pi}{3} \left(\frac{e^4}{m_i} \right) \left\langle \frac{1}{v} \right\rangle \left\langle \frac{1}{v^2} \right\rangle \ln \Lambda \right] \lambda(R), \quad (159)$$

where $\langle 1/v \rangle$ and $\langle 1/v^2 \rangle$ denote averages of $1/v$ and $1/v^2$, respectively, over a Maxwell-Boltzmann distribution, and $\lambda(R)$ is a function of the mirror ratio, approximated by

$$\lambda(R) \approx \frac{1}{\log_{10} R} \quad (160)$$

Note that the mass appearing in the right-hand side of Eq. (159) is that of an ion, not an electron.

Integrating Eq. (159) and substituting from Eq. (160),

$$\int_{n_e^{(o)}}^{n_e} \frac{dn_e}{n_e^2} = - \frac{4\pi e^4}{3m_i^2} \langle \frac{1}{v} \rangle \langle \frac{1}{v^2} \rangle \frac{\ln \Lambda}{\log_{10} R} \int_0^t dt \quad (161)$$

so that

$$\frac{1}{n_e} - \frac{1}{n_e^{(o)}} = \frac{4\pi e^4}{3m_i^2} \langle \frac{1}{v} \rangle \langle \frac{1}{v^2} \rangle \frac{\ln \Lambda}{\log_{10} R} t \quad (162)$$

Rearranging this expression, and defining a scattering time,

$$\tau_\lambda \equiv \frac{3m_i^2 \log_{10} R}{4\pi e^4 n_e^{(o)} \langle 1/v \rangle \langle 1/v^2 \rangle \ln \Lambda} \quad (163)$$

we can write

$$n_e = \frac{n_e^{(o)} \tau_\lambda}{t + \tau_\lambda} \quad (164)$$

Figure 18 is a plot of Eq. (164), and shows how the particle density falls off with time as a result of mirror losses, assuming there is no replenishment.

Performing the integrations implicit in the Maxwellian averages, we find that

$$\left. \begin{aligned} \left\langle \frac{1}{v} \right\rangle &= \frac{4}{\sqrt{\pi}} \left(\frac{m_i}{2kT} \right)^{3/2} \int_0^{\infty} v e^{-\frac{m_i v^2}{2kT}} dv \\ &= \sqrt{\frac{2m_i}{kT}} \end{aligned} \right\} \quad (165)$$

and

$$\left. \begin{aligned} \left\langle \frac{1}{v^2} \right\rangle &= \frac{4}{\sqrt{\pi}} \left(\frac{m_i}{2kT} \right)^{3/2} \int_0^{\infty} e^{-\frac{m_i v^2}{2kT}} dv \\ &= \frac{m_i}{kT} \end{aligned} \right\} \quad (166)$$

so that

$$\left\langle \frac{1}{v} \right\rangle \left\langle \frac{1}{v^2} \right\rangle = \sqrt{\frac{2}{\pi}} \left(\frac{m_i}{kT} \right)^{3/2} \quad (167)$$

Substituting Eq. (167), in Eq. (159) yields

$$\dot{n}_e = - \frac{4n_e^2 e^4 \ln \Lambda}{3kT \log R} \sqrt{\frac{2\pi}{m_i kT}} \quad (168)$$

where the factor n_e^2 appearing in the right-hand side is now the same as $n_e^{(0)2}$. Similarly, Eq. (163) becomes

$$\tau_\lambda = \frac{3kT \log_{10} R}{4 n_e^{(0)} e^4 \ln \Lambda} \sqrt{\frac{m_1 kT}{2\pi}} \quad (169)$$

Since B_0 is already as high as 117.8 kilogauss, it does not appear reasonable to postulate a mirror ratio greater than about 5.¹ For $R = 5$, $B_{\max} = 589$ kilogauss, which is about one-half the maximum magnetic field intensity ever achieved in the laboratory. Note that the volume over which B_{\max} need exist is very much smaller than the volume where the field is just B_0 . For $R = 5$,

$$\log_{10} R = 0.70. \quad (170)$$

Substituting this value into Eq. (168), we have

$$\begin{aligned} \dot{n}_e &= - \frac{4 \times 64 \times 10^{34} \times 5.32 \times 10^{-38} \times 4.00}{3 \times 1.38 \times 10^{-16} \times 2.5 \times 10^4 \times 0.70} \\ &\quad \times \sqrt{\frac{2\pi}{233 \times 1.67 \times 10^{-24} \times 1.38 \times 10^{-16} \times 2.5 \times 10^4}} \quad (171) \\ &= - 5.14 \times 10^{27} \text{ cm}^{-3} \text{ sec}^{-1}. \end{aligned}$$

In accordance with our earlier remarks, if $L = 10^3$ cm, the rate at which the particle density decreases should be $(N_\lambda)^{-1}$ times the value given in Eq. (171), where

$$\begin{aligned} N_\lambda &= 2 \times 10^3 / 2.50 \times 10^{-5} \\ &= 8 \times 10^7. \end{aligned} \quad (172)$$

¹From Eq. (168), the loss rate is inversely proportional to the logarithm of R . This weak dependence implies that large mirror ratios are simply not worthwhile.

Thus the effective loss rate is

$$\begin{aligned} \dot{n}_e &= 5.14 \times 10^{27} / 8 \times 10^7 \\ &= -6.45 \times 10^{19} \text{ cm}^{-3} \text{ sec}^{-1} . \end{aligned} \quad \left. \vphantom{\begin{aligned} \dot{n}_e &= 5.14 \times 10^{27} / 8 \times 10^7 \\ &= -6.45 \times 10^{19} \text{ cm}^{-3} \text{ sec}^{-1} . \end{aligned}} \right\} (173)$$

Similarly,

$$\begin{aligned} \tau_\lambda &= - \frac{n_e}{\dot{n}_e} = - \frac{8 \times 10^{17}}{-6.45 \times 10^{19}} \\ &= 1.24 \times 10^{-2} \text{ sec.} \end{aligned} \quad \left. \vphantom{\begin{aligned} \tau_\lambda &= - \frac{n_e}{\dot{n}_e} = - \frac{8 \times 10^{17}}{-6.45 \times 10^{19}} \\ &= 1.24 \times 10^{-2} \text{ sec.} \end{aligned}} \right\} (174)$$

Thus, according to Eq. (164), one-half of the original plasma will have escaped through the mirror after only 12.4 milliseconds. This loss rate is clearly intolerable. Eq. (169) tells us that the situation would be improved if $n \equiv n_e^{(0)}$ were decreased or T were increased. The latter is probably impractical for reasons previously mentioned. It should be noted, however, that one of these reasons; viz., the necessity of preventing propellant ionization; loses much of its importance in the present case of axial diffusion through a magnetic mirror relative to the previous case of radial diffusion. The explanation for this lies in the fact that $\tau_\lambda \propto m_i^{1/2}$ (or $\dot{n}_e \propto m_i^{-1/2}$). Hydrogen atoms which were ionized and trapped within the magnetic bottle could only be confined there $233^{-1/2}$ or about one-fifteenth as long as the uranium ions, so that there exists a convenient mechanism for preferentially rejecting the lighter ions in a composite plasma. In spite of this favorable circumstance, wall-cooling problems still may prohibit any further increase in T .

The alternative is almost as unattractive, because the only way to decrease n_e and still maintain reactor criticality is to increase the core volume, which is already very large. A further slight enlargement of the core is conceivable, although severely limited by the concomitant weight increase of the moderator-reflector, by the aggravated fabrication problems, and by the fact that the critical mass would be incremented by an amount δM_c , which is roughly proportional to the increment of a characteristic linear dimension. Because of this last point, n_e varies approximately

as R^{-2} instead of as R^{-3} . Considering the core as a cylinder of volume $\pi R^2 L$, we see that n_e is not significantly reduced by increasing L , although by virtue of Eq. (155) the scattering time, which is just the half-life of a plasma leaking through a magnetic mirror, is proportional to L . On the other hand, τ_λ is proportional to the square of the radius.

Obviously, no reasonable size increase could possibly improve τ_λ by a factor of 10^3 , which is the absolute minimum required for any degree of feasibility; (10^4 would keep mirror leakage to much more manageable proportions). Therefore, it is clear that some alternative method must be found to remedy this axial diffusion problem; otherwise the simple magnetic-bottle type of plasma core reactor must be deemed unsuitable for rocket propulsion. Several possible solutions of this problem can be imagined, but all entail further complication of the system. One of these involves addition of a Stellarator-type "divertor" just outside each magnetic mirror. (See Figure 19). This ingenious device; first proposed by Spitzer (Ref. 22), see also Burnett, et al. (Ref. 23); provides a magnetic trough wherein plasma particles which would otherwise strike the chamber wall are skimmed off before doing so. There are several obstacles to be overcome, however, before such a scheme could be applied in a practical manner. The most serious of these follows from the large uranium-hydrogen macroscopic interaction cross sections (particularly for scattering and charge-exchange) due to the relatively high-density of the hydrogen in the region which a uranium ion must traverse before reaching the divertor.

Perhaps the most promising approach to the problem of improving mirror confinement is to rotate the plasma. This will be discussed in more detail in subsection E, but before doing so, two points should be mentioned:

First, the present analysis has completely neglected ambipolar effects, which result in enhanced diffusion due to the fact that, at thermal equilibrium, electrons diffuse faster than ions (simply because they are moving faster). In order to prevent large space charges from developing, the ions are "dragged along" by the electrons. In principle, ambipolar effects can be minimized by maintaining the electrons at a lower temperature than the ions. This would, incidentally, diminish the radial diffusion. In practice, however, this might be exceedingly difficult to do.

Secondly, as in the radial diffusion case, a "Maxwell's-demon" effect seems to exist. The explanation is twofold: (a) From Eq. (168) it is seen that $\dot{n}_e \propto T^{-3/2}$ so that, just as with radial diffusion, the colder particles tend to escape earliest. (This is another reason, incidentally, for the preferential rejection of hydrogen ions from the magnetic bottle--on the average they would be colder than the uranium ions residing within the bottle). (b) The mean energy of the escaping particles is one-third the mean energy of the confined particles, or one-half kT (Ref. 24). This, of course, is intimately connected with (a), the result of preferential confinement of those particles whose (random) kinetic energy is greater.

E Plasma Rotation

The idea is to superimpose upon the axial and mirror B-fields, an electric field which is everywhere orthogonal to them. This essentially radial-electrical field would result from the maintenance of an electrostatic potential gradient between the wall of the core chamber, (which would then be designated as the outer electrode), and an inner coaxial electrode which need not be of solid material, but could be a plasma itself. The fissioning plasma would occupy the interelectrode volume, and would be electromagnetically pumped by the crossed electric and magnetic fields. The plasma would then tend to rotate on a coaxial surface of revolution in a direction orthogonal to both \vec{B} and \vec{E} . In this way an associated Hall electric field is produced which exactly cancels the externally imposed \vec{E} -field in the plasma frame of reference.

Crudely stated, the centrifugal force associated with plasma rotation serves to keep the plasma from approaching the axis ($\theta < \theta_c$) where, as we have seen, mirror leakage would occur. In principle, it is possible to truncate the escape cone arbitrarily far out in velocity space. This will be clarified in the subsequent analysis.

The geometry of the system is represented in Figure 20. This geometry, which is essentially that of a homopolar motor (the plasma corresponding to the armature), has been studied in conjunction with several thermonuclear projects (Ref. 25-28).

A criterion for confinement may be derived as follows. As before, let m_i , s_i , m_e , and v_e be the masses and velocities of ion and electrons, respectively. For ions, the balance of radial forces may be expressed as

$$\frac{m_i v_i^2}{r} + \frac{v_i e B}{c} + e E = 0, \quad (175)$$

where the first term on the left-hand side is the centrifugal force, the second term is the magnetic force, and the third term is the electric force. Similarly, the balance of radial forces for electrons may be written:

$$\frac{m_e v_e^2}{r} - \frac{v_e e B}{c} - e E = 0. \quad (176)$$

Multiplying both sides of Eqs. (175) and (176) by (r/m_i) and substituting the definitions:

$$v_L \equiv \frac{e B r}{m_i c}, \quad (177)$$

$$v_E \equiv \frac{c E}{B}, \quad (178)$$

we have

$$v_i^2 + v_L v_i + v_L v_E = 0 \quad (179)$$

and

$$(m_e/m_i) v_e^2 - v_L v_e - v_L v_E = 0. \quad (180)$$

v_L is just the Larmor velocity of the ions ($=\omega_i r$), and v_E is the first-order $\bar{E} \times \bar{B}$ drift velocity of both electrons and ions. Eqs. (179) and (180) are quadratic equations in v_i and v_e whose solutions are

$$v_i = \frac{v_L}{2} \left[-1 + \left(1 - 4 \frac{v_E}{v_L} \right)^{1/2} \right], \quad (181)$$

$$v_e = \frac{v_L}{2} \left(\frac{m_i}{m_e} \right) \left[1 - \left(1 + \frac{m_e}{m_i} \frac{v_E}{v_L} \right)^{1/2} \right]. \quad (182)$$

For $v_E/v_L \ll 1$ we can expand the radicals and drop all terms above first-order. In this case

$$v_i \approx v_e \approx v_E = cE/B. \quad (183)$$

Rewriting Eqs. (179) and (180),

$$v_i^2 = -v_L v_i - v_L v_E = -v_L(v_i + v_E), \quad (184)$$

$$\left(\frac{m_e}{m_i} \right) v_e^2 = v_L v_E + v_L v_i = v_L(v_e + v_E). \quad (185)$$

Adding Eqs. (184) and (185), we get

$$v_i^2 + \left(\frac{m_e}{m_i} \right) v_e^2 = v_L(v_e - v_i), \quad (186)$$

so that

$$\left. \begin{aligned} v_i - v_e &= -\frac{1}{v_L} \left(v_i^2 + \frac{m_e}{m_i} v_e^2 \right) \\ &= \frac{m_e c}{e B r} \left(v_i^2 + \frac{m_e}{m_i} v_e^2 \right) \end{aligned} \right\} \quad (187)$$

The azimuthal diamagnetic drift-current density is just

¹For the system which will be considered, this is equivalent to be the condition that the electric field intensity be small compared with about 4000-statvolt cm^{-1} or 1.2×10^6 volt cm^{-1} .

$$j_{\theta} = \frac{n_e e}{c} (v_i - v_e). \quad (188)$$

Substituting Eq. (187) in Eq. (188) yields

$$j_{\theta} = - \frac{n_e m_i}{B r} \left[v_i^2 + \left(\frac{m_e}{m_i} \right) v_e^2 \right]. \quad (189)$$

We can now solve Maxwell's equation:

$$\nabla \times \bar{\mathbf{B}} = 4\pi \bar{\mathbf{j}} + \frac{1}{c} \frac{\partial \bar{\mathbf{E}}}{\partial t}, \quad (190)$$

or, since we are dealing with a steady-state electric field,

$$\nabla \times \bar{\mathbf{B}} = 4\pi \bar{\mathbf{j}}. \quad (191)$$

The only nonvanishing component of curl $\bar{\mathbf{B}}$ is in the azimuthal direction:

$$\left. \begin{aligned} \nabla \times \bar{\mathbf{B}} &= (\nabla \times \bar{\mathbf{B}})_{\theta} = \frac{\partial B_r}{\partial z} - \frac{\partial B_z}{\partial r} \\ &= \frac{\partial B_z}{\partial r}, \end{aligned} \right\} \quad (192)$$

since the magnetic mirrors at the ends are here neglected for the sake of simplicity. Thus, combining Eqs. (191) and (192), we can write

$$- \partial B_z = 4\pi j_{\theta} \partial r, \quad (193)$$

or, since the other components of $\bar{\mathbf{B}}$ and $\bar{\mathbf{j}}$ are assumed to vanish, we can replace the partial differentials in Eq. (193) by total differentials:

$$- dB_z = - dB = 4\pi j_{\theta} dr. \quad (194)$$

Substituting Eq. (183) into Eq. (189) yields

$$j_{\theta} = - \frac{n_e m_i}{Br} \left[\frac{c^2 E^2}{B^2} \left(1 + \frac{m_e}{m_i} \right) \right] \quad (195)$$

Substituting this expression for j_{θ} in Eq. (194) and integrating:

$$- \int_{B(a)}^{B(b)} dB = 4\pi \int_a^b \frac{n_e m_i}{Br} \left[\frac{c^2 E^2}{B^2} \left(1 + \frac{m_e}{m_i} \right) \right] dr \quad (196)$$

or

$$- \int_{B(a)}^{B(b)} B^3 dB = 4\pi n_e m_i c^2 \left(1 + \frac{m_e}{m_i} \right) \int_a^b \frac{E^2}{r} dr. \quad (197)$$

Now the electric-field intensity between coaxial-cylindrical electrodes is given by

$$E \equiv E(r) = \frac{\varphi}{\ln \left(\frac{b}{a} \right)} \frac{1}{r}, \quad (198)$$

where φ is the electrostatic potential difference between the inner electrode at $r = a$ and the outer electrode at $r = b$. Substituting Eq. (198) in the integrand on the right-hand side of Eq. (197) yields

$$\left. \begin{aligned} - \frac{B^4(b)}{4} &= 4\pi n_e m_i c^2 \left(1 + \frac{m_e}{m_i} \right) \int_a^b \frac{\varphi}{\left[\ln \left(\frac{b}{a} \right) \right]^2} \frac{1}{r^3} dr \\ &= \frac{4\pi n_e m_i c^2 \left(1 + \frac{m_e}{m_i} \right) \varphi^2}{\left[\ln (b/a) \right]^2} \left(-\frac{1}{2} \right) \left[r^{-2} \right]_a^b, \end{aligned} \right\} (199)$$

where the magnetic field has been assumed to vanish at the inner electrode, in accordance with the diamagnetism of the plasma. Thus

$$\frac{B^4(b)}{4} = \frac{4\pi n_e m_i c^2 \left(1 + \frac{m_e}{m_i}\right) \varphi^2}{2 \left[\ln(b/a) \right]^2} \left(\frac{b^2 - a^2}{a^2 b^2} \right) \quad (200)$$

or

$$B^4(b) = \frac{8\pi n_e m_i c^2 \left(1 + \frac{m_e}{m_i}\right) \varphi^2}{\left[\ln(b/a) \right]^2} \left(\frac{b^2 - a^2}{a^2 b^2} \right) \quad (201)$$

This can also be written as

$$n_e = \frac{B^4(b)}{8\pi m_i c^2} \left\{ \frac{a^2 b^2}{b^2 - a^2} \left[\ln\left(\frac{b}{a}\right) \right]^2 \right\} \frac{1}{\varphi^2 \left(1 + \frac{m_e}{m_i}\right)} \quad (202)$$

Defining

$$\left. \begin{aligned} \alpha &= \frac{1}{8\pi m_i c^2} \\ &= 0.1136 \text{ gm}^{-1} \text{ sec}^2 \text{ cm}^{-2} \end{aligned} \right\} \quad (203)$$

and

$$Q \equiv \frac{a^2 b^2}{b^2 - a^2} \left[\ln\left(\frac{b}{a}\right) \right]^2 \quad (204)$$

and taking

$$1 + \frac{m_e}{m_i} \approx 1 \quad (205)$$

which is a good approximation, since

$$\frac{m_e}{m_i} < 3 \times 10^{-6} \quad (206)$$

we can write Eq. (202) as

$$n_e = a Q \frac{B^4(b)}{\varphi^2} \quad (207)$$

This is the confinement criterion sought, which relates the particle density to the magnetic-field intensity and the electric potential.

Over the range of inner electrode radii of interest, Q varies by more than three orders of magnitude. It is therefore of interest to examine the behavior of $Q(a)$, where b is a parameter, especially since nucleonic, structural and plasma diffusion considerations will, to a large extent, fix the radius of the outer electrode. Figure 21 plots $Q(a)$ for different values of the parameter b . For any value of b , Q attains a maximum for that value of a , which satisfies the relation:

$$\frac{b}{a} = e^{\frac{b^2 - a^2}{b^2}} \quad (208)$$

This may be seen immediately by setting

$$\frac{\partial Q}{\partial a} = 0 \quad (209)$$

Thus

$$\begin{aligned} \frac{\partial Q}{\partial a} = & \frac{2ab^2}{b^2 - a^2} \left[\ln \left(\frac{b}{a} \right) \right]^2 + \frac{2a^3 b^2}{(b^2 - a^2)^2} \left[\ln \left(\frac{b}{a} \right) \right]^2 \\ & - \frac{a^2 b^2}{b^2 - a^2} \left[2 \ln \left(\frac{b}{a} \right) \right] \frac{1}{a} = 0 \end{aligned} \quad (210)$$

Canceling and rearranging terms, this condition becomes

$$\ln \left(\frac{b}{a} \right) \left[1 + \frac{a^2}{b^2 - a^2} \right] = 1, \quad (211)$$

which is equivalent to Eq. (208). The maximum is found to occur for

$$b \approx 2.22 a; \quad (212)$$

i. e., where the radius of the inner electrode is about 45 percent that of the outer electrode. This maximum value of Q is numerically

$$Q_{\max} = 0.16 b^2. \quad (213)$$

Figure 21 shows, however, that the peak is rather flat, so that not much is lost by going to values of a which are substantially less than optimum, in order not to sacrifice too much interelectrode volume. In particular, let us select as a typically desirable value

$$b/a = 6. \quad (214)$$

We are now in a position to apply several conditions for plasma confinement in a device with homopolar geometry. These conditions take the form of inequalities derived by Anderson et al.¹ to describe the limitations of the Livermore Homopolar Device. The first says that the electric-energy density multiplied by a "mechanical-advantage" factor ($\rho c^2 / 2nkT$), must greatly exceed the thermal-energy density:

$$\frac{E^2(r)}{8\pi} \left(\frac{\rho c^2}{2nkT} \right) \gg nkT, \quad (215)$$

where $E(r)$ is the electric-field intensity, ρ the plasma density, and $n = 2n_e$ is the total particle density of the plasma. Ineq. (215) represents a necessary condition for confinement. The following expression, however, represents a sufficient condition:

$$nkT < \frac{1}{2} \rho \left(\frac{E(v)}{B_1} c \right)^2 \frac{\omega_2}{\omega_1} < < \frac{B_1^2}{8\pi}. \quad (216)$$

¹Op. cit., Eqs. (60)-(62).

Here $B_1 \equiv B_0$ is the magnetic field at $r = R$, in the median region (midway between the mirrors). At the mirrors, this magnetic field is incremented by the magnitude B_2 , so that the resultant field is $B_{\max} = B_1 + B_2$, and the mirror ratio is

$$R = 1 + (B_2/B_1) . \quad (217)$$

In this notation, the angular velocities appearing in Ineq. (216) are

$$\omega_j = \frac{eB_j}{2m_1c} , \quad (j = 1, 2) . \quad (218)$$

Thus

$$\omega_2/\omega_1 = B_2/B_1 . \quad (219)$$

We can therefore write the first part of Ineq. (216) as

$$nkt < \frac{1}{2} \rho \left[\frac{E(r)}{B_1} c \right]^2 \frac{B_2}{B_1} . \quad (220)$$

Essentially, this says that the rotational kinetic-energy density of the plasma must exceed the thermal-energy density. The quantity in brackets will be recognized from Eq. (183) to be the azimuthal $\bar{E} \times \bar{B}$ drift velocity of the plasma.

The second part of Ineq. (216) says that the rotational kinetic-energy density must, in turn, be greatly exceeded by the magnetic-energy density:

$$\frac{1}{2} \rho \left[\frac{E(r)}{B_1} c \right]^2 \frac{B_2}{B_1} \ll \frac{B_1^2}{8\pi} . \quad (221)$$

This condition obtains from considerations of centrifugal force balance and plasma stability.

Let us evaluate Ineq. (215) to see numerically what lower bound it places upon the electric-field intensity and the voltage. We make the following substitutions:

$$\begin{aligned} \rho &= n_i A / N \\ &= 1.93 \times 10^{-4} \text{ gm cm}^{-3} \end{aligned} \quad \left. \vphantom{\begin{aligned} \rho &= n_i A / N \\ &= 1.93 \times 10^{-4} \text{ gm cm}^{-3} \end{aligned}} \right\} (222)$$

where $A = 233 \text{ gm mole}^{-1}$, N is Avogadro's number, and $n_i = n_e = 5 \times 10^{17} \text{ cm}^{-3}$. Also

$$\begin{aligned} nkT &= 2n_e kT = 10^{18} \times 1.38 \times 10^{-16} \times 2.5 \times 10^4 \\ &= 3.45 \times 10^6 \text{ erg cm}^{-3} \end{aligned} \quad \left. \vphantom{\begin{aligned} nkT &= 2n_e kT = 10^{18} \times 1.38 \times 10^{-16} \times 2.5 \times 10^4 \\ &= 3.45 \times 10^6 \text{ erg cm}^{-3} \end{aligned}} \right\} (223)$$

Thus Ineq. (215), which can be written in the form

$$E(r) \gg \frac{4nkT}{c} \sqrt{\frac{\pi}{\rho}} \quad ,$$

becomes

$$E(r) \gg \frac{4 \times 3.45 \times 10^6}{3.00 \times 10^{10}} \sqrt{\frac{\pi}{1.93 \times 10^{-4}}} \quad (224)$$

or

$$E(r) \gg 5.87 \times 10^{-2} \text{ statvolt cm}^{-1} \quad (225)$$

Recalling the upper bound on E established in the footnote on p. 54, we may write the resultant condition as

$$4 \times 10^3 \gg E(r) \gg 5.87 \times 10^{-2} \text{ esu} \quad (226)$$

This is not a particularly difficult condition to satisfy. We may translate it into upper- and lower-bounds on the electrostatic potential difference between the plasma annulus and an electrode by the use of Eqs. (198), and (214). Let b vary between 300 and 500 cm and a vary between 50 and 83.33 cm. Then, if we approximate the radial position of the plasma annulus by the arithmetic mean of the radial coordinates of the two electrodes, it follows that the corresponding values of $r = \langle r \rangle$ vary between 66.67 and 175 cm. Substituting each of these values for r into Eq. (198) yields

¹We will consider here cores of slightly greater radial dimension than the 269-cm core treated previously.

$$E(r) = \frac{\varphi}{1.7918 \times 175} = \frac{\varphi}{313.57} \quad (\text{larger chamber}) \quad (227)$$

and

$$E(r) = \frac{\varphi}{1.7918 \times 66.67} = \frac{\varphi}{119.45} \quad (\text{smaller chamber}) \quad (228)$$

Let us use the more stringent case for each inequality. Thus we substitute from Eq. (228) in the left-hand part of Ineq. (226), and from Eq. (227) in the right-hand part. This enables us to write

$$4.78 \times 10^5 \text{ esu} \gg \varphi \gg 18.41 \text{ esu} \quad (229)$$

or

$$1.43 \times 10^8 \text{ volts} \gg \varphi \gg 5523 \text{ volts.} \quad (230)$$

Let us turn next to Ineq. (220). In order to avoid boundary-layer problems and complications such as supersonic shock waves, we take the rotational drift velocity of the plasma to be simply

$$E(r) \ c/B_1 = 10^6 \text{ cm sec}^{-1} \quad (231)$$

which approximately corresponds to the speed of sound in hydrogen at 10^4 -deg K and 1 atm. The ratio B_2/B_1 will vary typically between 2 and 4. Let us use the former value, since it will result in the more stringent condition. Making the above substitutions, Ineq. (220) becomes

$$3.45 \times 10^6 < \frac{1}{2} \times 1.93 \times 10^{-4} \times 10^{12} \times 2 \quad ,$$

or

$$3.45 \times 10^6 < 1.93 \times 10^8 \quad , \quad (232)$$

so we see that the condition is indeed satisfied.

Finally, we consider Ineq. (221). This says that

$$B_1^2 \gg 8\pi \times 1.93 \times 10^8$$

or

$$B_1^2 \gg 48.60 \times 10^8 \text{ gauss}^2 \quad . \quad (233)$$

If we relax the \gg sign to $>$, upon taking the square root of both sides, we obtain the condition

$$B_1 > 69.7 \text{ kilogauss} . \quad (234)$$

This completes the limiting conditions which govern homopolar confinement.

Figures 22 and 23 summarize the juxtaposition of the foregoing inequalities with the confinement criterion expressed by Eq. (207). The intersection of the "forbidden zones" in these figures defines a parallelogram-shaped region, within which the corresponding values of system parameters are at least theoretically compatible (if not practically feasible). Within this region a smaller parallelogram has been inscribed with dotted lines. This area represents the preferred regime of operation, where the azimuthal drift velocity of the plasma exceeds 5×10^5 cm sec⁻¹, and B_1 does not exceed 150 kilogauss. A typical set of values might be selected as follows:

$$\left. \begin{aligned} B_1 &= 100 \text{ kilogauss} \\ \varphi &= 180 \text{ kilovolts} \\ v_i &= v_e = 5 \times 10^5 \text{ cm sec}^{-1} \\ n_e &= 5 \times 10^{17} \text{ cm}^{-3} \\ b &= 400 \text{ cm} \\ a &= 66.7 \text{ cm} \end{aligned} \right\} (235)$$

The most severe problems affecting such a system are those associated with the maintenance of a 180-kilovolt potential drop within the core; that B_1 be of the order of 100 kilogauss and the mirror field be upwards of 200 kilogauss; and, of course, the heat transfer problems endemic to all high-temperature propulsion devices. There is no reason to believe, however, that some system resembling that characterized by Eq. (235) could not eventually be built. Let us then examine the question of what has been "bought" by discarding a simple magnetic bottle in favor of a homopolar scheme with its concomitant complication and strong electrostatic field. In particular, how has the problem of axial confinement (in the face of mirror leakage) been alleviated?

The well-known reflection criterion for a simple magnetic mirror is

$$\mu B_{\max} > W \quad , \quad (236)$$

where $B_{\max} = B_1 + B_2$ is the field intensity at the mirror, W is the total particle kinetic energy, and μ is the magnetic moment, which is defined as the ratio of rotational kinetic energy to magnetic field intensity:

$$\mu \equiv \frac{W_{\perp}}{B} = \frac{m_i v_{\perp}^2}{2B} \quad , \quad (237)$$

where W_{\perp} and v_{\perp} are the components of the particle's kinetic energy and velocity, respectively, perpendicular to the mirror axis. Using Eq. (237), we can write Ineq. (236) as

$$\frac{W}{W_{\perp}} < R \quad , \quad (238)$$

where R is the mirror ratio, B_{\max}/B_1 , and all energies and velocities are referred to the median or B_1 region of the magnetic bottle (i. e., midway between the mirrors at $z = L/2$). Writing

$$W = W_{\perp} + W_{\parallel} \quad , \quad (239)$$

where W_{\parallel} is the component of kinetic energy parallel to the mirror axis, we can put Ineq. (238) into the form

$$W_{\parallel} < W_{\perp} (R - 1) \quad . \quad (240)$$

For a magnetic bottle within which the plasma rotates, such as in the present homopolar geometry, it is easy to show that the condition which corresponds to Ineq. (240) is

$$W_{\parallel} < W_{\perp} (R-1) + \frac{1}{2} m_i v_E^2 \left(\frac{R-1}{R} \right) \quad , \quad (241)$$

where $v_E = v_i = v_e$ is the $\bar{E} \times \bar{B}$ drift velocity given by Eq. (183). Ineq. (241) says that those particles are confined whose parallel component of kinetic energy is less than the sum of the two terms on the right-hand side. The first of these terms is identical with the right-hand side of Ineq. (240), so that the second term represents what has been gained in plasma confinement by resorting to $\bar{E} \times \bar{B}$ drift. Let us see what this gain would be for a typical system. With

$$v_{\perp} = \sqrt{\frac{8kT}{\pi m_i}} \quad (242)$$

and

$$W_{\perp} = \frac{1}{2} m_i v_{\perp}^2 = 4 k T / \pi \quad (243)$$

and with $R = 2$, the right-hand side of Ineq. (240) becomes

$$\left. \begin{aligned} W_{\perp} (R-1) &= \frac{8kT}{\pi} \\ &= \frac{8 \times 1.38 \times 10^{-16} \times 2.5 \times 10^4}{\pi} \\ &= 8.79 \times 10^{-12} \text{ erg} . \end{aligned} \right\} (244)$$

On the other hand, for $v_E = 10^6 \text{ cm sec}^{-1}$, the right-hand side of Ineq. (241) becomes

$$\left. \begin{aligned} W_{\perp} (R-1) + \frac{1}{2} m_i v_E^2 \left(\frac{R-1}{R} \right) \\ &= 8.79 \times 10^{-12} + \frac{233 \times 1.67 \times 10^{-24} \times 10^{12}}{4} \\ &= (8.79 + 97.28) \times 10^{-12} \\ &= 106.07 \times 10^{-12} \text{ erg} . \end{aligned} \right\} (245)$$

This is some 12 times the value in Eq. (244). If v_E were chosen as $5 \times 10^5 \text{ cm sec}^{-1}$, the homopolar contribution to the rotational kinetic energy would be only 25 percent of the value given in Eq. (245), and the combined thermal- and drift-rotational kinetic energy components would be only about 3.8 times the thermal component alone (nonrotating plasma). Although this is still a significant improvement, rotating the plasma loses much of its appeal when v_E gets much less than $5 \times 10^5 \text{ cm sec}^{-1}$. That is why the preferred region in Figures 22 and 23 (dashed parallelogram) is bounded on the left-hand side by this velocity.

In passing, it might be mentioned that homopolar confinement has been found experimentally, both at Los Alamos¹ and at Livermore,² to

¹Anderson et al., op. cit.

²Boyer et al., op. cit.

result in a relatively high degree of plasma stability.

A further advantage of the present scheme follows from the greater number of reactor control mechanisms, which are naturally afforded, compared with the simple magnetic bottle. Some of the more obvious methods for controlling the multiplication constant of a rotating plasma-core reactor of the type, discussed above are:

1. Variation of the constituency (poison, fuel and moderator) of the plasma inner electrode.
2. Doping of the hydrogen propellant with material of appropriately variable constituency.
3. Variation of the mirror separation, L , by axial motion of one or both mirrors.
4. Variation of the plasma re-injection rate.
5. Variation of the intensity of the axial magnetic field.
6. Variation of the mirror ratio.
7. Variation of the electric field intensity.

It will be noted that methods 1 and 7 are peculiar to homopolar geometry. Methods 5 - 7, being electromagnetic in nature, are particularly attractive because the relatively fast response-times characteristics of electromagnetic controls make them amenable to an electronic negative-feedback system.

In concluding this analysis of plasma motion and diffusion, it is worthwhile to check the adiabaticity of the plasma under the conditions repeatedly employed above. All previous calculations have implicitly assumed that the usual adiabatic approximations are valid and, in particular, that the magnetic moment is an integral of the motion. Post (Ref. 29) gives the following useful criterion for adiabaticity in mirror machines:

$$\frac{2\pi a_L}{L} < 0.2 , \quad (246)$$

where a_L is the Larmor radius (radius of gyration) of an ion, given by

$$a_L = \frac{m_i c v_{\perp}}{eB} = \frac{m_i c}{eB} \sqrt{\frac{8kT}{\pi m_i}} \quad (247)$$

Substituting Eq. (247) into Ineq. (246), and taking B to be 10^5 gauss and L to be 400 cm (which is the smallest value which can be contemplated for an actual device) we find

$$\begin{aligned} \frac{2\pi a_L}{L} &= \frac{2\pi m_i c}{eBL} \sqrt{\frac{8kT}{\pi m_i}} \\ &= \frac{2\pi \times 233 \times 1.67 \times 10^{-24} \times 3 \times 10^{10}}{4.8 \times 10^{-10} \times 10^5 \times 400} \\ &\quad \times \sqrt{\frac{8 \times 1.38 \times 10^{-16} \times 2.5 \times 10^4}{\pi \times 233 \times 1.67 \times 10^{-24}}} \\ &= 5.74 \times 10^{-4} \end{aligned} \quad (248)$$

This is some 348 times smaller than 0.2, so that μ is indeed constant to very high order over the course of a single cyclotron orbit.

SECTION IV

GENERAL DISCUSSION

Let us briefly recapitulate what has thus far been determined about the characteristics of a plasma core reactor, and attempt to indicate the areas of uncertainty or technical lacunae, and the direction indicated for further research.

From a strictly nuclear point of view, it is quite feasible to construct a critical plasma core of reasonable dimensions and fuel inventory. It is found, however, that the core must be greatly enlarged beyond its theoretically minimum size for non-nuclear reasons. In addition to the necessity of enlarging the core dimensions in order to minimize plasma diffusion processes (which has already been discussed in some detail), there is also the need for maximizing the optical depth of the hydrogen layer, which has not been considered quantitatively in this paper. Another reason for enlarging the core stems from our initial constraint upon the system variables requiring that we end up with a high-acceleration vehicle. This implies thrust levels upwards of 10^7 lb and, therefore, propellant flow rates at least of the order of several tons per second. In order to pump hydrogen longitudinally across the core at such rates without resorting to excessive axial velocities (which have the effect of aggravating Helmholtz instabilities), it is clear that the cross-sectional area of the hydrogen annulus coaxial with the plasma must be rather large.

Although we have Maxwellianized Safonov's nucleonic calculations, thereby accounting for the possibility of steady-state moderator-reflector kinetic temperatures significantly above 0.0253 ev, the results are nevertheless crude. The principal simplification, which must be removed by more detailed calculation in the future, is the omission of hydrogen in the core and, more significantly, the neglect of the fuel void represented by the hydrogen. There exists some indication (based on machine computations at Los Alamos with the "S_n" code of the criticality of an assembly consisting of Godiva surrounded by a reflector-enclosed void) that the void occupied by propellant will not be as detrimental to criticality as had been

previously anticipated, provided certain very definite relationships between plasma radius and distance to the inner reflector wall are maintained.

In addition to a careful neutronic analysis of the plasma-core system using one of the appropriate machine codes, a quantitative investigation of reactor kinetics is also indicated for the future. As we have seen, the plasma state of the fissionable material in some ways actually simplifies the potentially serious problem of control. This is because the existence of electromagnetic fields augments the multiplicity of available control mechanisms which are naturally suited to a gas-phase cavity reactor. Moreover, while magnetic field fluctuation does not promise instantaneous control (due to inductance problems), it may easily afford much faster response times than would be possible with any mechanical system; and in the homopolar scheme, electric field fluctuation appears most promising of all.

Nucleonic calculations have effectively fixed the plasma particle densities required for criticality at $10^{17} - 10^{18} \text{ cm}^{-3}$. Although U-233 was consistently assumed to be the fuel in the subsequent (plasma physics) numerical calculations, Figures 3-11 show that results remain substantially the same if U-235 or plutonium are used instead. Indeed, although the former appears slightly more favorable from theoretical considerations, the latter two are more likely candidates from the viewpoint of net fuel cost. Particle densities much below 10^{17} cm^{-3} imply impractically large core volumes, while values much above 10^{18} cm^{-3} tend to be too difficult to confine for a sufficient period of time, and appear nucleonically unnecessary. The next step, then, is to graft onto these nuclear requirements a framework of restrictions which are imposed by considerations of plasma physics -- particularly diffusion phenomena.

Our analysis has shown that, at the price of enormous field strength and physical dimension, it is possible to sufficiently ameliorate the radial diffusion losses. Axial (mirror) losses, however, pose a more serious problem; one which demands further complication of the system in order to cope with it. One is thus led to consider solutions which almost present more problems than they solve, such as the addition of gadgetry like the divertor, or rotation of the plasma. The latter approach, however, holds great interest, in spite of its problems, and lends itself (conceptually) to a

variety of field configurations and propellant flow geometries. One of the more promising of these schemes is the homopolar field arrangement where the inner electrode is a plasma. For this reason, and for the sake of concreteness within the confines of a study of such limited scope as this, the latter has been selected for detailed investigation. In particular, of the two propellant-flow geometries which appear natural for a crossed-field cylindrical device (radial flow through the rotating plasma annulus and axial flow along it), only the latter is expected to lead to a high-thrust device, for reasons which will become apparent from the following discussion.

Let us consider the former flow pattern. It is clear that, a homopolar arrangement where the dominant propellant flow is radially inward (if limited to the same subsonic propellant velocities as in the hydrodynamically-driven free vortex) would be inferior to the latter for the following reasons:

1. The free-vortex device does not require heavy field-generating and heat-rejection paraphernalia.
2. The magnetohydrodynamic device cannot expel hydrogen at temperatures much above 12,000-deg K, whereas the hydrodynamic device is not necessarily limited by ionization phenomena (although it is probably limited by problems of fission-fragment heating).
3. The greater the magnitude of the axial magnetic-field intensity in the homopolar device, the further the maximum allowable radial inward flow of hydrogen is depressed below its free-vortex value (for the same Mach number in both cases).

The latter parenthetical qualification gives an indication as to why, in the face of the foregoing objections, one might nevertheless be interested in a homopolar device in which the propellant is forced radially through the plasma from a peripheral-injection region to an axial-expulsion region. The maximum radial flow rate of propellant which can be tolerated without collapsing the plasma is proportional to the square of the vortex Mach number and, at least conceptually, it is much easier to accelerate a plasma to great supersonic velocities by electromagnetic means than it is to accelerate a non-ionized gas by means of fluid jets. It is this second-power

velocity dependence which makes supersonic rotational velocities attractive, but there are several serious drawbacks. First, there are the boundary-layer and shock-wave problems associated with such velocities. Although supersonic velocities are not absolutely necessary for a homopolar device with axial propellant flow, such as treated analytically in subsection E of Section III, as they are for a radial flow device, they would nevertheless be advantageous for stabilizing the plasma against Helmholtz waves and axial erosion. In subsection E, however, the maximum rotational velocity was taken to be 10^6 -cm sec⁻¹ (i. e., Mach 1 for hydrogen), precisely in order to avoid supersonic flow problems. This option is not available for a radial flow device, so supersonic problems must be faced.

Even more serious is the problem of the electrical power which is wasted in rotating the hydrogen. This problem arises in the following manner. In a radial-flow homopolar device, the propellant would be forced through the material wall of the chamber which comprises the moderator-reflector (thereby cooling the latter by transpiration). The propellant would then find itself confronting the rapidly rotating plasma annulus (through which it would proceed to diffuse) until it emerged on the other side into the interior void encompassing the cylindrical axis of the core -- from which region it would be axially exhausted through a nozzle. In the process of traversing the plasma, it is clear that the propellant must, of necessity, achieve a tangential velocity comparable with that of the rotating plasma driving it, because at the relatively high densities of both plasma and propellant the interaction cross sections are extremely large. The difficulty lies in the fact that the rotating propellant, when finally expelled, carries off a substantial quantity of energy with it. If the propellant attains a rotational velocity of only Mach 1, for example, while its flow rate is, say, two-metric tons per second, the power dissipated in "corkscrewing" the hydrogen out the nozzle is of the order of 100,000 MW! Moreover, this power must be supplied electrically, because the plasma drift is maintained by work done on it by the electric and magnetic fields. In order to estimate how much core power is thus wasted, this electrical energy must, therefore, be multiplied by the reciprocal of an overall efficiency factor governing the conversion of nuclear energy in the core into electrical energy in the fields. The extra coil weight, not to mention heat-rejection problems due to energy

conversion efficiencies a good deal less than unity (which are associated with the power dissipation by this mechanism alone) are obviously intolerable.

One method, which might be employed to recover some fraction of the rotational kinetic energy of the propellant, may be described as follows: A profile of propellant azimuthal velocity will exist between the inner- and outer-boundaries of the plasma annulus. The propellant will have minimum azimuthal velocity at the outer interface (which would equal zero in the absence of hydrogen viscosity), and will achieve its maximum rotational velocity near the inner boundary where it emerges in the course of its inward radial flow. If the plasma were periodically compressed and expanded by means of periodic fluctuations in the intensities of the confining fields, the result would be that, after plasma compression, each region of hydrogen bounded by the surfaces of revolution at r_1 and $r_1 + dr_1$ would find itself immersed in a region of plasma, formerly located at $r_2 (>r_1)$, whose rotational kinetic energy is now less, instead of more, than that of the hydrogen itself. The latter would thus tend to drive the plasma, imparting kinetic energy to it in the process, and losing some of its own rotational energy (which is directed energy, not heat). As the plasma expands, it does work against the confining magnetic field, which may be tapped off the external coils as electrical energy. The mechanism, therefore, is to convert the mechanical energy of the non-ionized gas into mechanical energy of the plasma, and then to convert the latter directly into electricity.

It is evident that the need for detailed analysis of the foregoing proposal is indicated. Should results show the scheme to be impractical, or of inadequate efficiency, it is conceivable that some other way might be found of recovering the power spent in uselessly spinning the propellant.

Thus we see that a radial flow homopolar device in which the plasma rotates subsonically would not only result in a low-acceleration propulsion system, but also one which could not compete favorably with a free-vortex system. High (vehicle) acceleration could be achieved with a radial flow homopolar system only by resorting to supersonic velocities which, in turn, engender very formidable difficulties. These considerations appear to justify the preference of an axial propellant flow scheme where the plasma need not rotate supersonically. This is why the latter type has been studied in some detail in subsection E, even though a radial flow scheme seems to

afford superior heat transfer properties such as high propellant-outlet temperatures. The axial flow pattern appears to be the one most adaptable to the enormous propellant flow rates necessary for high-acceleration propulsion -- rates which even a matrix of thousands of parallel free vortices could not accommodate.

In passing, it is interesting to note that, should it indeed prove feasible to have $V_E = 10^7$ cm sec⁻¹ (about Mach 10), the right-hand side of Ineq. (241) would be 9.7×10^{-9} erg, which is some 1,100 times the value of the right-hand side of Ineq. (240). In such a case, the axial-diffusion problem, characteristic of the simple magnetic bottle, will have been essentially solved by rotating the plasma.

Next, we come to some of the most formidable problem areas of all. These have not been treated here, but could well comprise the subject-matter of additional papers. The first of these areas concerns plasma instability. Perhaps the greatest source of instability in the simple magnetic bottle, and in the axial-flow homopolar device, will prove to be Helmholtz waves generated at the plasma-propellant interface because of the relative motion of the gasses. Other instabilities, such as those of the flute, kink- and sausage-types, must also be investigated. Furthermore, it is necessary that an analysis be made of the assorted types of oscillations to which plasma cores of several configurations would be susceptible, and the methods for damping them.

The remaining problem area is probably the most crucial of all. The central question within this area is: Given a hot ionized gas, which is itself a heat source, and given a region of non-ionized gas (such as hydrogen), whose function is to absorb radiant energy and which is situated between the hot source and a physical wall enclosing the entire cavity, what is the temperature profile throughout the absorber as a function of its thickness? This would appear to be a trivial problem of applying the Stefan-Boltzmann law, except for a number of serious complications. First, the absorptivities and emissivities of hydrogen, and particularly of uranium, at the temperatures and pressures of interest, are not well known. To calculate these quantities theoretically as functions of temperature, well

into the range of ionization, is a problem of great magnitude and complexity. Experimental measurements would appear to be highly desirable for direct empirical use and also as checks for any theoretical analysis. Since the radiation properties of various fissionable materials at extreme temperatures represent unknown factors shared by all truly advanced (i.e., post-Rover) controlled nuclear rockets, it follows that a broad experimental program directed toward measurement of these and related properties would be of great interest for large classes of systems in addition to those discussed here.

Another factor complicating theoretical analysis of the heat transfer properties of a plasma core reactor with longitudinal propellant flow is the radial distribution function for plasma particles in configuration space. In practice, fuel ions will be distributed in the steady-state throughout the hydrogen, falling off from maximum density at the interface to some minimum value at the wall, according to a law which will depend upon the field geometry and other factors. These fuel ions, while diffusing out of the core and therefore constituting an undesirable economic loss, also constitute a doping of the relatively transparent hydrogen by particles which are much more opaque to the incident radiation, thereby enormously alleviating the wall-cooling problem. Indeed, the possibility exists of further doping the hydrogen with a good radiation absorber having suitable nuclear properties (low atomic mass, poor neutron absorber). All these points introduce the tantalizing hope of solving the all-important problem of maintaining the wall temperature within manageable bounds, but vastly complicate the analysis.

Further complications of the heat-transfer problem involve taking into account (1) the absorption by plasma particles of radiation emitted by other plasma particles, (2) hydrogen re-emission, (3) effects of wall impurities dislodged into the chamber interior, and a host of other factors.

In addition to the foregoing, several ancillary, but nevertheless significant problems exist within the area of heat transfer. One of these involves the quantitative determination of the relative importance of conduction and convection processes compared with thermal radiation. While the latter is likely to be the dominant mode of heat transfer at the high core temperatures envisaged, it is of interest to make detailed calculations of the other

processes for purposes of comparison. Another problem is that of fission fragment heating. By far the largest fraction of usable energy produced by fission reactions within the core appears in the form of kinetic energy of pairs of fission fragments whose charge-to-mass ratios greatly exceed that for singly ionized uranium. These fragments quickly dissipate their energy by an assortment of interactions with the surrounding matter. In the process, the latter gets somewhat ionized and, of course, heats up. The range of these fragments in hydrogen at the densities of interest is such that any optically sufficient thickness would probably also suffice to stop them. Difficulties arise, however, if one tries to imagine a rotating plasma scheme where centrifugal force throws the fuel ions out to the wall, with only a minimal thickness of hydrogen intervening. In this case, which is typical of the hydrodynamic vortex scheme, a fraction approaching one-half of the fission energy is dissipated inside the wall -- an intolerable situation for any device attempting to achieve temperatures more than twice that possible in solid-core reactors.

It is interesting to note that, should the heat-transfer problem (that is to say, the aggregate of all the foregoing heat-transfer difficulties) prove, that in the final analysis, to be tractable, it would be tempting to reconsider a possibility which has been rejected a priori; viz., to allow the plasma temperature to greatly exceed 25,000-deg K, and to hold the average propellant temperature constant by increasing its flow rate by the necessary amount. The obvious drawback would be the creation of a layer of propellant (of indeterminate depth) in the immediate vicinity of the plasma interface which is ionized. The advantage in terms of decreased plasma radius or increased confinement time (or both), however, is equally obvious.

If the foregoing problems appear formidable, it should be apparent that they are far from exhaustive. To cite several further areas requiring attention, there is the problem of maintaining, without breakdown, very intense electrical fields between a solid (or liquid film) electrode and a plasma electrode, while another plasma occupies the intervening region. Also, the problems of coil construction and plasma particle-dynamics in the face of strong pulsating magnetic fields of different geometries bear close scrutiny. For that matter, the strictly hardware problem of generating a 100-kilogauss steady-state field with lightweight equipment itself represents a major project.

A further area of investigation of potential interest concerns the possibility of loading the moderator-reflector with fuel, thereby decreasing the particle density of the plasma which must be magnetically confined for criticality. It is clear that order-of-magnitude decreases in core density are impractical because the fission power density is directly proportional to the fuel density. However, even a factor-of-two core density decrease, achieved by depositing half the fuel inventory within the moderator cladding, would be welcome indeed. The maximum practical moderator loading will very likely be the largest value for which the fission heat generated may be removed entirely by heat exchange to the propellant; i.e., the value beyond which preheating the propellant can no longer cope with the heat transfer requirements and heavy radiators become necessary.

SECTION V

CONCLUSIONS

The above discussion gives some indication of the extremely limited scope of the present treatment of the plasma core reactor relative to the bewildering variety of problems which beset this concept. We have, however, been able to establish some upper- and lower-bounds within which the values of the principal variables of any working system must lie. The factors governing these limitations are summarized in Table III.

The very existence of such a large number of constraints serves to emphasize, not only the intrinsic difficulties which a plasma-core reactor system possesses, but also the many directions from which help is possible. A breakthrough in any of these directions could significantly alter the prognosis.

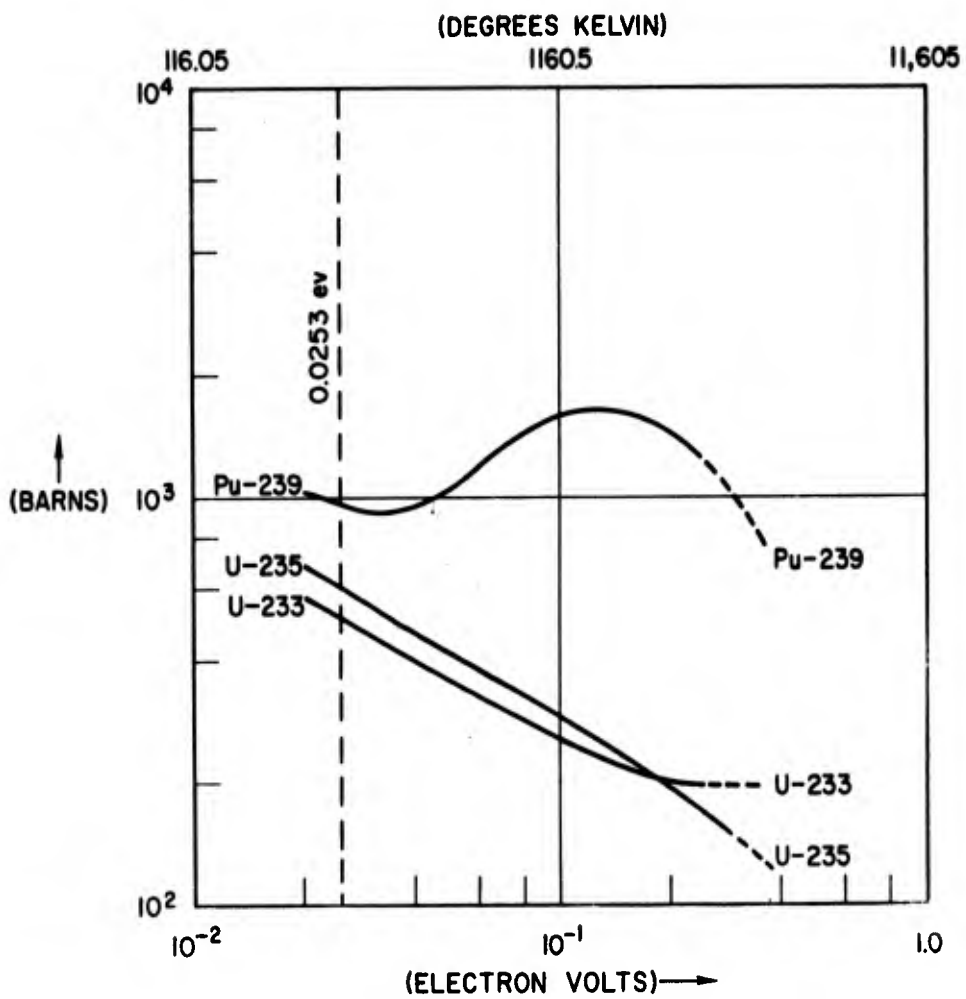


Figure 1 - $\langle \sigma_a \rangle$ vs Neutron Energy

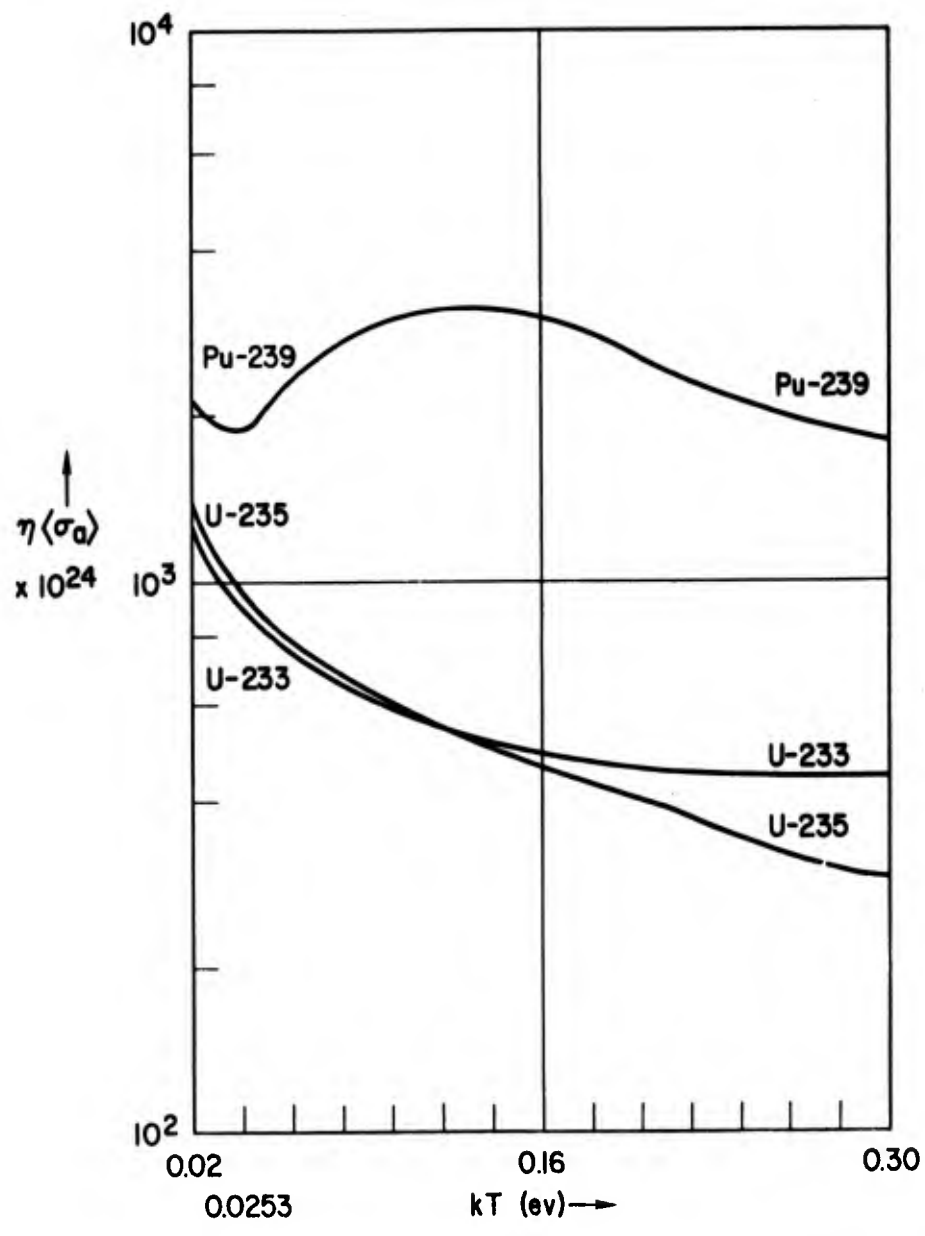


Figure 2 - $\eta \langle \sigma_a \rangle$ vs Neutron Energy

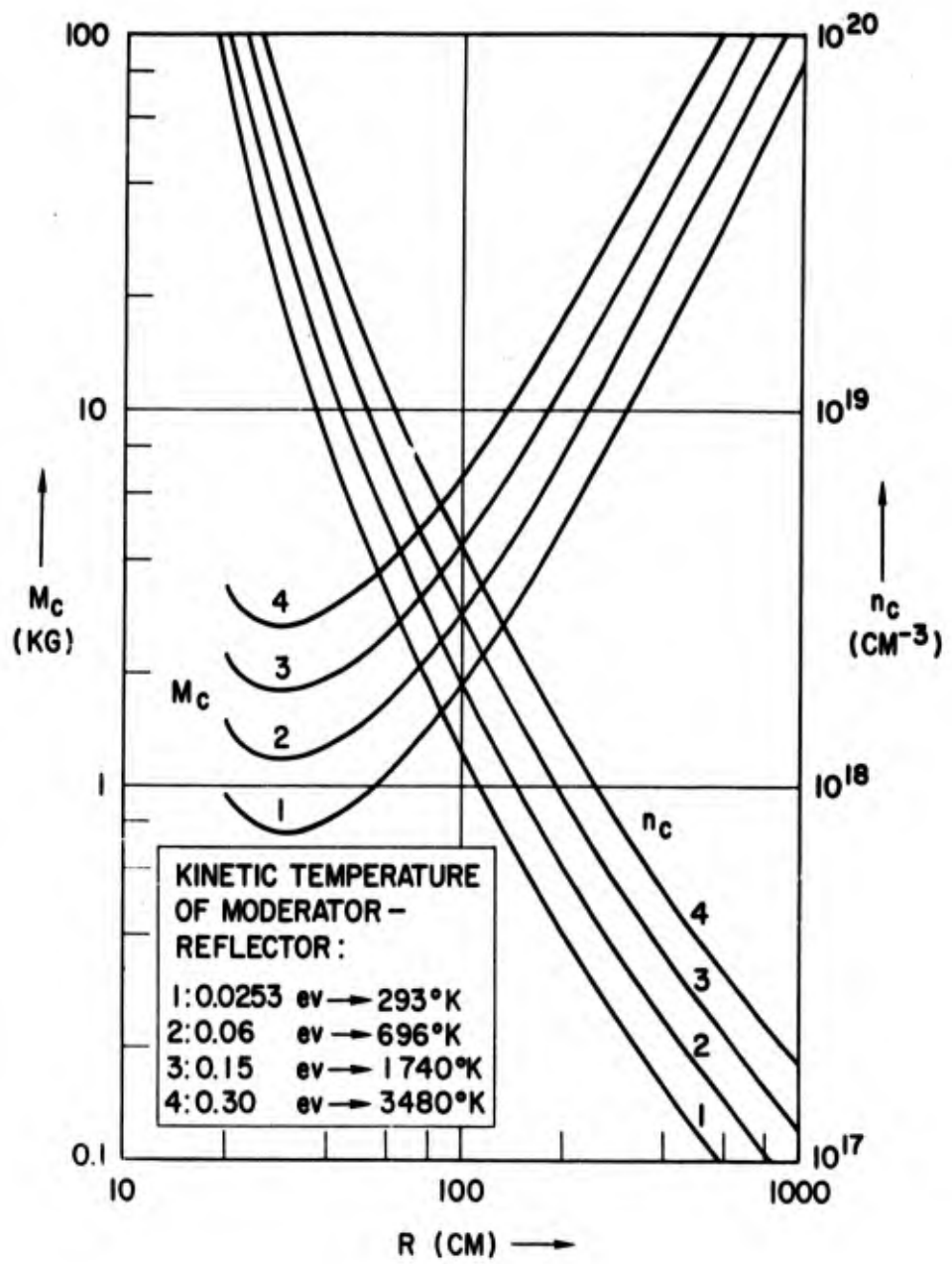


Figure 3 - Critical Mass and Particle Density vs Radius for U-233/D₂O

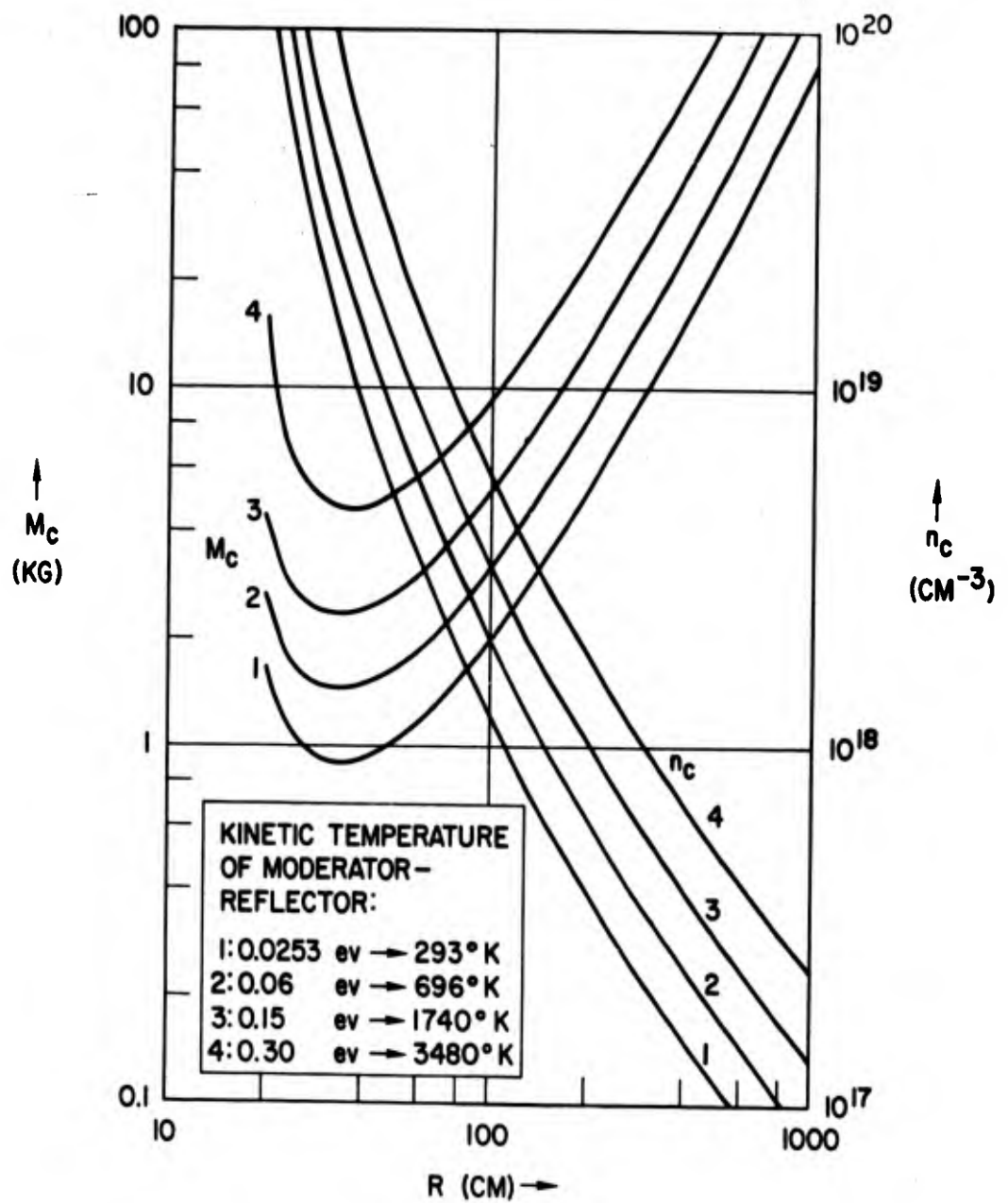


Figure 4 - Critical Mass and Particle Density vs Radius for U-235/D₂O

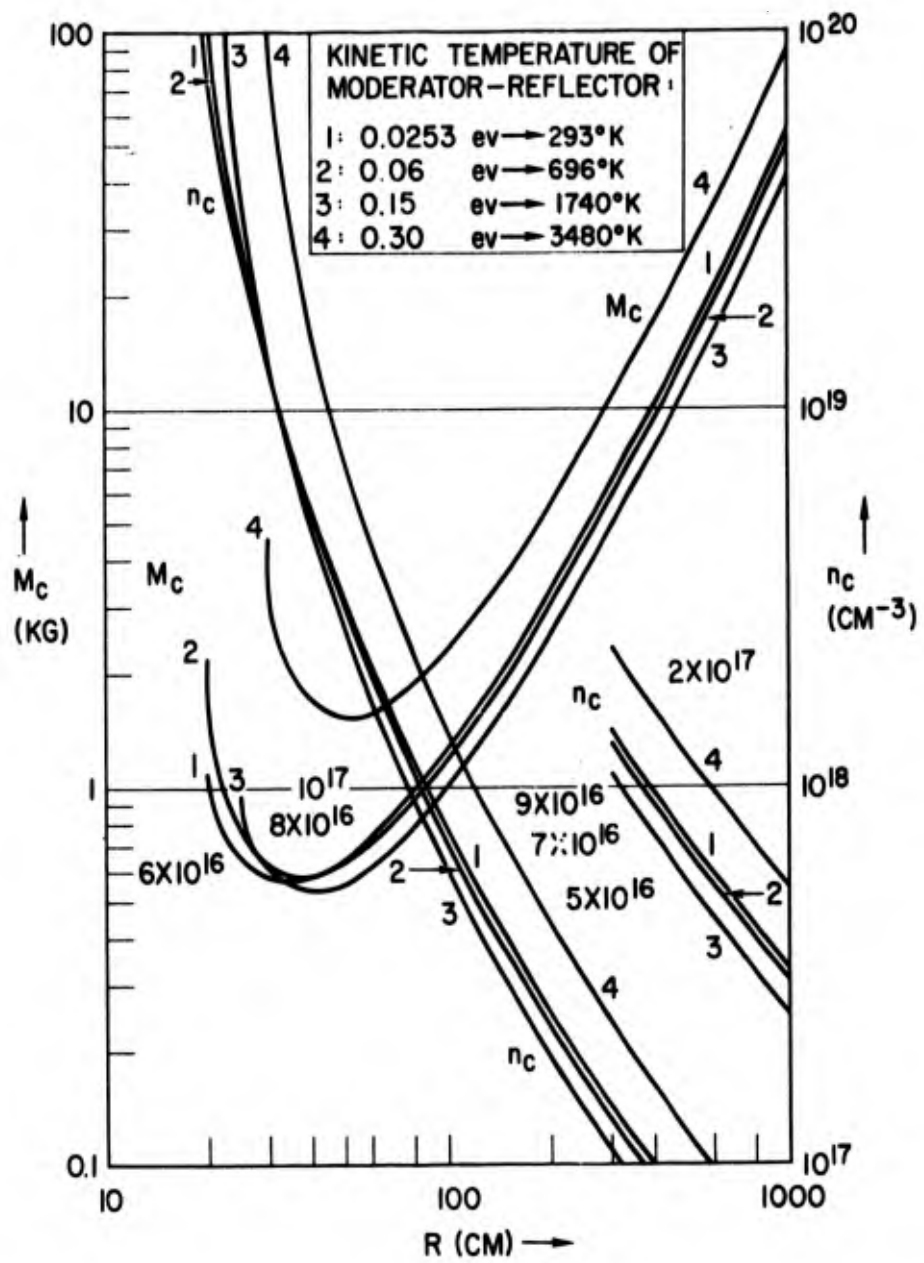


Figure 5 - Critical Mass and Particle Density vs Radius for Pu-239/D₂O

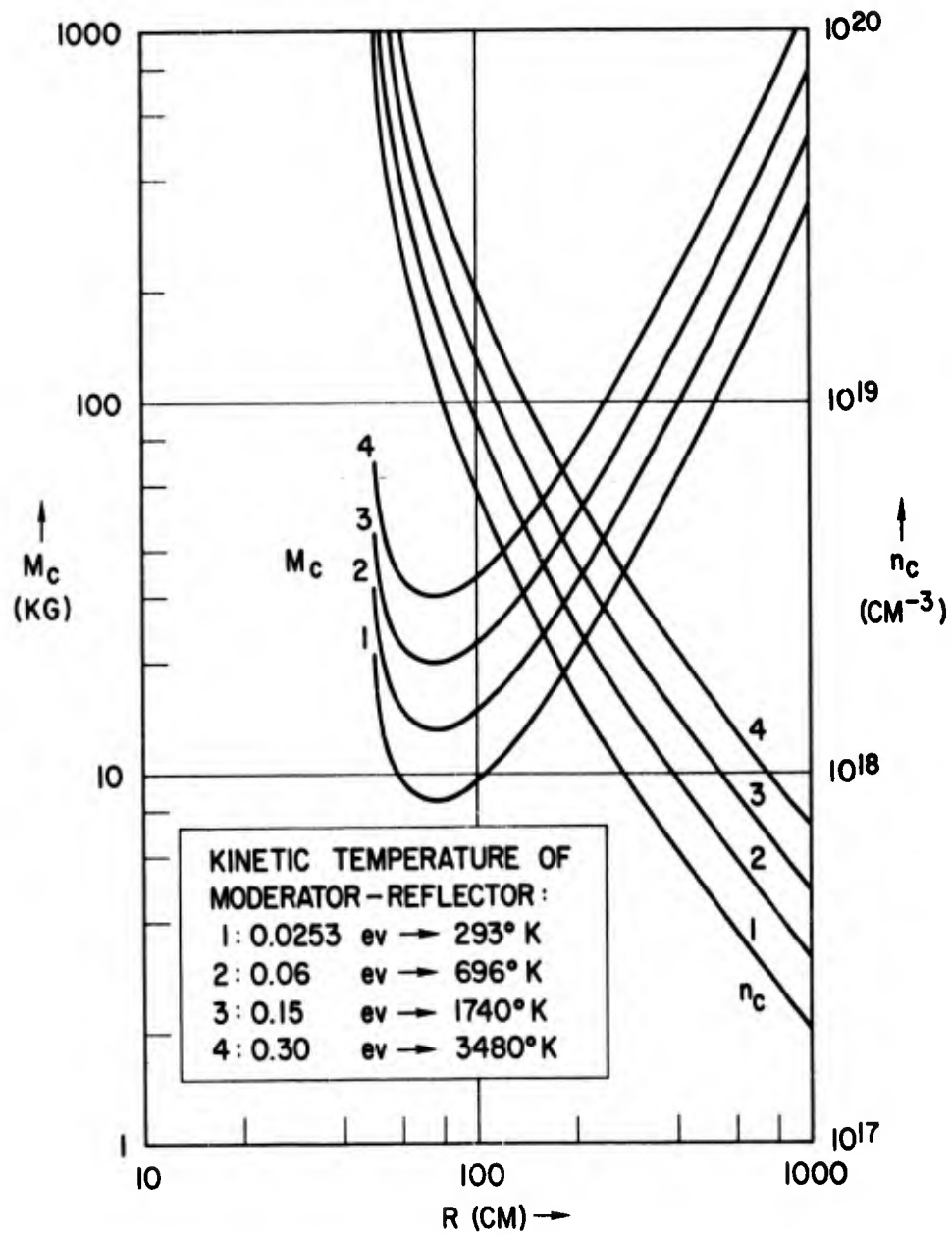


Figure 6 - Critical Mass and Particle Density vs Radius for U-233/C

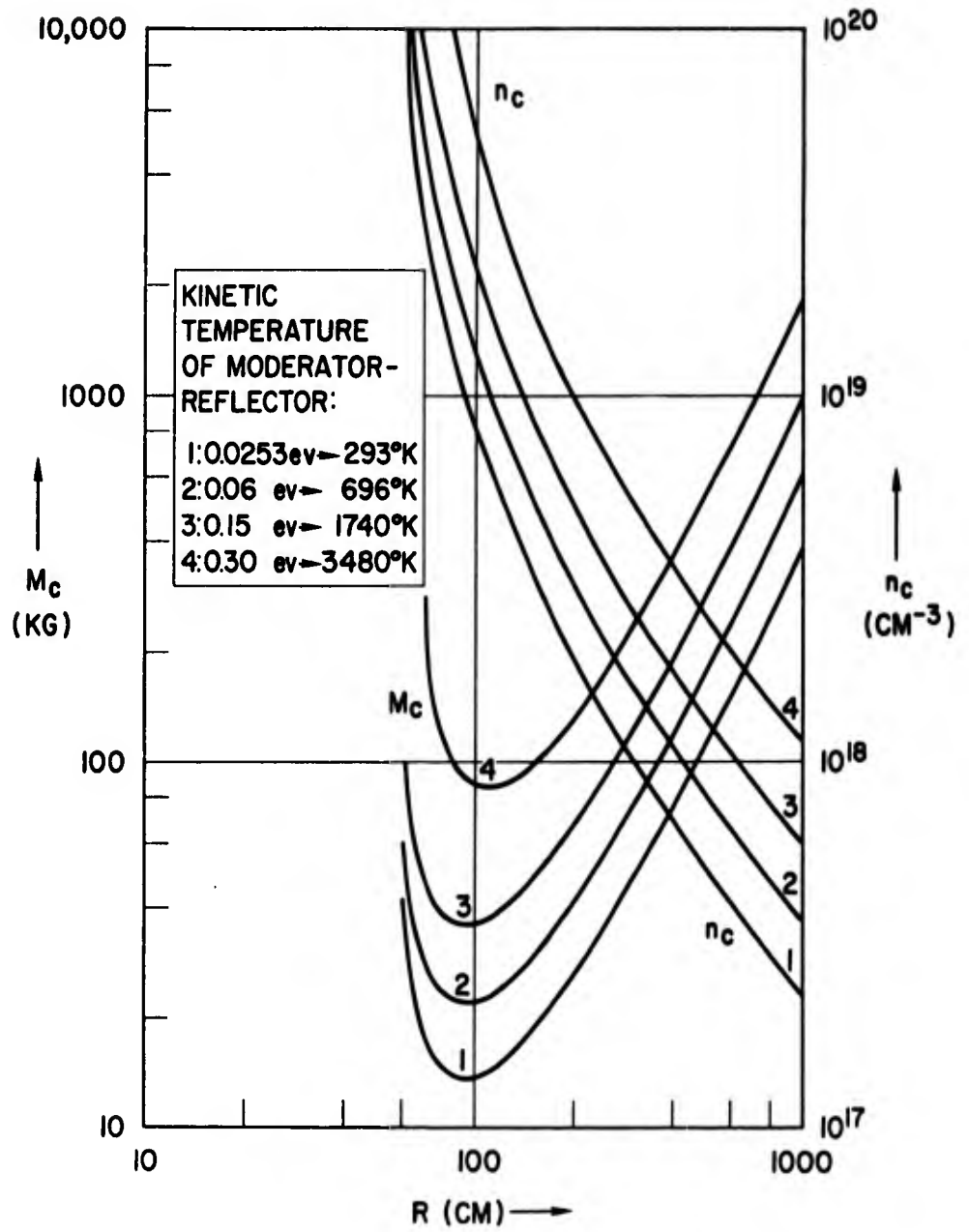


Figure 7 - Critical Mass and Particle Density vs Radius for $^{235}\text{U}/\text{C}$

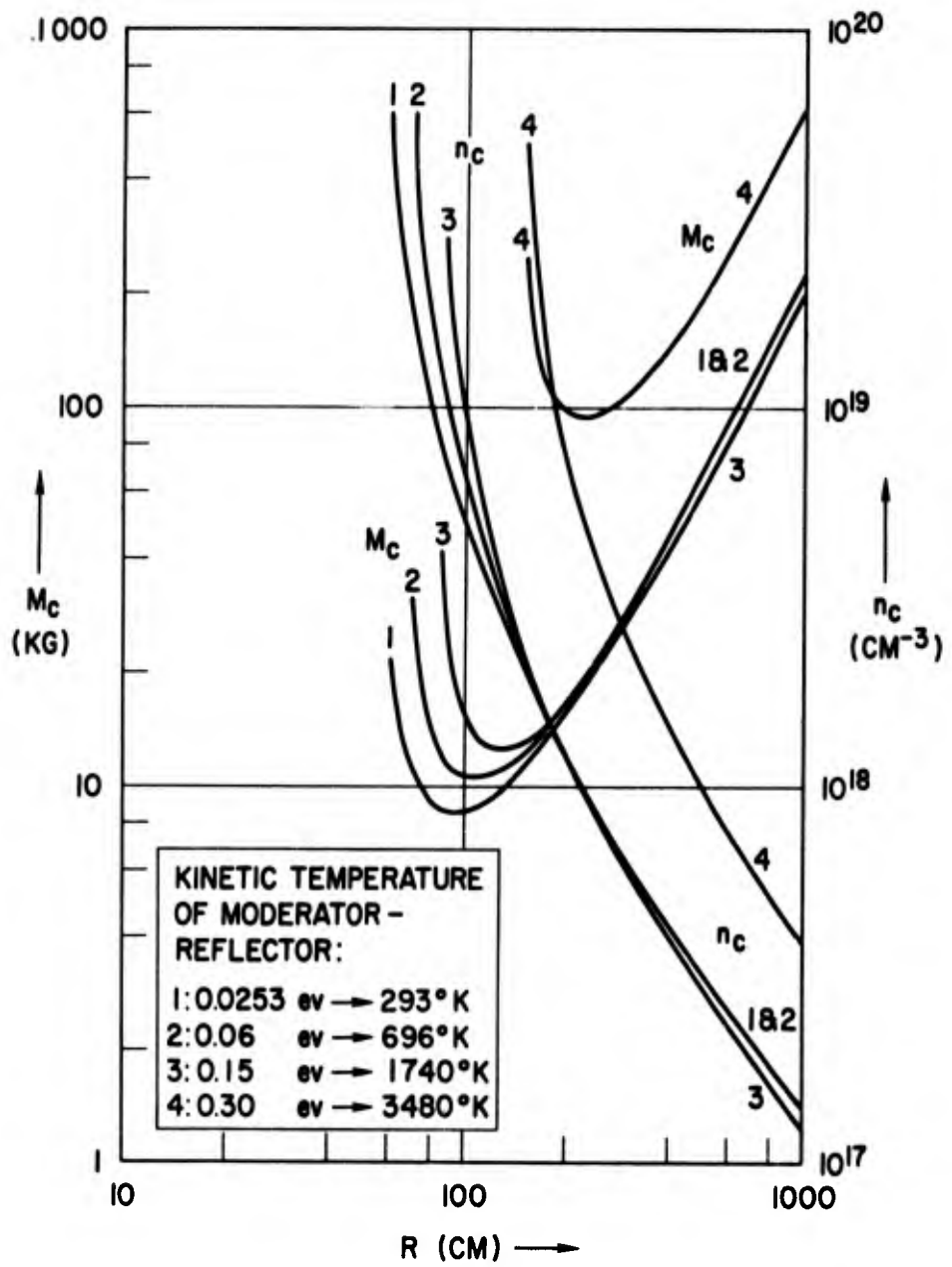


Figure 8 - Critical Mass and Particle Density vs Radius for Pu-239/C

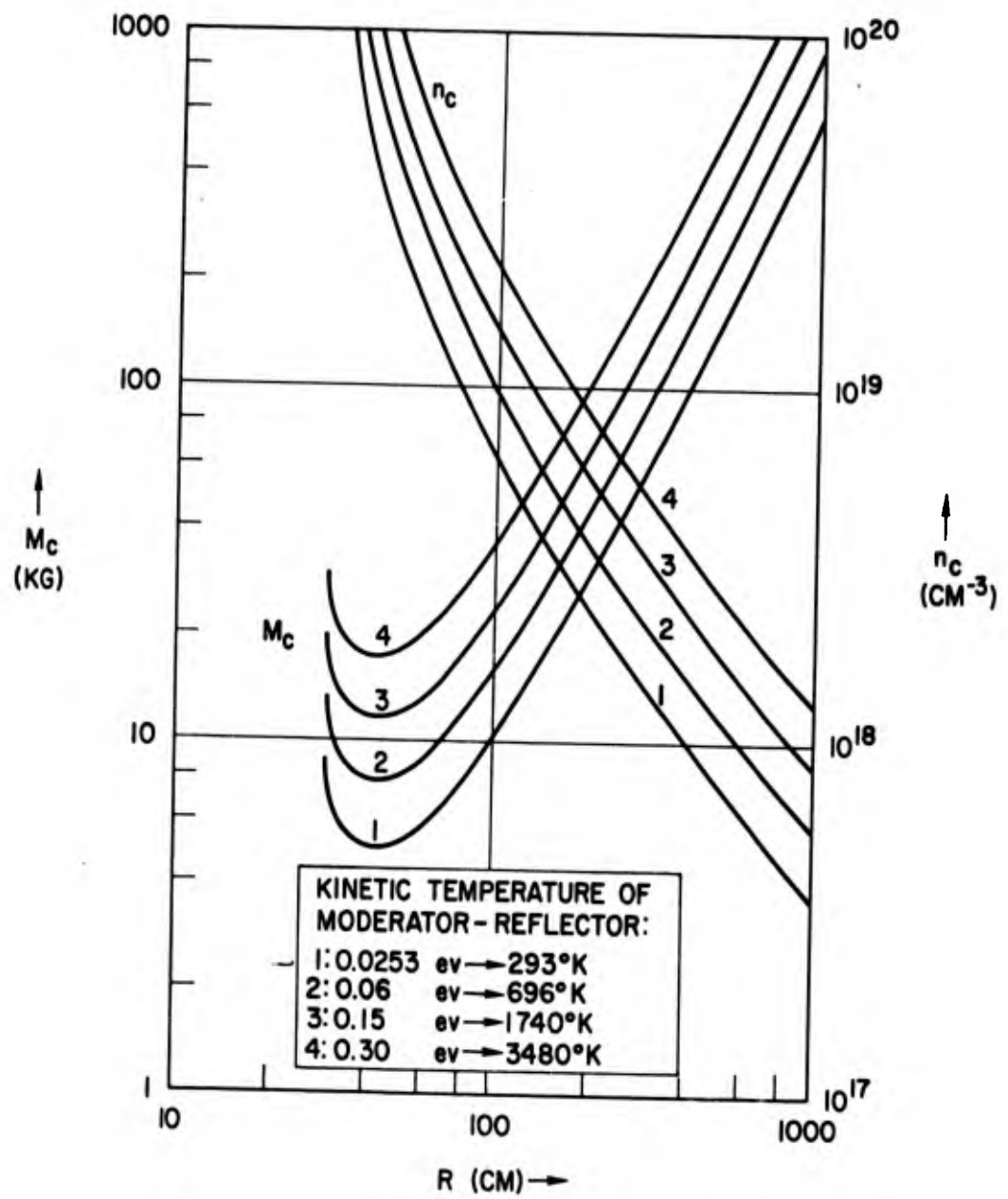


Figure 9 - Critical Mass and Particle Density vs Radius for U-233/Be

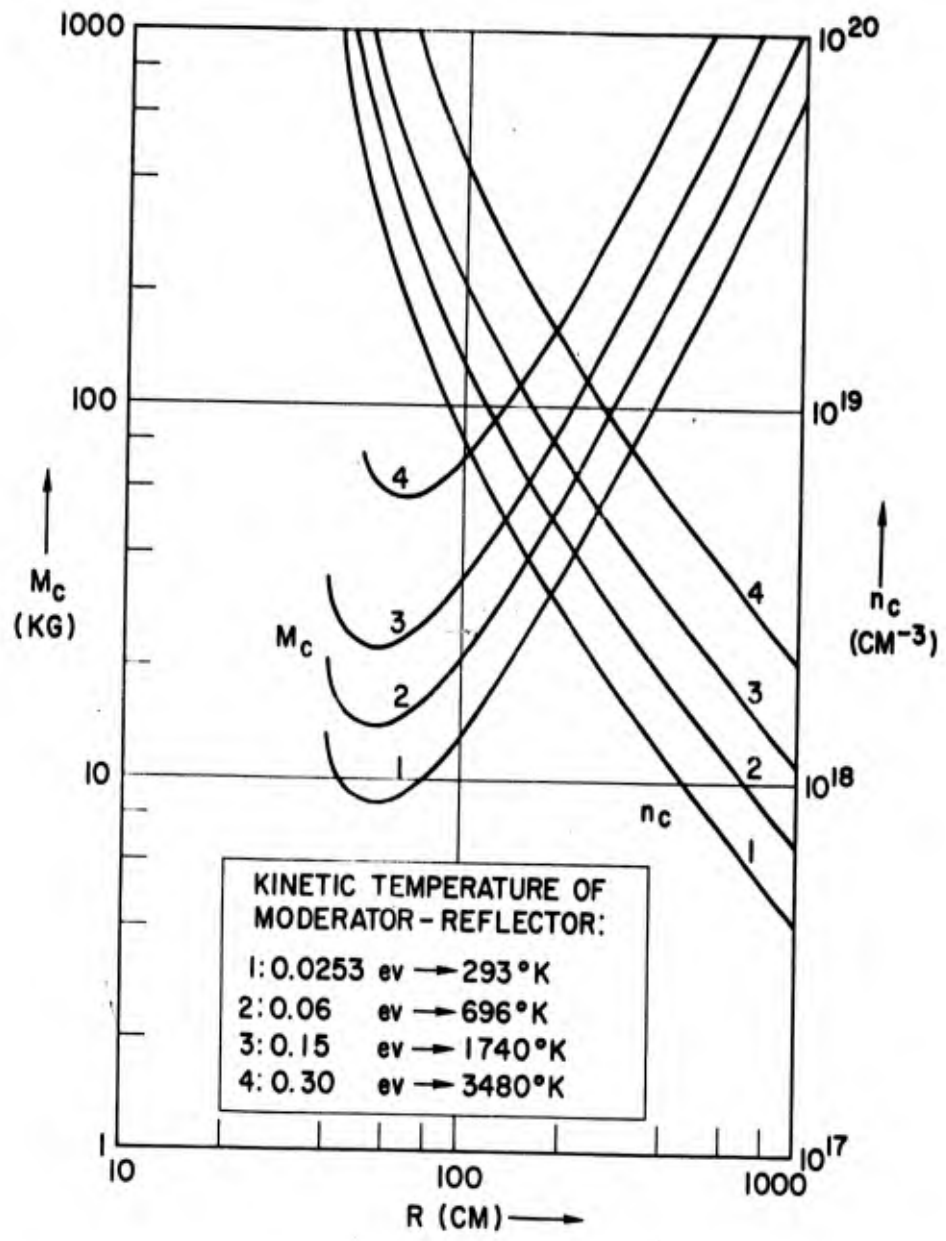


Figure 10 - Critical Mass and Particle Density vs Radius for U-235/Be

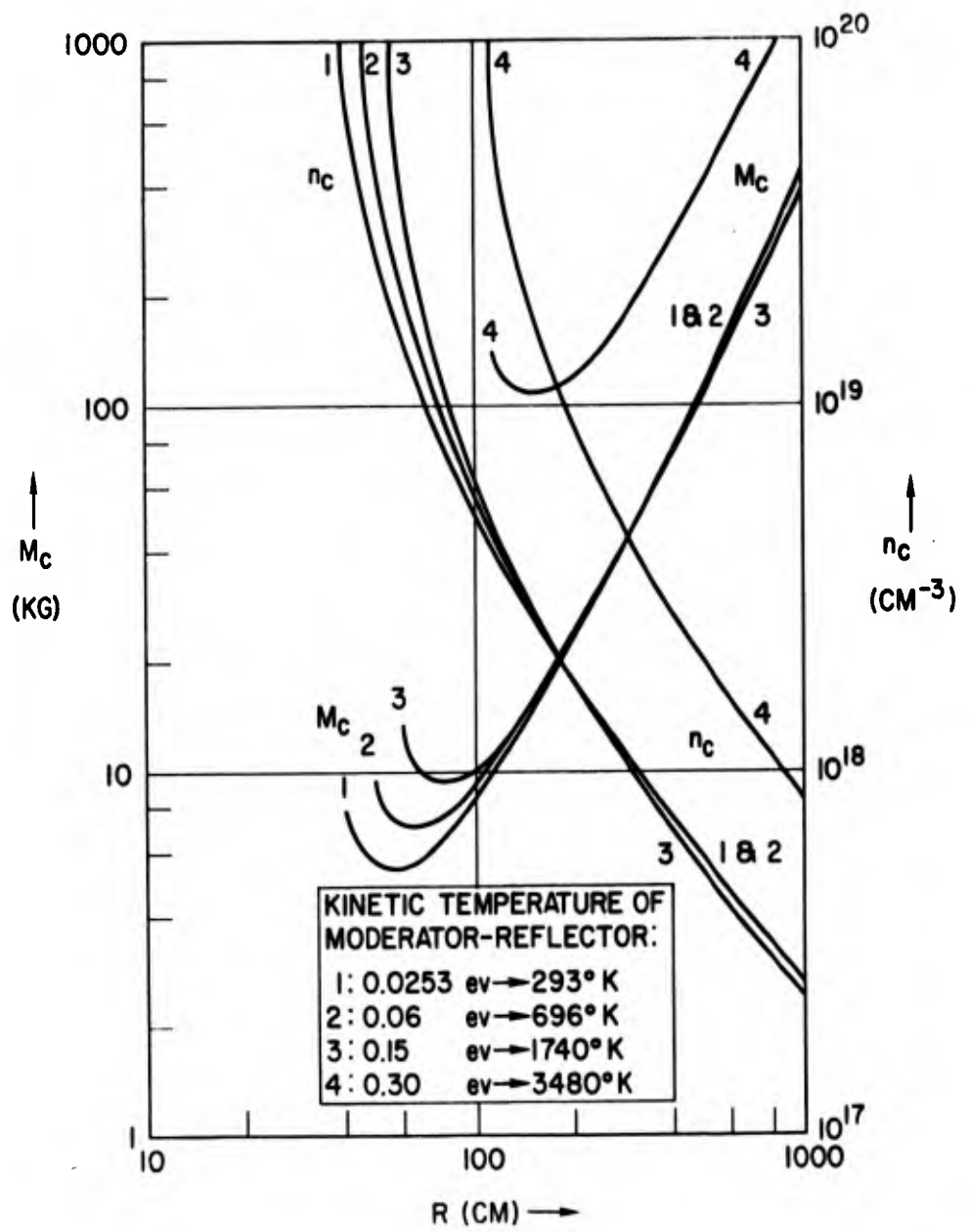


Figure 11 - Critical Mass and Particle Density vs Radius for Pu-239/Be

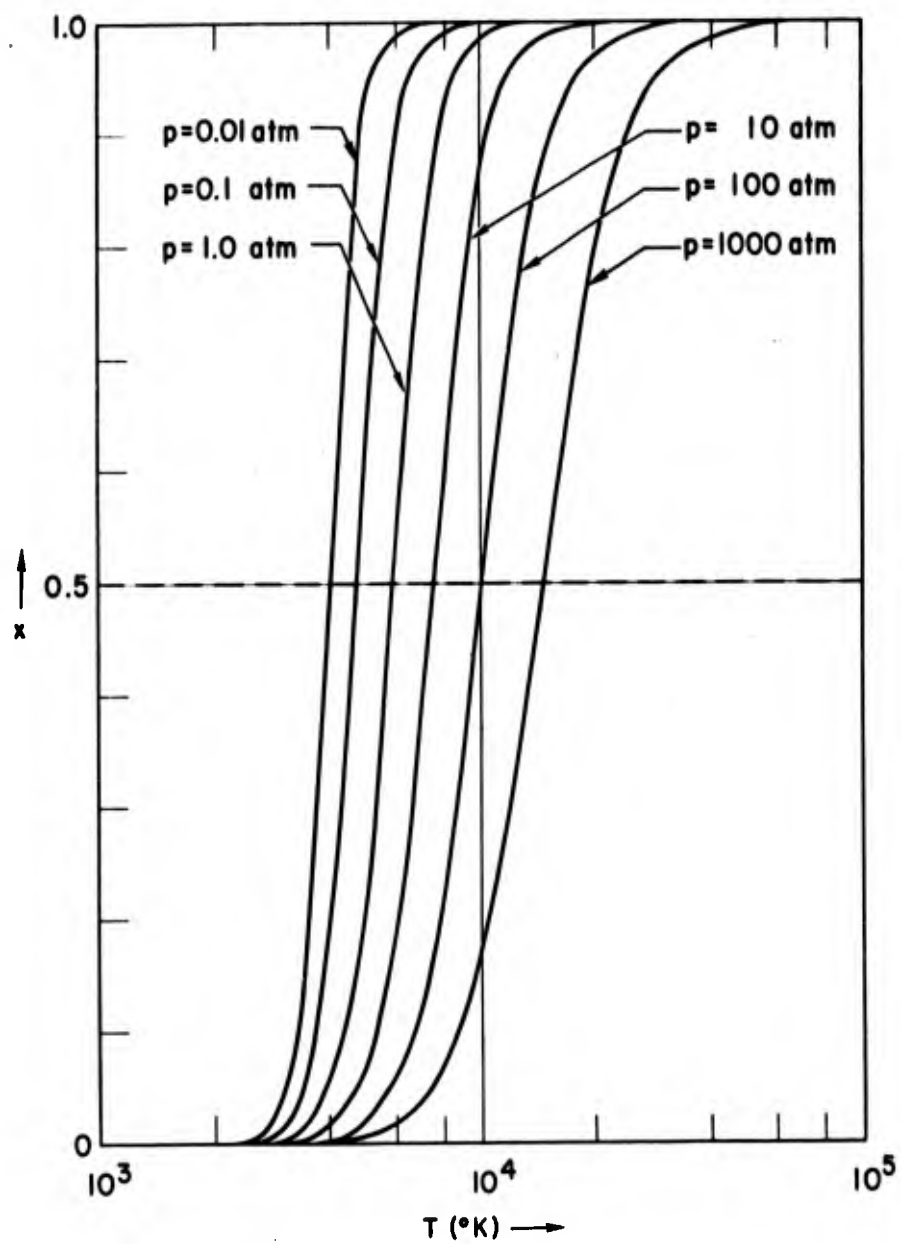


Figure 12 - Fraction of Singly Ionized Uranium Atoms vs Temperature for Various Pressures

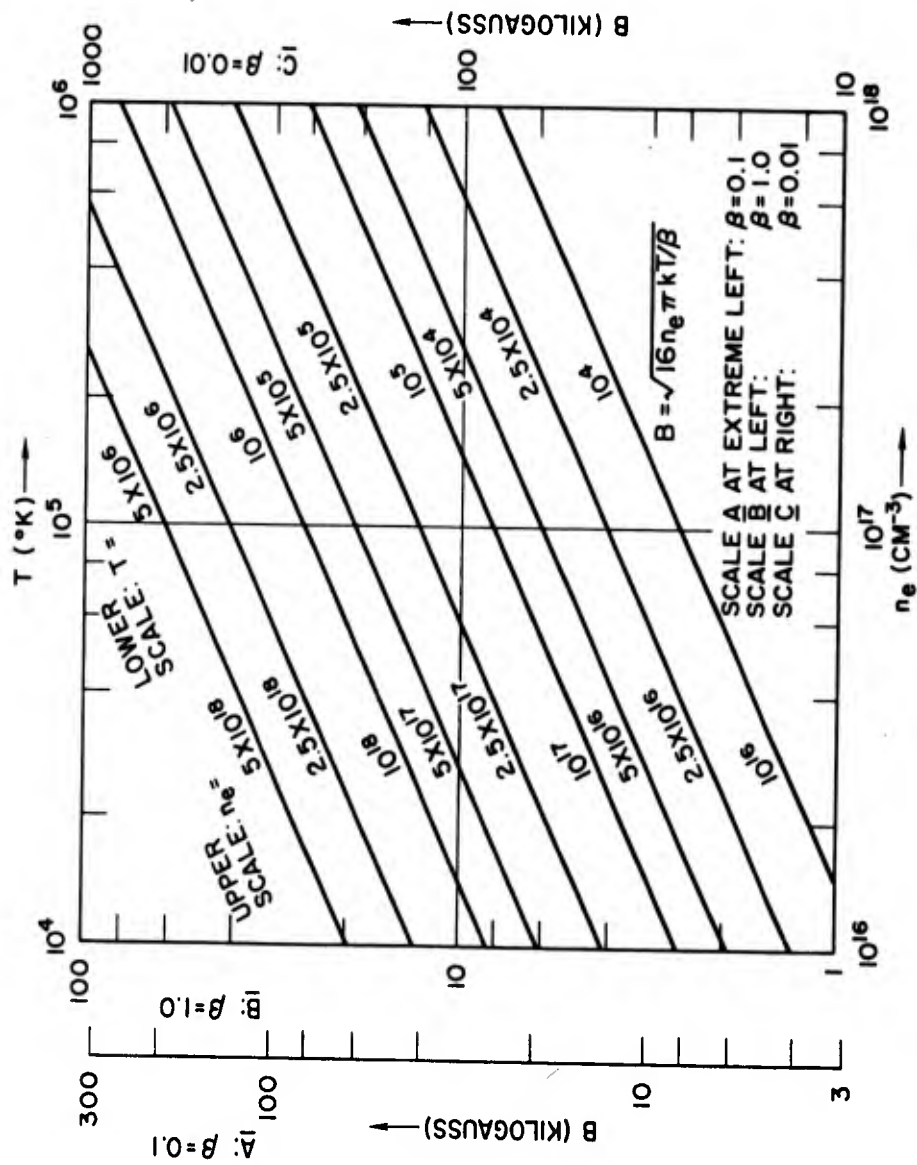


Figure 13 - B vs n_e and T

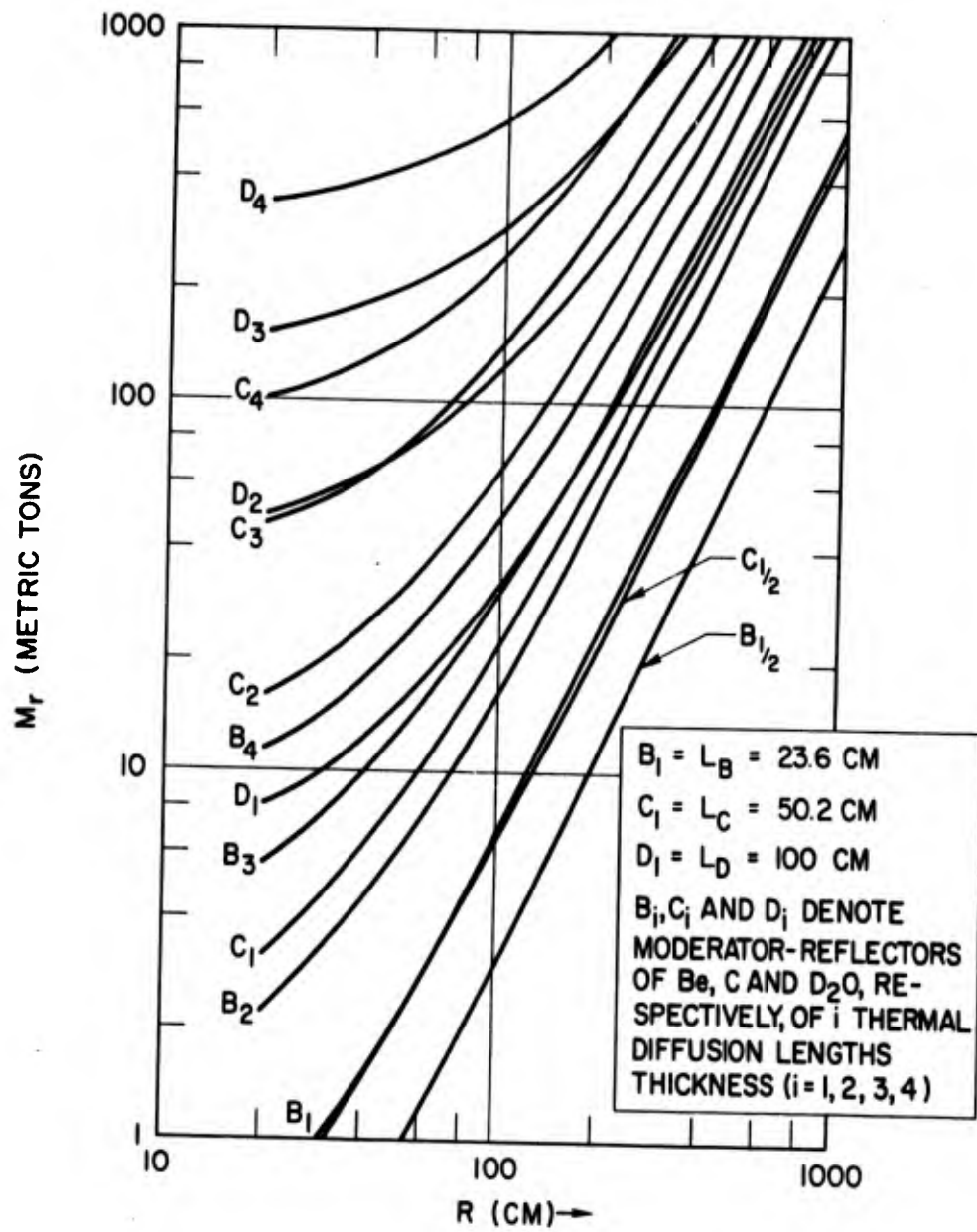


Figure 14 - Moderator-Reflector Mass vs Radius of Spherical Critical Cavity

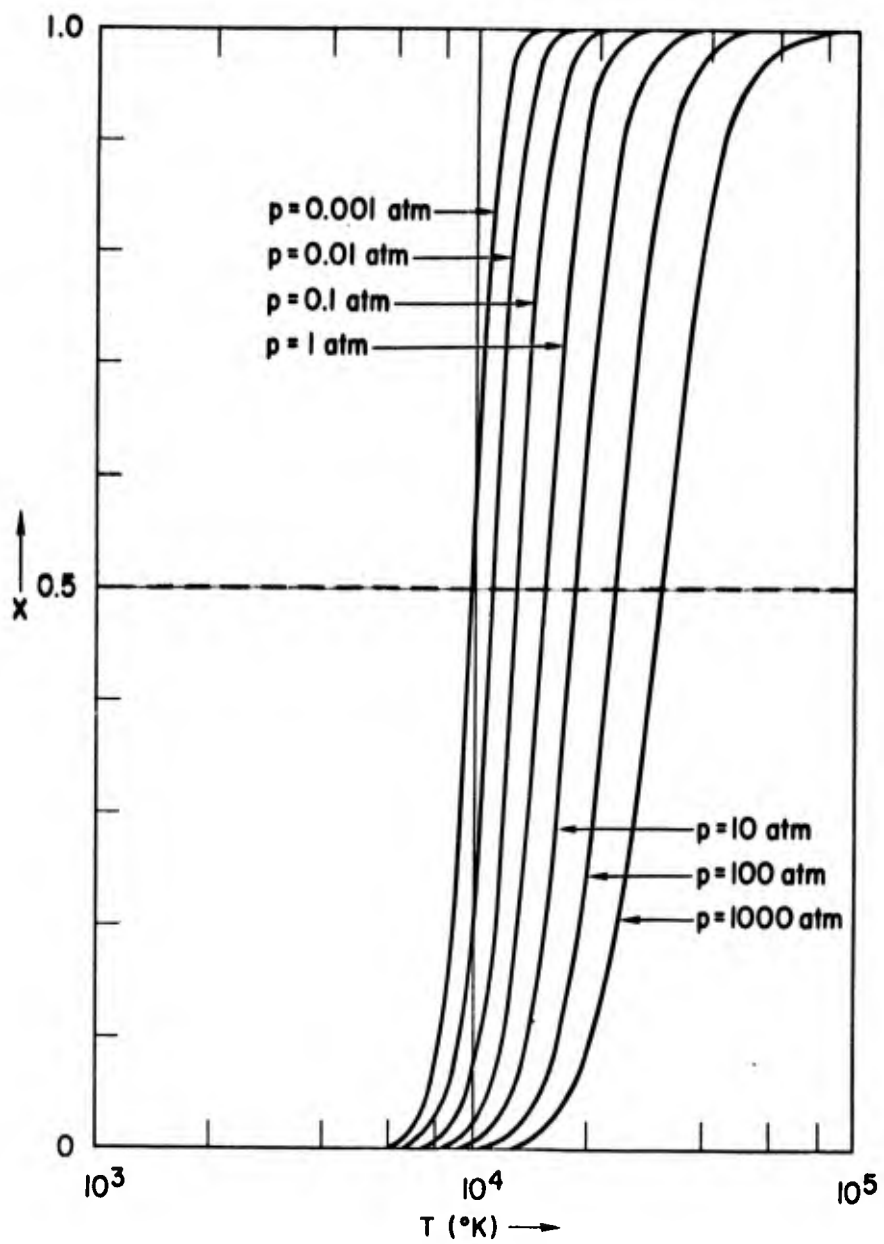


Figure 15 - Fraction of Singly Ionized Hydrogen Atoms vs Temperature for Various Pressures

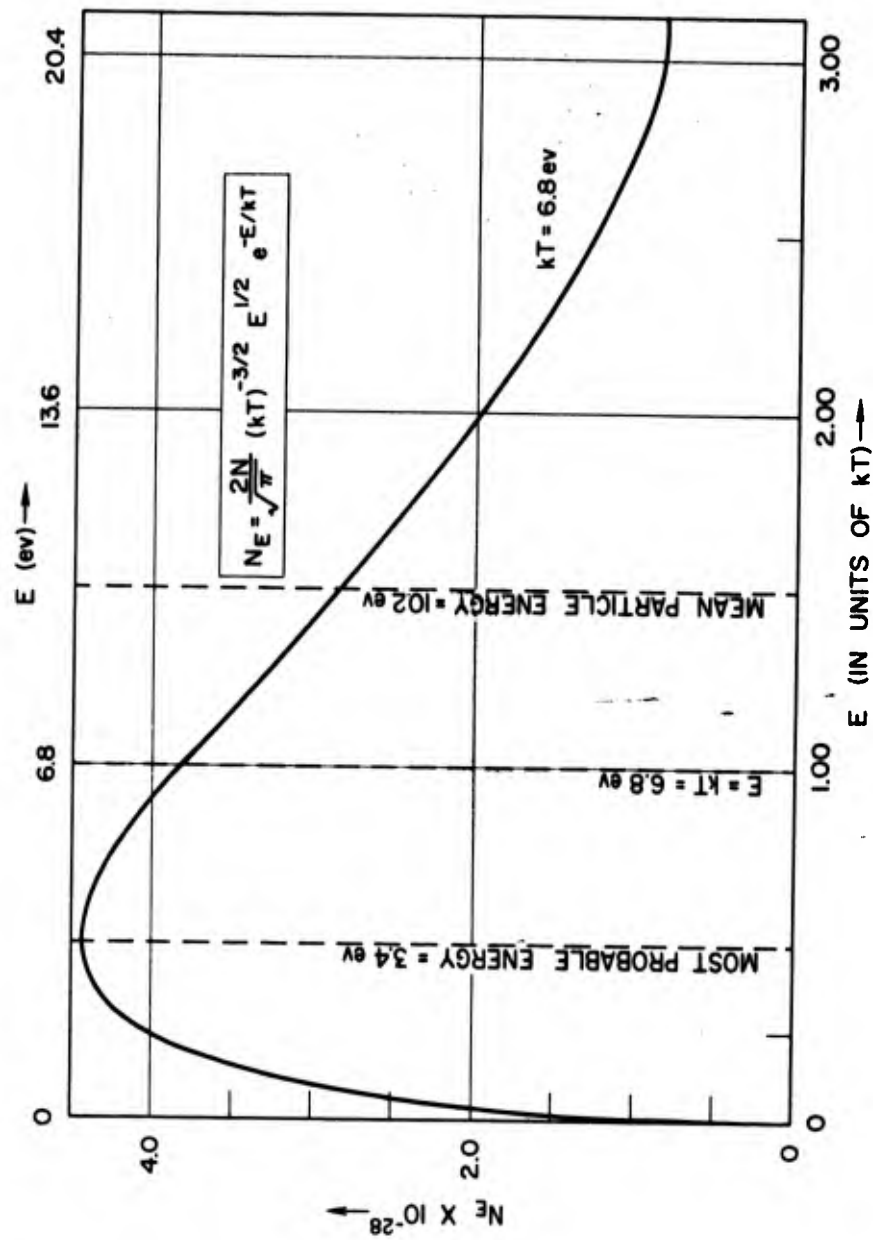


Figure 16 - Maxwell-Boltzmann Energy Distribution

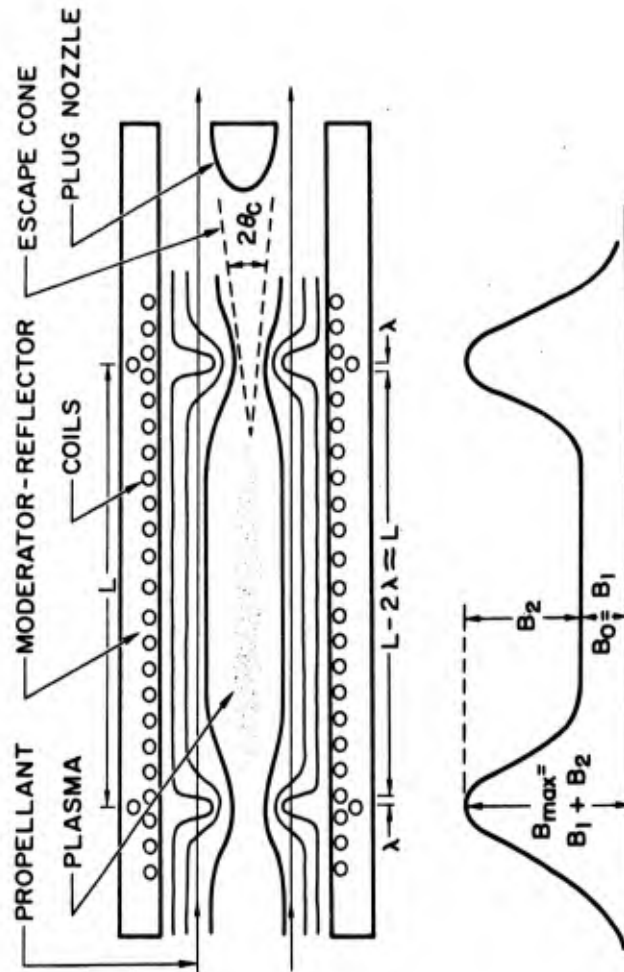


Figure 17 - Schematic Diagram of Magnetic-Bottle Type of Plasma Core Reactor

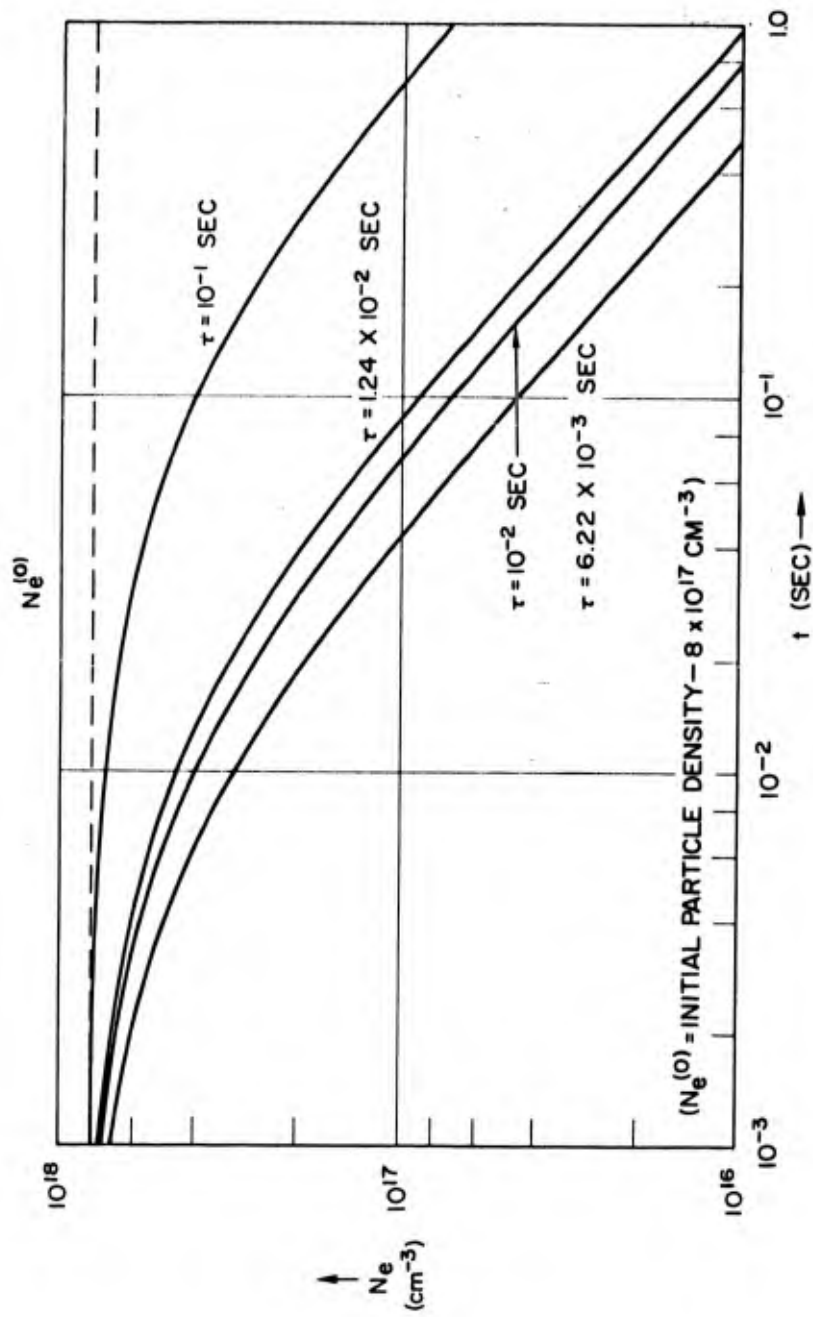


Figure 18 - Particle Density Decay Due to Plasma Loss Through a Magnetic Mirror

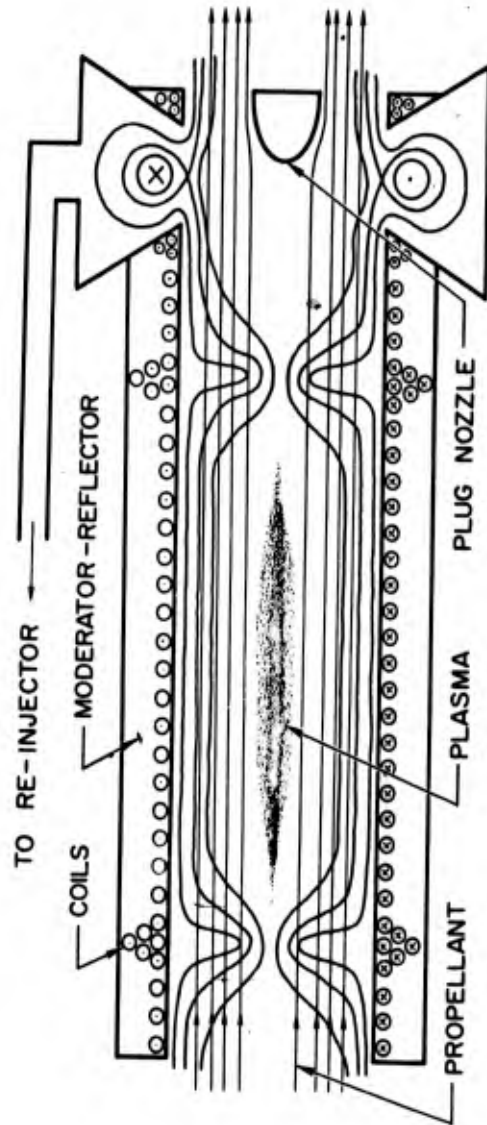


Figure 19 - Magnetic-Bottle Type of Plasma Core Reactor with Divertor

(MAGNETIC COILS AND AXIAL FLOW OF PROPELLANT HAVE BEEN OMITTED FROM DIAGRAM FOR SIMPLICITY)

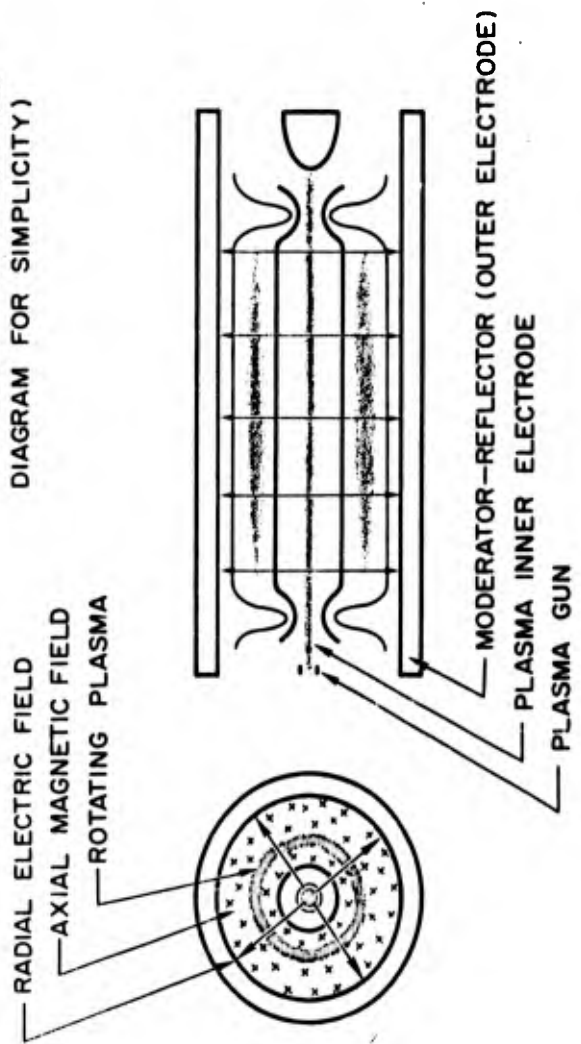


Figure 20 - Plasma Core Reactor with Homopolar Geometry

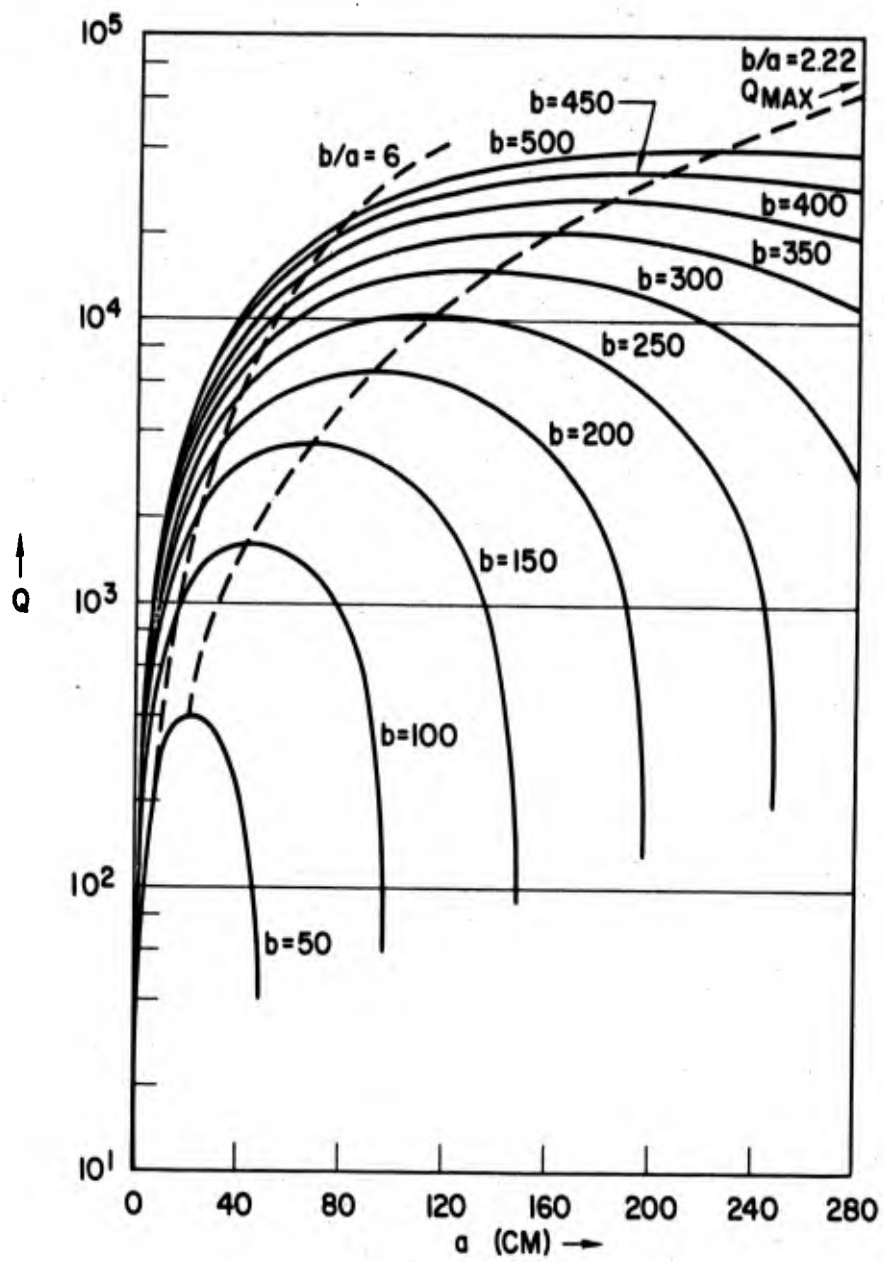


Figure 21 - Q vs a for Different Values of b

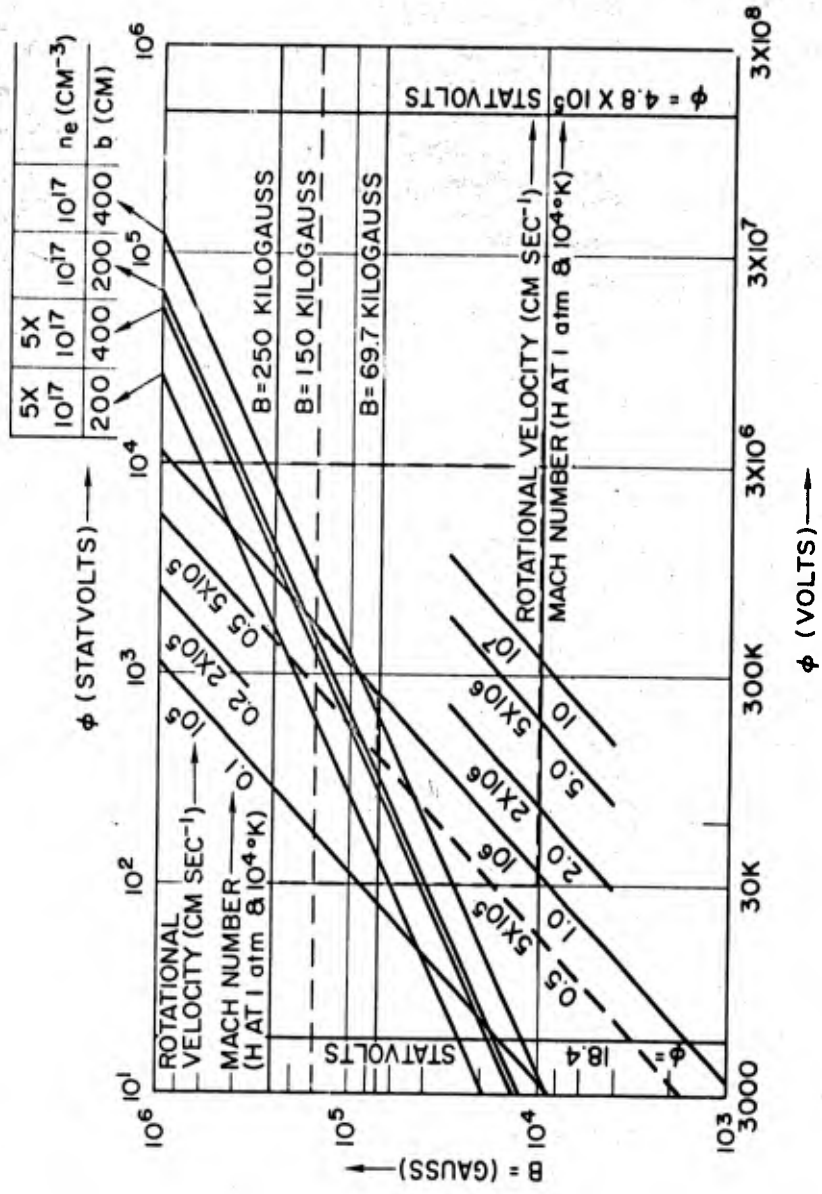
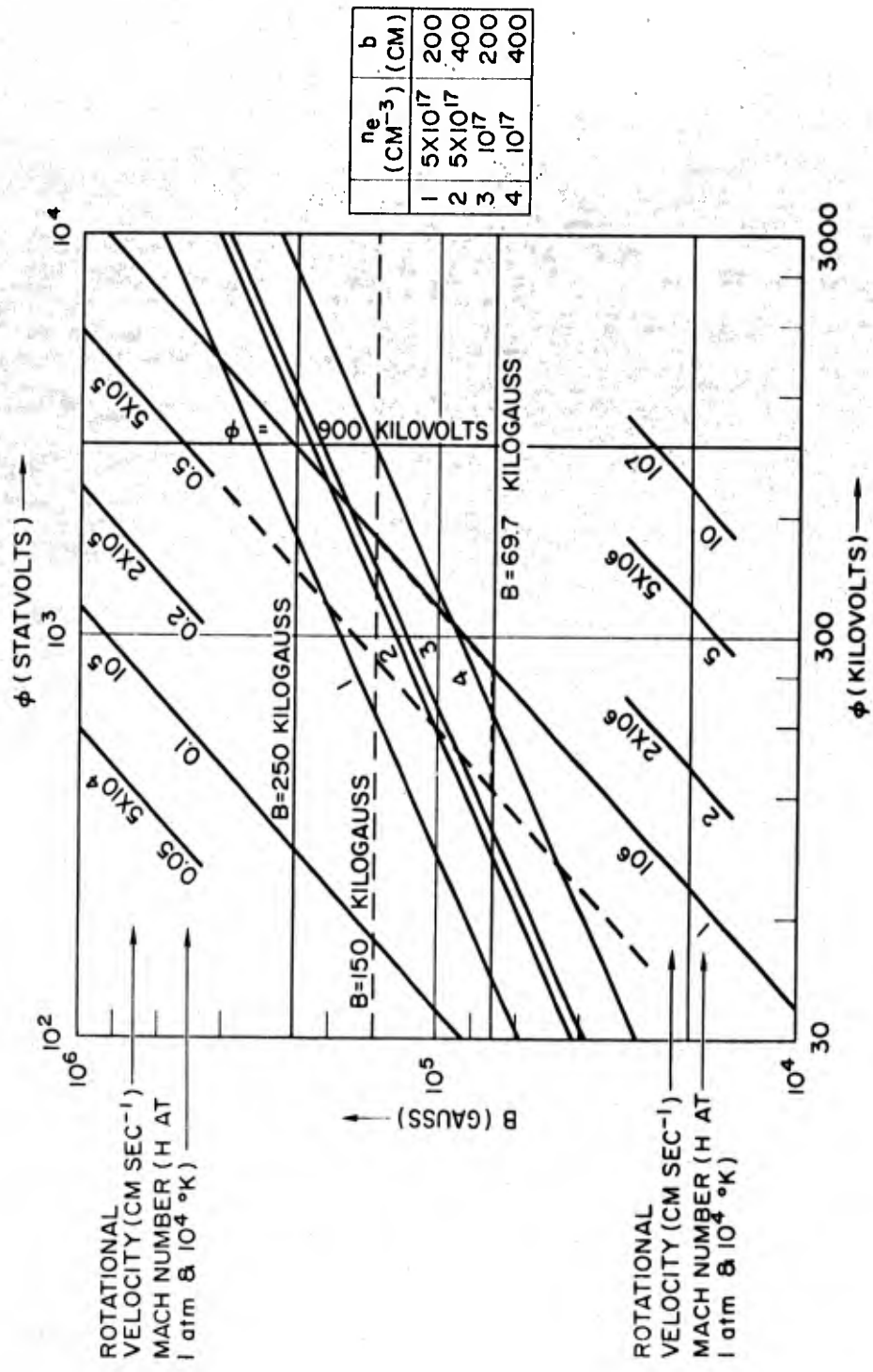


Figure 22 - Homopolar Confinement



	n_e (CM ⁻³)	b (CM)
1	5×10^{17}	200
2	5×10^{17}	400
3	10^{17}	200
4	10^{17}	400

Figure 23 - Homopolar Confinement (Detail)

Table 1

Nucleonic Temperature Data

U-233							
E (ev)	T (°K)	T ^{1/2}	g _a (T)	g _a /T ^{1/2}	<σ _a >	η	η <σ _a >
0.02	232.19	15.237	0.988	.064842	572.6	2.3	1316.98
0.0253	293.71	17.138	0.986	.057533	508.1	2.3	1168.63
0.04	464.37	21.548	0.980	.045480	401.7	2.3	923.91
0.06	696.56	26.392	0.980	.037132	327.9	2.3	754.17
0.08	928.74	30.475	0.984	.032289	285.2	2.3	655.96
0.10	1160.93	34.073	0.993	.029143	257.4	2.3	592.02
0.12	1393.11	37.324	1.004	.026900	237.6	2.3	546.48
0.125	1451.16	38.094	1.007	.026435	233.5	2.3	537.05
0.13	1509.21	38.849	1.010	.025999	229.6	2.3	528.08
0.14	1625.30	40.315	1.018	.025251	223.0	2.3	512.90
0.15	1741.39	41.730	1.026	.024587	217.1	2.3	499.33
0.16	1857.48	43.099	1.036	.024038	212.3	2.3	488.29
0.17	1973.58	44.425	1.049	.023613	208.5	2.3	479.55
0.18	2089.67	45.713	1.062	.023232	205.2	2.3	471.96
0.19	2205.76	46.966	1.077	.022931	202.5	2.3	465.75
0.20	2321.86	48.186	1.093	.022683	200.3	2.3	460.69
0.22	2554.04	50.538	1.129	.022340	197.3	2.3	453.79
0.24	2786.23	52.785	1.173	.022222	196.3	2.3	451.49
0.26	3018.45	54.940					
0.28	3250.46	57.013					
0.30	3482.83	59.016					

NOTE: $\langle \sigma_a \rangle = g_a(T) \sigma_{oa} \sqrt{\pi T_o/4T} = 8831 g_a(T) T^{-1/2}$

Table I

Nucleonic Temperature Data (Continued)

U-235							
E (ev)	T (°K)	T ^{1/2}	g _a (T)	g _a /T ^{1/2}	<σ _a >	η	η<σ _a >
0.02	232.19	15.237	0.985	.064645	681.0	2.1	1430.10
0.0253	293.71	17.138	0.974	.056833	598.7	2.1	1257.27
0.04	464.37	21.548	0.949	.044041	464.0	2.1	974.40
0.06	696.56	26.392	0.936	.035465	373.6	2.1	784.56
0.08	928.74	30.475	0.934	.030648	322.9	2.1	678.09
0.10	1160.93	34.073	0.932	.027353	288.2	2.1	605.22
0.12	1393.11	37.324	0.926	.024810	261.4	2.1	548.94
0.125	1451.16	38.094	0.924	.024256	255.5	2.1	536.55
0.13	1509.21	38.849	0.922	.023733	250.0	2.1	525.00
0.14	1625.30	40.315	0.918	.022771	239.9	2.1	503.79
0.15	1741.39	41.730	0.913	.021879	230.5	2.1	484.05
0.16	1857.48	43.099	0.908	.021068	222.0	2.1	466.20
0.17	1973.58	44.425	0.902	.020304	213.9	2.1	449.19
0.18	2089.67	45.713	0.896	.019601	206.5	2.1	433.65
0.19	2205.76	46.966	0.889	.018929	199.4	2.1	418.74
0.20	2321.86	48.186	0.883	.018325	193.1	2.0	386.2
0.22	2554.04	50.538	0.870	.017215	181.4	2.0	362.8
0.24	2786.23	52.785	0.858	.016255	171.2	2.0	342.4
0.26	3018.45	54.940	0.846	.015399	162.2	2.0	324.4
0.28	3250.46	57.013	0.833	.014611	153.9	2.0	307.8
0.30	3482.83	59.016	0.822	.013928	146.7	2.0	293.4

NOTE: $\langle \sigma_a \rangle = g_a(T) \sigma_{oa} \sqrt{\pi T_o/4T} = 10535 g_a(T) T^{-1/2}$

Table I

Nucleonic Temperature Data (Continued)

Pu-239							
E (ev)	T (°K)	T ^{1/2}	g _a (T)	g _a /T ^{1/2}	<σ _a >	η	η<σ _a >
0.02	232.19	15.237	1.013	.066483	1041.3	2.1	2186.73
0.0253	293.71	17.138	1.057	.061676	966.0	2.1	2028.60
0.04	464.37	21.548	1.302	.060423	946.4	2.0	1892.80
0.06	696.56	26.392	1.972	.074720	1170.3	2.0	2340.60
0.08	928.74	30.475	2.783	.091321	1430.4	1.9	2717.76
0.10	1160.93	34.073	3.431	.100960	1577.2	1.9	2996.68
0.12	1393.11	37.324	3.907	.104678	1639.6	1.9	3115.24
0.125	1451.16	38.094	3.996	.104898	1643.0	1.9	3121.70
0.13	1509.21	38.849	4.075	.104893	1642.9	1.9	3121.51
0.14	1625.30	40.315	4.203	.104254	1632.9	1.9	3102.51
0.15	1741.39	41.730	4.297	.102971	1612.8	1.9	3064.32
0.16	1857.48	43.099	4.361	.101186	1584.9	1.9	3011.31
0.17	1973.58	44.425	4.400	.099043	1551.3	1.9	2947.47
0.18	2089.67	45.713	4.417	.096625	1513.4	1.9	2875.46
0.19	2205.76	46.966	4.418	.094068	1473.4	1.9	2799.46
0.20	2321.86	48.186	4.404	.091396	1431.5	1.7	2433.55
0.22	2554.04	50.538	4.345	.085975	1346.6	1.7	2289.22
0.24	2786.23	52.785	4.255	.080610	1262.6	1.7	2146.42
0.26	3018.45	54.940					
0.28	3250.46	57.013					
0.30	3482.83	59.016					

NOTE: $\langle \sigma_a \rangle = g_a(T) \sigma_{oa} \sqrt{\pi T_o/4T} = 15663 g_a(T) T^{-1/2}$

Table II

 $\ln \Lambda$

	n_e (cm ⁻³)						
		10^{14}	10^{15}	10^{16}	10^{17}	5×10^{17}	10^{18}
T (°K)	10^4	7.14	5.97	4.83	3.68	2.86	2.53
	2×10^4	8.16	7.01	5.86	4.71	3.90	3.56
	2.5×10^4	8.50	7.34	6.19	5.04	4.24	3.89
	10^5	10.6	9.43	8.28	7.13	6.32	5.97
	10^6	13.6	12.4	11.2	10.1	9.34	8.96
	10^7	15.9	14.7	13.6	12.4	11.6	11.2

Table III
 Limitations Upon Principal System Variables

	LOWER LIMIT	UPPER LIMIT
SIZE (R)	1. CRITICALITY	1. WT. OF MODERATOR - REFLECTOR 2. EXCESSIVE FUEL INVENTORY 3. EXCESSIVE MAG. FIELD VOLUME 4. FABRICATION DIFFICULTIES
TEMPERATURE (T)	1. FUEL IONIZATION TEMP.	1. RADIATIVE HEAT TRANSFER TO WALLS 2. PROPELLANT IONIZATION
MAGNETIC FIELD STRENGTH (B)	1. PLASMA CONFINEMENT 2. COST OF MAX. TOLERABLE FUEL LOSS BY DIFFUSION	1. ELECTRIC POWER REQUIREMENTS 2. COIL WEIGHT
ELECTRIC FIELD STRENGTH (E) (HOMOPOLAR CONFIGURATION)	1. PLASMA ROTATES TOO SLOWLY a. THEREFORE UNSTABLE b. THEREFORE AXIAL DIFFUSION INTOLERABLE	1. SUPERSONIC FLOW PROBLEMS 2. EXCESSIVE VOLTAGE DROP ACROSS PLASMA
PROPELLANT FLOW RATE	1. FLOW CHANNEL CROSS SECTION EXCESSIVE (THEREFORE MODERATOR TOO HEAVY)	1. EXCESSIVE PRESSURE 2. HELMHOLTZ WAVES (THEREFORE PROPELLANT SWEEP THROUGH NOZZLE)
PLASMA ROTATIONAL VELOCITY (HOMOPOLAR CONFIGURATION)	1. PLASMA INSTABILITY (THEREFORE MAX. PERMISSIBLE PROPELLANT FLOW RATE TOO SLOW) 2. APPROACHES DIFFUSION PROPERTIES OF SIMPLE MAGNETIC BOTTLE	1. SHOCK WAVES AND BOUNDARY LAYER TURBULENCE 2. ROTATIONAL KINETIC ENERGY WASTED IN SPINNING PROPELLANT

SYMBOLS

LOWER CASE ROMAN

a	plasma radius -- Section II
a	radius of inner electrode in crossed-field device
a_L	radius of gyration (Larmor radius)
b	radius of outer electrode in crossed-field device
c	velocity of light
$\bar{c}_0, \bar{c}'_0, \bar{c}_1, \bar{c}'_1$	particle velocities -- Eq. (151)
e	electric charge (If no subscript appears, e denotes the electronic charge)
f	velocity space distribution function
g	acceleration due to gravity at the earth's surface
$g=g_a(T)$	cross section correction factor (see Table I)
g, h	factors of velocity space distribution function with separated variables
h	Debye length or "shielding distance"
j	current density
k	reactor multiplication constant
k	Boltzmann constant
m	particle mass
m	reduced mass -- Eq. (27)
n	particle density
p	pressure, atm -- Eq. (19)
p_0	value of the classical impact parameter corresponding to $\pi/2$ deflection of an electron by an ion
$q(r)$	thermal neutron source strength per unit volume at a distance r from the center of the system
r	radial coordinate
t	time
v	particle velocity
x	fractional ionization--Eq. (19)
x_1	x-coordinate of the guiding center of a plasma particle whose coordinates in phase space are x, v -- Eqs. (26) and (27)

UPPER CASE ROMAN

A	atomic mass, amu
A	parameter defined in Eq. (74)
B	magnetic field intensity
D	diameter of plasma core
D_0	diffusion coefficient in the absence of a magnetic field
D'	diffusion coefficient in the presence of a magnetic field
E	energy
E	electric field intensity
F	diffusion flux
I_{sp}	specific impulse
J	net neutron current -- Section II
L	thermal diffusion length -- Section II
L	length of plasma core
M	molecular mass of propellant exhaust gas
M	mass, gm
N	Avogadro's number
N'	number of times which magnetic energy must be supplied to coils to overcome ohmic dissipation in the plasma
N	parameter defined in Eq. (155)
P	Plasma pressure -- Section III
Q	parameter defined in Eq. (204)
R	mirror ratio -- Eq. (154)
R	radius of plasma -- Section III, same as a of Section II
S	total fast neutron source strength
T	temperature
V	volume
V_D	relative velocity of unlike particles -- Eq. (26)
W	total particle kinetic energy
Y	thickness of propellant layer surrounding plasma and flowing axially
Z	atomic number

SCRIPT

l	transport mean free path for thermal neutrons in the moderator
D	degree of ionization
n	total number of "throughputs" of critical mass during one mission

LOWER CASE GREEK

α	parameter defined in Eq. (203)
β	parameter defined in Eq. (47)
γ	dimensionless constant defined on p. 7
η	number of neutrons born per thermal neutron captured in the core -- Section II
θ	scattering angle in center of mass system
θ	angle between the directional neutron flux and the radial vector from the center of the system -- Section II
λ	ion-electron collision mean free path
μ	magnetic moment
ν_c	ion - electron collision frequency
ρ	radial coordinate of a unit shell source of thermal neutrons -- Section II
ρ	plasma density -- Section III
δ	cross section
τ	Fermi age of thermal neutrons in the moderator -- Section II
τ	time constant (e-folding time) -- Eq. (113)
τ	mean time between ion - electron collisions -- Section III, Subsection C
τ	time for 1/2 the plasma to leak through a magnetic mirror -- Eq. (163)
ϕ	thermal diffusion kernel -- Section II
ϕ	external potential (such as gravitational potential) Section III
φ	electrostatic potential across plasma annulus in homopolar core
ω	electron cyclotron (Larmor) frequency
ω	angular velocity

UPPER CASE GREEK

Λ	absorption mean free path of thermal neutrons in the core -- Section II
Λ	parameter defined in Eqs. (29) - (31)
Φ	thermal neutron flux -- Section II
Φ	magnetic flux -- Eqs. (109) - (112)
Ω	solid angle

SUBSCRIPTS

a	absorption (fission + capture)
b	rocket burnout
c	criticality -- Section II
c	cone of escape in velocity space -- Eq. (153)
d	diffusion
e	electron
E	$\mathbf{E} \times \mathbf{B}$ plasma drift -- Eq. (178)
H	hydrogen -- Eq. (22)
H	hydrostatic -- Eq. (90)
i	ion
L	Lorentz gas -- Eq. (114)
L	Larmor gyration -- Eq. (177)
M	magnetic -- Eq. (89)
max	maximum
min	minimum
r	reflector (moderator-reflector cladding)
r	radial direction
R	Plasma boundary
s	scattering
tot	total -- Eq. (120)
v	ionization -- Eq. (19)
z	axial direction
θ	azimuthal direction
o	thermal temperature (0.0253 ev or 293 deg K)
o	axis
1, 2	different species of particles

SUPERSCRIPTS

(o) initial conditions
(th) thermal

MISCELLANEOUS SYMBOLS

\bar{x} vector of magnitude x
 $\langle x \rangle$ mean value of x (generally averaged over a Maxwell-Boltzmann distribution)
 \dot{x} time rate of change of $x = \delta x / \delta t$
 δx increment of x
 x_{\perp} component of x in the plane perpendicular to magnetic lines of force
 x_{\parallel} component of x parallel to magnetic lines of force
 x^{\dagger} peak value -- p. 33

REFERENCES

1. J. L. Kerrebrock and R. W. Maghreblian; "An Analysis of Vortex Tubes for Combined Gas-Phase Fission Heating and Separation of the Fissionable Material;" Oak Ridge National Laboratory Memorandum CF 57-11-3, Nov. 1, 1957. Classification AEC-C86, Declassified Dec. 21, 1959.
2. Lawnie Taylor; Aerojet Report 1279-A; 1957, (Secret Restricted Data).
3. R.H. Fox; "Study of a Nuclear Gaseous Reactor Rocket;" UCRL-4996, (Secret Restricted Data).
4. R. W. Bussard and R.D. DeLauer; Nuclear Rocket Propulsion; McGraw-Hill, N. Y., 1958.
5. George Safonov; "Externally Moderated Reactors;" The RAND Corporation Report R-316, July 1957.
6. George Safonov; "The Criticality and Some Potentialities of 'Cavity Reactors';" The RAND Corporation Report RM-1835, ASTIA Document No. AD 112410, 17 July 1955.
7. George I. Bell; "Calculations of the Critical Mass of UF_6 as a Gaseous Core, with Reflectors of D_2O , Be and C;" LA-1874, February 1955.
8. P.R. Wallace and J. LeCaine; "Elementary Approximations in the Theory of Neutrons Diffusion;" National Research Council of Canada, Chalk River, Ontario, Report N.R.C. No. 1480.
9. H. Etherington (ed); Nuclear Engineering Handbook; McGraw-Hill, N. Y., 1958.
10. Argonne National Laboratory, "Reactor Physics Constants;" ANL-5800.
11. A. Simon, Phys. Rev. 100 , 1557, 1955.
12. C.L. Longmire and M.N. Rosenbluth, Phys. Rev. 103 . 507, 1956.
13. M.N. Saha, Phil. Mag 40, 472, 1920.
14. J.D. Cobine; Gaseous Conductors; Dover, N. Y., 1958.
15. C.L. Longmire; Report LA-2055; Part III-C (T-702); Los Alamos Scientific Laboratory, 1956.
16. Lyman Spitzer, Jr.; Physics of Fully Ionized Gases; Interscience, N. Y., 1956.
17. H. P. Furth, M.A. Levine, and R. W. Waniek, Rev. Sci. Instr. 28, 949; November, 1957; (See also Furth and Waniek. Rev. Sci. Instr. 27, 195, April 1956).

18. H. Aroeste and W. C. Benton, *J. Appl. Phys.* 27, 117, 1956.
19. A. Simon, An Introduction to Thermonuclear Research; (See Chapter III), Pergamon Press, 1959.
20. D. Judd, W. MacDonald and M. Rosenbluth; "End Leakage Losses From the Mirror Machine;" AEC Report WASH-289, Conference on Controlled Thermonuclear Reactions, Berkeley, California, February 1955.
21. A.A. Garren, R.J. Riddell, L. Smith, G. Bing, J.E. Roberts, T.C. Northrup and L.R. Henrick; "Individual Particle Motion and the Effect of Scattering in an Axially Symmetric Magnetic Field;" UCRL-8076. (Also appears as P/383, Vol. 31, Second U.N. Conference on the Peaceful Uses of Atomic Energy, Geneva, September 1958.)
22. Lyman Spitzer, Jr.; "A Proposed Stellarator;" AEC Report No. NYO 993 (PM-S-1, 1951).
23. C.R. Burnett, D.J. Grove, R.W. Palladino, T.H. Stix and K.E. Wakefield; "The Divertor, A Device for Reducing the Impurity Level in a Stellarator;" P/359, Vol. 32, Second U.N. Conference on the Peaceful Uses of Atomic Energy, Geneva, September 1958.
24. G.I. Budker, "Thermonuclear Reactions in a System with Magnetic Stoppers and the Problem of Direct Transformation of Thermonuclear Energy into Electrical Energy," Vol. III of Plasma Physics and the Problem of Controlled Thermonuclear Reaction; M. A. Leontovich and J. Turkevich, eds., Trans. by J.B. Sykes, Pergamon Press, 1959.
25. O.A. Anderson, W.R. Baker, A. Bratenahl, H.P. Furth, J. Ise, Jr., W.B. Kunkel, and J.M. Stone; "The Homopolar Device;" AEC Report UCRL-8062, January 1958. (This also appears in abbreviated form as P/373, Vol. 32, Second U.N. Conference on the Peaceful Uses of Atomic Energy, Geneva, September 1958.)
26. K. Boyer, J.E. Hammel, C.L. Longmire, D. Nagle, F.L. Ribe and W.B. Riesenfeld; "Theoretical and Experimental Discussion of Ixion, A Possible Thermonuclear Device;" P/2383, Vol. 31, Second U.N. Conference on the Peaceful Uses of Atomic Energy, Geneva, September 1958.
27. Wilcox, Gow and Smith, *Bull. Amer. Phys. Soc. Ser. II*, 4, 55, 1959; "The Ion Magnetron," AEC Report UCRL-8579.
28. E.E. Yushmanov; Vol. IV of Plasma Physics and the Problem of Controlled Thermonuclear Reactions; M.A. Leontovich and J. Turkevich, eds., trans. by J.B. Sykes, Pergamon Press, 1959.
29. R.F. Post, "Summary of UCRL Pyrotron (Mirror Machine) Program" P/377, Vol. 32, Second U.N. Conference on the Peaceful Uses of Atomic Energy, Geneva, 1958.

UNCLASSIFIED

Aerospace Corporation, El Segundo, California. THE PLASMA CORE REACTOR, by Seymour T. Nelson. 10 May 1961. 111p. incl. illus. (Report No. TDR-594(1555-01)TN-1) (Contract AF 04(647)-594).

Unclassified report

Two types of plasma core reactor, considered as a space propulsion system of thrust-to-weight ratio exceeding unity, are investigated; viz, the simple magnetic bottle and the bipolar configurations. The principal system variables are indicated, and some upper- and lower-bounds are derived. The major problem areas and difficulties affecting feasibility are discussed.

UNCLASSIFIED

UNCLASSIFIED

Aerospace Corporation, El Segundo, California. THE PLASMA CORE REACTOR, by Seymour T. Nelson. 10 May 1961. 111p. incl. illus. (Report No. TDR-594(1555-01)TN-1) (Contract AF 04(647)-594).

Unclassified report

Two types of plasma core reactor, considered as a space propulsion system of thrust-to-weight ratio exceeding unity, are investigated; viz, the simple magnetic bottle and the bipolar configurations. The principal system variables are indicated, and some upper- and lower-bounds for these are derived. The major problem areas and difficulties affecting feasibility are discussed.

UNCLASSIFIED

UNCLASSIFIED

Aerospace Corporation, El Segundo, California. THE PLASMA CORE REACTOR, by Seymour T. Nelson. 10 May 1961. 111p. incl. illus. (Report No. TDR-594(1555-01)TN-1) (Contract AF 04(647)-594).

Unclassified report

Two types of plasma core reactor, considered as a space propulsion system of thrust-to-weight ratio exceeding unity, are investigated; viz, the simple magnetic bottle and the bipolar configurations. The principal system variables are indicated, and some upper- and lower-bounds for these are derived. The major problem areas and difficulties affecting feasibility are discussed.

UNCLASSIFIED

UNCLASSIFIED

Aerospace Corporation, El Segundo, California. THE PLASMA CORE REACTOR, by Seymour T. Nelson. 10 May 1961. 111p. incl. illus. (Report No. TDR-594(1555-01)TN-1) (Contract AF 04(647)-594).

Unclassified report

Two types of plasma core reactor, considered as a space propulsion system of thrust-to-weight ratio exceeding unity, are investigated; viz, the simple magnetic bottle and the bipolar configurations. The principal system variables are indicated, and some upper- and lower-bounds for these are derived. The major problem areas and difficulties affecting feasibility are discussed.

UNCLASSIFIED

UNCLASSIFIED

Aerospace Corporation, El Segundo, California. THE PLASMA CORE REACTOR, by Seymour T. Nelson. 10 May 1961. 111p. incl. illus. (Report No. TDR-594(1555-01)TN-1) (Contract AF 04(647)-594).

Unclassified report

Two types of plasma core reactor, considered as a space propulsion system of thrust-to-weight ratio exceeding unity, are investigated; viz, the simple magnetic bottle and the homopolar configurations. The principal system variables are indicated, and some upper- and lower-bounds for these are derived. The major problem areas and difficulties affecting feasibility are discussed.

UNCLASSIFIED

Aerospace Corporation, El Segundo, California. THE PLASMA CORE REACTOR, by Seymour T. Nelson. 10 May 1961. 111p. incl. illus. (Report No. TDR-594(1555-01)TN-1) (Contract AF 04(647)-594).

Unclassified report

Two types of plasma core reactor, considered as a space propulsion system of thrust-to-weight ratio exceeding unity, are investigated; viz, the simple magnetic bottle and the homopolar configurations. The principal system variables are indicated, and some upper- and lower-bounds for these are derived. The major problem areas and difficulties affecting feasibility are discussed.

UNCLASSIFIED

UNCLASSIFIED

Aerospace Corporation, El Segundo, California. THE PLASMA CORE REACTOR, by Seymour T. Nelson. 10 May 1961. 111p. incl. illus. (Report No. TDR-594(1555-01)TN-1) (Contract AF 04(647)-594).

Unclassified report

Two types of plasma core reactor, considered as a space propulsion system of thrust-to-weight ratio exceeding unity, are investigated; viz, the simple magnetic bottle and the homopolar configurations. The principal system variables are indicated, and some upper- and lower-bounds for these are derived. The major problem areas and difficulties affecting feasibility are discussed.

UNCLASSIFIED

UNCLASSIFIED

UNCLASSIFIED

UNCLASSIFIED